FACULTY OF TECHNOLOGY

Uncertainty and Sensitivity Analysis for Nuclear Reactor Core and Thermal-Hydraulic System Models

Rebekka Komu

ENVIRONMENTAL ENGINEERING

Master's Thesis

December 2019

FACULTY OF TECHNOLOGY

Uncertainty and Sensitivity Analysis for Nuclear Reactor Core and Thermal-Hydraulic System Models

Rebekka Komu

Supervisors:
Ph.D., M.Sc. (Tech.) Antonio Caló
M.Sc. (Tech.) Elina Syrjälahti

ENVIRONMENTAL ENGINEERING
Master's Thesis
December 2019

ABSTRACT
FOR THESIS

University of Oulu Faculty of Technology

Degree Programme (Bachelor's Thesis, Master's Thesis) Degree Programme in Environmental Engineering		Major Subject (Licentiate Thesis)	
Author Komu, Rebekka		Thesis Supervisor Caló A, Ph.D., M.Sc. (Tech.)	
Title of Thesis Uncertainty and Sensitivity Analysis for Nuclear Reactor Core and Thermal-Hydraulic System Models			
Major Subject Energy Systems and Cleaner Production	Type of Thesis Master's Thesis	Submission Date December 2019	Number of Pages 81 p., 3 app.

Abstract

In order to ensure the safe operation of nuclear power plants, safety analyses are needed during the design, licensing and operation of the plant. It has been an increasing interest to substitute conservative safety analyses with best-estimate analyses including their uncertainty limits. For this purpose, uncertainty and sensitivity analysis methods have been under investigation, discussion and development in the nuclear community during the past few decades, from which OECD/NEA's UAM (Uncertainty Analysis in Modelling) benchmark is a good example.

In this thesis, uncertainty and sensitivity analyses were done using UAM benchmark as a framework. The benchmark is divided into three phases: neutronics, core, and system phase, from which this thesis focuses on the last phase. The goal of the benchmark is to recognize the sources of uncertainty in each phase and how uncertainties propagate from one calculation stage to another. Uncertainty and sensitivity analyses were done for a separate core model, a system thermal-hydraulics model and a coupled core-system model using HEXTRAN, TRACE and the coupled HEXTRAN-SMABRE codes, respectively. The modelled case was the Kalinin-3 main coolant pump switching off at nominal power transient, which is a well-documented experiment and one of the studied cases in UAM benchmark. TRACE is a new code at VTT, and it was taken into use and the Kalinin-3 model development was started as a part of this thesis. The goal of this thesis was to identify what are the most important sources of uncertainty in each model, what are the capabilities of the used sensitivity analysis tools, and could the models and tools be improved somehow.

The used sensitivity analysis tools were VTT's own code Sensla for HEXTRAN-SMABRE and DAKOTA for TRACE. Both tools used a statistical method, in which the input uncertainty parameters are recognized and given probability distributions, then random samples are selected from the distributions and calculated. The sample size is determined with the Wilks' formula by using 95 % probability and 95 % confidence limits for the results. The results give mean, minimum and maximum values, and standard deviations for the output parameters as well as plots from all the simulations. Sensitivity measurements, which tell about the effect each input variable has on the results, are calculated between every input variable and outputs of interest. The sensitivity measurements used in this thesis were the Rank correlation coefficient (RCC) and the Partial rank correlation coefficient (PRCC).

In each model, a couple input variables among the selected variations clearly affected results the most: gas gap conductance and core inlet temperature in HEXTRAN, gas gap conductance and homologous pump curves in HEXTRAN-SMABRE, and liquid-to-wall heat transfer coefficient and wall drag in the TRACE model. Adding neutronics uncertainties to the simulations increased standard deviations in HEXTRAN and HEXTRAN-SMABRE results, which indicates that many of the uncertainties in this case come from the earlier calculation steps. Overall the standard deviations were the same scale or smaller than measurement error. No new scenarios or unexpected events emerged with the chosen input variations. This may be due to the mildness of the transient or that there are not many uncertainties in this case.

Final tuning for the HEXTRAN and SMABRE models can be done after the final specifications are received from the benchmark team, for example, data concerning the homologous pump curves, which has been ambiguous so far. The development of the Kalinin-3 model for TRACE was started, but it still needs more work. Some control systems must be added and boundary conditions removed, and a three-dimensional core model is needed for further use. PRCC calculation was coded to Sensla, but the results were unsuccessful. In the future, some other method could be tested or the PRCC values could be calculated with another program. Due to this thesis TRACE was taken into use at VTT, and Sensla is now ready to be used once the final specifications are received from the benchmark team and these analyses can be done again with the suggested input variations.

Additional Information

TIIVISTELMÄ
OPINNÄYTETYÖSTÄ Oulun yliopisto Teknillinen tiedekunta

Koulutusohjelma (kandidaatintyö, diplomityö) Ympäristötekniikan tutkinto-ohjelma	Pääaineopintojen ala (lisensiaatintyö)
Tekijä Komu, Rebekka	Työn ohjaaja yliopistolla Caló A, FT, DI

Työn nimi
Epävarmuus- ja herkkyysanalyysi ydinvoimalan reaktorisydän- ja laitosmalleille

Opintosuunta	Työn laji	Aika	Sivumäärä
Energy Systems and Cleaner Production	Diplomityö	Joulukuu 2019	81 s., 3 liitettä

Tiivistelmä

Turvallisuusanalyysit ovat olennainen työkalu ydinvoimalaitoksen turvallisuuden takaamiseen sen suunnittelun, lisensioinnin ja käytön aikana. Viime vuosikymmenten aikana ydinalalla on ollut kasvava mielenkiinto korvata konservatiiviset turvallisuusanalyysit best-estimate-analyyseillä niiden epävarmuusrajojen kanssa. Tätä varten epävarmuus- ja herkkyysanalyysimenetelmät ovat olleet tutkimuksen, kehityksen ja keskustelun aiheena, mistä OECD/NEA:n UAM (Uncertainty Analysis in Modelling) vertailuanalyysi on hyvä esimerkki.

Epävarmuus- ja herkkyysanalyysit tähän diplomityöhön tehtiin UAM vertailutehtävien mukaisesti. Vertailuanalyysi on jaettu kolmeen vaiheeseen: neutroniikka-, reaktorisydän- ja laitosvaihe, joista jälkimmäiseen tässä työssä keskityttiin. Tehtävien tarkoituksena on tunnistaa epävarmuuden lähteet kussakin vaiheessa sekä kuinka epävarmuudet kumuloituvat laskentaketjun vaiheesta toiseen. Epävarmuus- ja herkkyysanalyysi tehtiin irtosydän-, laitos- ja yhdistetylle sydän-laitosmallille käyttäen vastaavasti HEXTRAN, TRACE ja yhdistettyä HEXTRAN-SMABRE koodeja. Mallinnettu tapaus oli Kalinin-3 ydinvoimalaitoksella suoritettu käyttöhäiriökoe, jossa yksi neljästä pääkiertopumpusta sammutettiin täydellä tehotasolla. TRACE on VTT:llä uusi koodi, joka otettiin käyttöön osana tätä työtä, ja Kalinin-3 mallin kehitys koodille aloitettiin. Työn tavoitteena oli tunnistaa tärkeimmät epävarmuuden lähteet kussakin mallissa, verrata käytettyjen herkkyysanalyysityökalujen ominaisuuksia ja tunnistaa, tulisiko malleja ja työkaluja parantaa jotenkin.

Työssä käytetyt herkkyysanalyysityökalut olivat VTT:llä kehitetty Sensla HEXTRAN-SMABRE:lle ja DAKOTA TRACE:lle. Kumpikin työkaluista käytti tilastollista menetelmää, jossa epävarmoiksi tunnistetuille syöteparametreille annettiin todennäköisyysjakaumat, ja useita simulaatiota suoritettiin poimien kullekin ajolle satunnaiset syöteparametrien arvot jakaumista. Simulaatioiden lukumäärä laskettiin Wilksin kaavalla, jolloin tuloksille saatiin luottamusväli, jolle 95 % tuloksista sijoittuu 95 % todennäköisyydellä. Tulossuureille saatiin keskiarvo, minimi- ja maksimiarvot, ja keskihajonta. Syöteparametrien ja tulossuureiden väliset riippuvuudet laskettiin käyttäen tunnuslukuina järjestyskorrelaatiokerrointa ja osittaista järjestyskorrelaatiokerrointa.

Jokaisessa mallissa havaittiin pari syötemuuttujaa, jotka vaikuttivat tuloksiin kaikkein eniten: jäähdytteen sisäänmenolämpötila ja kaasuraon lämmönjohtavuus irtosydänmallissa (HEXTRAN), nesteen ja seinämän välinen lämmönsiirtokerroin ja putkien kitkakerroin laitosmallissa (TRACE), sekä kaasuraon lämmönjohtavuus ja homologinen pumppukäyrä yhdistetyssä sydän-laitosmallissa (HEXTRAN-SMABRE). Neutroniikkaepävarmuudet lisäsivät keskihajontaa huomattavasti HEXTRAN ja HEXTRAN-SMABRE tuloksissa, mistä voi päätellä ison osan epävarmuuksista tulevan tässä tapauksessa aiemmista laskentavaiheista. Tuloksien keskihajonta oli kaikissa tulossuureissa pienempi tai korkeintaan yhtä suuri kuin mittausvirhe. Mikään simulaatioista ei johtanut uusiin skenaarioihin tai odottamattomiin tuloksiin. Tämä saattaa johtua mallinnetun tapahtuman lievyydestä tai siitä, ettei tapahtuma sisällä paljon epävarmuuksia.

HEXTRAN ja SMABRE malleja tulee vielä hienosäätää, kunhan vertailuanalyysin järjestäjiltä saadaan varmistus työssä käytettävästä datasta, esimerkiksi pumppukäyristä, joista tähän mennessä on saatu ristiriitaista tietoa. TRACE mallia muokattiin paljon tätä työtä varten, ja mallin kehitystä tulee jatkaa edelleen. Muun muassa säätöjärjestelmiä tulee lisätä ja reunaehtoja poistaa, lisäksi kolmitulotteinen sydänmalli tulee liittää TRACE:en jatkokäyttöä varten. Osittaisen järjestyskorrelaation laskeminen koodattiin Senslaan, mutta tulokset epäonnistuivat. Jatkossa tulisi kokeilla toista laskentatapaa tai suorittaa korrelaatiokertoimen laskeminen toisella ohjelmalla. Tämän työn myötä TRACE otettiin käyttöön VTT:llä, ja Senslaa muokattiin niin, että se on valmis käyttöä varten, kunhan vertailuanalyysin järjestäjiltä saadaan lopulliset spesifikaatiot ja nämä analyysit voidaan tehdä uudestaan ehdotetuilla parametrien variaatioilla.

Muita tietoja

ACKNOWLEDGEMENTS

This thesis was carried out at VTT Technical Research Centre of Finland between June and December 2019. I would like to thank the Finnish Research Programme on Nuclear Power Plant Safety 2019 – 2022 (SAFIR2022) for funding this study. The aim of this thesis was to conduct uncertainty and sensitivity analyses for nuclear reactor core and thermal-hydraulic system models.

I am grateful to my supervisor Elina Syrjälahti from VTT for making this thesis possible and for her valuable advice and contribution during the work. Her counsel was instrumental in setting up and conducting this study. I would like to thank my supervisor Antonio Caló from University of Oulu for guiding me through this process and for his insightful comments and enthusiastic encouragement.

I want to express my gratitude to Hanna Räty and Anitta Hämäläinen from VTT for all their support and expertise. Their help was invaluable while finishing this work. I must also thank all my co-workers at VTT for a great work environment.

Finally, I want to thank my family for supporting me and especially my sisters for showing me the way. Special thanks to my friends for being there throughout my studies and making those years unforgettable.

Espoo, 9.12.2019 Rebekka Komu

CONTENTS

APPENDICES:

ABBREVIATIONS

BEPU	best-estimate plus uncertainty
BWR	boiling water reactor
CAMP	Code Application and Maintenance Program
CFD	computational fluid dynamics
DEC	design extension condition
FA	fuel assembly
GRS	Gesellschaft für Anlagen- und Reaktorsicherheit
HTC	heat transfer coefficient
ICSM	in-core monitoring system
LHS	Latin hybercube sampling
LOCA	loss of coolant accident
LWR	light-water reactor
MCP	main coolant pump
NEA	Nuclear Energy Agency
NSC	Nuclear Science Committee
NSCI	Committee on Safety of Nuclear Installations
NPP	nuclear power plant
OECD	The Organisation for Economic Co-operation and Development
PRCC	partial rank correlation coefficient
PRZ	pressurizer
PWR	pressurized water reactor
RCC	rank correlation coefficient
RPV	reactor pressure vessel
SD	standard deviation
SG	steam generator
STUK	Radiation and Nuclear Safety Authority
UAM	Uncertainty Analysis in Modelling
USNRC	United States Nuclear Regulatory Commission
VTT	Technical Research Centre of Finland
XS	cross-section

1 INTRODUCTION

In order to ensure the safe operation of nuclear power plants (NPP), safety analyses are needed and their methods constantly developed. Recently it has been a subject of interest to replace traditional, conservative safety analysis methods with best estimate analyses including their uncertainty limits. The problem with conservative analysis, in which pessimistic assumptions about initial and boundary conditions are made, is that with complex models it is difficult to known whether the assumptions actually lead to conservative results (Peltokorpi 2009). In order to add uncertainty limits to best-estimate simulations, uncertainty and sensitivity analysis is needed.

During the past decades, the Nuclear Energy Agency of the Organisation for Economic Co-operation and Development (OECD/NEA) has organized expert groups and workshops to chart the best uncertainty analysis methods for NPP safety analyses (OECD/NEA/CSNI 1994, OECD/NEA/CSNI 2013). There have been programs such as BEMUSE (Best Estimate Methods – Uncertainty and Sensitivity Evaluation), which focused on loss of coolant accident (LOCA) analysis (OECD/NEA/CSNI 2011). Latest effort for international co-operation on the topic is the Uncertainty Analysis in Modelling (UAM) for design, operation and safety analysis of light-water reactors (LWRs) benchmark organized by OECD/NEA Nuclear Science Committee (NSC) (Hou et al. 2019a). It is divided into three phases: neutronics, core, and system phase, from which the latter two are still ongoing. The benchmark focuses on coupled simulations' uncertainties in all stages of the system calculations, and their propagation through the calculation chain by using six well-documented cases as examples. One of these cases is Kalinin-3 Coolant Transient, which is studied in this thesis.

During the past few years, interest in VVER-1000 reactors, such as Kalinin-3, has increased at VTT due to Fennovoima's Hanhikivi-1 project planned in Finland, and in 2018, the model for Kalinin-3 was created (Syrjälahti 2018a). Because the Kalinin-3 coolant transient is a part of the UAM benchmark, and it has previously been its own benchmark, it is a well-documented case and therefore well suited for code development and model validation purposes (OECD/NEA 2016). The model was created for VTT's own code, HEXTRAN-SMABRE, and this thesis starts the work of Kalinin-3 model development for a new code at VTT's Reactor analysis team, TRACE. In the future,

TRACE will be a part of VTT's new calculation system for reactor analyses thus increasing the diversity principle of nuclear safety analyses at VTT.

In this thesis, uncertainty analyses are done for a separate reactor core model (HEXTRAN), a thermal-hydraulic system model (TRACE), and two scenarios with a coupled core-system model (HEXTRAN-SMABRE) using the UAM benchmark as a guideline. The goal is to recognize the most important sources of uncertainty in each model. Two sensitivity analysis tools are used: Sensla for HEXTRAN-SMABRE and DAKOTA for TRACE. Sensla is a used and validated sensitivity analysis tool developed at VTT, and some upgrades were done to it for this thesis' purposes. Since DAKOTA – like TRACE – is a new tool at VTT, its features and capabilities were explored while doing this study. Comparing the two sensitivity analysis tools helped to recognize the advantages and shortcomings of each, and see how they could be improved.

Because the UAM benchmark System Phase is still ongoing, the final benchmark specifications are still missing and there are no results about the Kalinin-3 whole core and thermal-hydraulic system models yet. There have been many studies about the uncertainty in coupled code models, but most of the studied cases have been vastly different from Kalinin-3 coolant transient. More severe accidents, such as LOCAs, or BWR (boiling water reactor) transients have very different characteristics due to their two-phase nature compared to milder transients such as this, which makes comparison of the results difficult. Langenbuch et al. (2005) have studied two milder transient scenarios for VVER-440 and VVER-1000 plants – load-drop of one turbo generator and switch-off of one feedwater pump – which could be somewhat comparable to this case even though the transients are different.

Research questions studied in this thesis are:

- What are the most important sources of uncertainties in reactor core, thermal-hydraulic system, and coupled core-system models?
- Based on the uncertainty and sensitivity results, how should the models be improved?
- What are the capabilities of used sensitivity analysis tools? Could they be improved somehow?

In Chapter 2, the baseline for this work is established by familiarizing with the modelled NPP and the framework for the sensitivity analyses set by UAM benchmark. Chapter 3 discusses the goals and outcomes of uncertainty and sensitivity analysis, touches briefly on the different methods, and describes in more detail the method used in this thesis. In Chapter 4, the used codes – HEXTRAN, SMABRE and TRACE – and respective models are introduced, as well as the changes made to the models. Chapter 5 covers the sensitivity analysis runs done for this study. First, the sensitivity analysis tools are presented. Then the sources of uncertainty in each model are identified and the variations used in the sensitivity runs are decided. The results are presented in Chapter 6 and discussed in detail in Chapter 7. The final conclusions and follow-up measures are presented in Chapter 8.

2 BACKGROUND

OECD/NEA's UAM benchmark was used as a framework for the uncertainty and sensitivity analyses done for this thesis. In this chapter, the benchmark and its goals are introduced. In order to do uncertainty and sensitivity analysis, a deep understanding about the modelled system and transient is required. The modelled NPP and transient are presented in this chapter, as well as some of the measurements from the experiment.

2.1 UAM benchmark

Uncertainty and sensitivity analyses done for this thesis are part of NEA's Uncertainty Analysis in Modelling benchmark. Need for this benchmark arises from the increasing demand for best estimate predictions to be provided with their confidence bounds. It provides well-defined problems with input specifications and reference experimental data as well as guidance on assumptions and sources of uncertainty. The goal is to map the current status of uncertainty and sensitivity analysis and help developing and validating the used methods. (Hou et al. 2019a)

The UAM benchmark is divided into three phases – Neutronics, Core, and System Phase – with three to four exercises in each. The phases and exercises can be carried out consecutively or separately. This thesis focuses on Phase III – System Phase with four exercises: Core Multi-Physics, System Thermal-Hydraulics and Coupled Core-System performances, and Comparison of Best Estimate Plus Uncertainty (BEPU) vs. Conservative Calculations. (Hou et al. 2019a) In thesis, the first three exercises are addressed.

Kalinin-3 Coolant Transient was selected as one of the studied scenarios in the UAM benchmark, because it is an existing benchmark, therefore many participants have already tested models for that case. It is a transient test case with well-documented plant measurement data available. (Hou et al. 2019a) The measurements are done with a quite high frequency and the measurement errors are known for almost all parameters, which makes the data valuable for the uncertainty analysis (Tereshonok et al. 2008).

2.2 Kalinin-3 NPP

Kalinin NPP is located in Tver Oblast, Russia, about 200 kilometres from Moscow. It has four units, each with installed capacity of 1000 MW. (Rosenergatom 2018) In this thesis, Kalinin unit 3 is being modelled.

Kalinin-3 is a VVER-1000 reactor, which is a Soviet-Russian designed pressurized water reactor (PWR) using water as coolant and moderator. It has four primary coolant circuits each with a horizontal steam generator. (USDOE Assistant Secretary for Nuclear Energy 1987) A schematic picture of a VVER-1000 reactor and one of its primary circuits is presented in Figure 1.

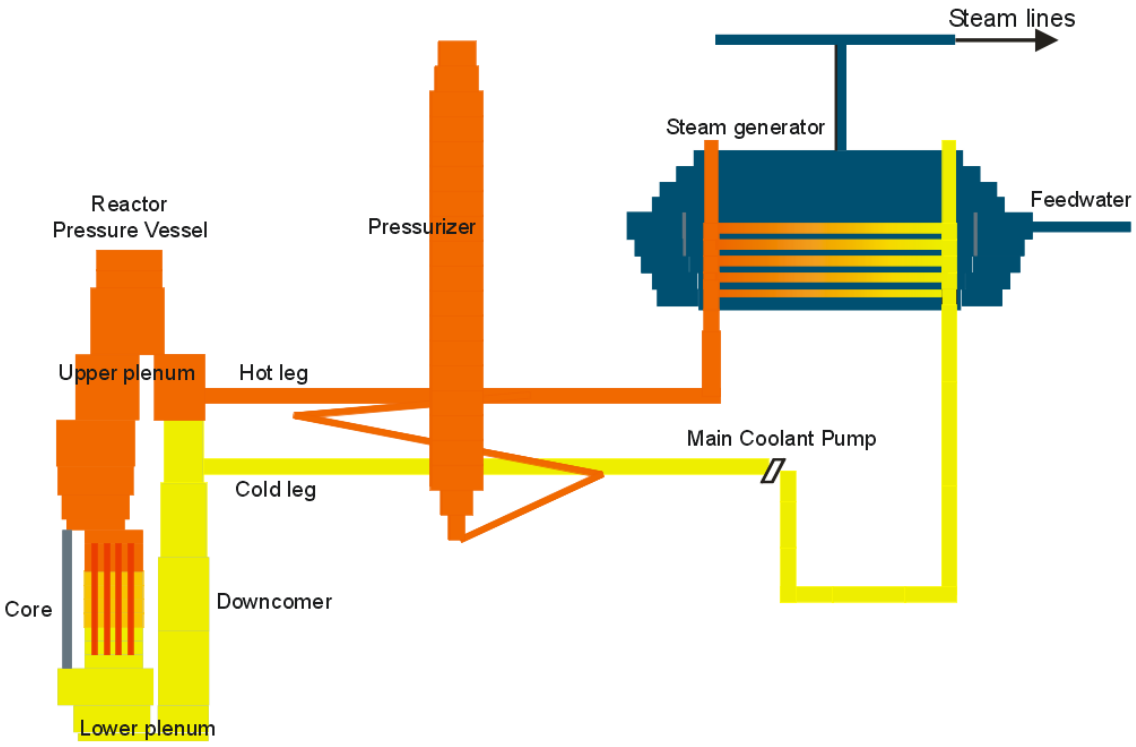

Figure 1. A schematic picture of a PWR reactor and one of the primary coolant circuits (VTT).

Nuclear reactor core is contained in a reactor pressure vessel (RPV). Main coolant pump (MCP) feeds coolant through cold leg piping to the RPV, where it flows through downcomer to the lower plenum of RPV and up through the core to upper plenum. Heated water exits the RPV through hot leg piping and continues towards steam generators (SG), where heat is exchanged between primary and secondary coolant circuits. Pressure is kept high in the primary circuit so that water does not boil in the

reactor core, but on the secondary side of SG water evaporates due to lower pressure and generates steam for electricity production. After going through turbines, water in the secondary circuit is condensed and fed back to the SG through the feedwater system. (Sandberg 2018, p. 45)

High system pressure is maintained with a pressurizer, which contains both water and steam. Pressure is controlled with four groups of heaters and a cooling spray. Activating the heaters increases the pressure, whereas the cooling spray decreases it by spraying cold water from the cold leg piping into the steam. Coolant volume in the primary circuit is controlled with make-up and letdown systems, which feed and extract water from the system as needed. (Ivanov et al. 2002, p. 29)

The Kalinin-3 reactor core has 163 hexagonal fuel assemblies (FA) with uranium-gadolinium fuel (Tereshonok et al. 2008). One FA consists of a bundle of fuel rods, which are zirconium alloy tubes filled with pellets of fissile material (Sandberg 2018, p. 83). The fuel-loading map in Appendix 1 Figure 47 shows the fuel composition in each FA, the location of control rod groups 1-10, as well as the position of the four cooling circuits in relation to the core, numbered from 1 to 4. This is the first fuel loading at Kalinin-3 unit. It is good to notice, that one defected FA in position 07-32 was replaced in the middle of a cycle with a fresh FA different from the others causing some asymmetry in the core. It has only uranium pellets and instead of zirconium alloy cladding, it has spacers and leading tubes made of stainless steel. (Tereshonok et al. 2008)

In order to understand, how power output is controlled in the core, some basics about core neutronics need to be known. Energy, which heats up water in the reactor core, is produced in a fission reaction in the fuel. In a fission reaction, a heavy nucleus splits producing two lighter nuclei, neutrons and energy. Generated neutrons hit other nuclei near them causing them to split, thus creating a chain reaction. When the chain reaction is stable and power production stays the same, a reactor is said to be critical. Power output in PWRs is controlled by affecting the neutron flux mainly with control rods and boron that is dissolved in the coolant. For example, insertion of neutron absorbing control rods causes the reactor to become subcritical and the power output is decreased until it stabilizes on a lower power level and the reactor becomes critical again. Reactivity describes the changes in the neutron flux and power production. A critical

reactor has the reactivity of zero, subcritical reactor has negative reactivity and supercritical positive reactivity. In addition to control rods and boron, reactivity is affected by other physical properties, for example fuel temperature and water temperature and density. For example, if water temperature is increased, it brings negative reactivity to the system. This causes decrease in power output, which again lowers the temperature thus affecting the power output again until the reactor stabilizes. This is called reactivity feedback. (Sandberg 2018, p. 26-31)

2.3 Transient description

The purpose of safety analyses is to demonstrate that the nuclear system has sufficient safety features and margins during a variety of postulated events. These events are categorized by frequency to anticipated transients, postulated accidents, design extension conditions (DEC) and severe accidents. Transients have an anticipated probability of more than 10^{-2} events per year, which means that they are expected to happen at least once during the plant lifetime. (STUK 2018) Events like this are, for example, reactor scram, pump trips, turbine trips and loss of feedwater (Miettinen 2000). Postulated accidents have been divided into two classes: Class 1 with a probability of occurrence between 10^{-2} and 10^{-3} events per year and Class 2 with a probability of less than 10^{-3} events per year (STUK 2018). This category includes, for example, loss of coolant accidents and other cases where the integrity of main coolant system is lost (Miettinen 2000). DEC includes occurrences where required safety functions fail, for example transient or Class 1 accident that involves a common cause failure in safety system (STUK 2018). In severe accidents, a significant part of fuel is damaged and the analyses focus on a severe accident management strategy (Peltokorpi 2009).

In this thesis, the Kalinin-3 Coolant Transient experiment is modelled. During the transient, one of the main circulation pumps is switched off at nominal power. This causes the control systems to lower reactor power to an automatically chosen set point by operating control rod groups 9 and 10. Both of these events cause spatial asymmetry in the core. (Tereshonok et al. 2008)

The time interval of interest is 300 seconds. The main coolant pump in loop 1 (MCP-1) is switched off at t = 0 s. After 1.41 seconds, a ‘one pump out of operation’ signal is

generated and the reactor limiting controller starts to decrease the power to a level of 67.2 %. Control rod group 10 starts to move downwards from its initial position of 82.95 % (with 100 % being fully drawn out) until it reaches 43.3 % where it remains until the end of the transient. Group 9 starts to move when group 10 has reached 50 % insertion depth. It moves to a position of 93.1 % where it stays until 180th second of the transient before returning to its initial position of 100 %. (Tereshonok et al. 2008)

Partial insertion of control rods causes axial asymmetry in the power distribution. Relative power as a function of axial location calculated with HEXTRAN-SMABRE at four different times is presented in Figure 2. As seen from the figure, insertion of control rods from the top pushes the power profile downwards.

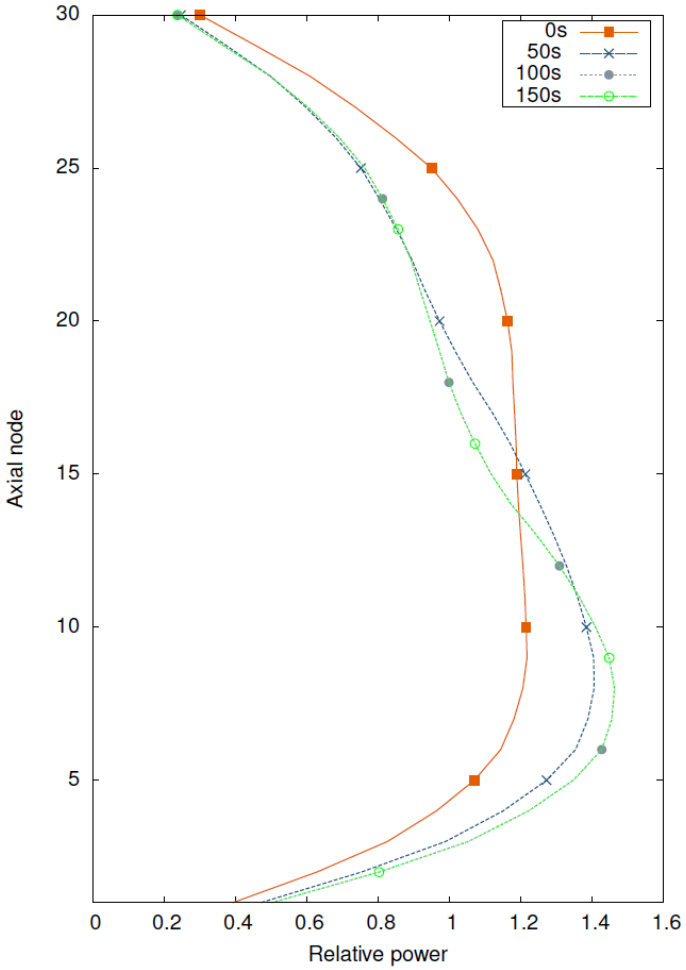

Figure 2. Axial power distribution at different times during the transient calculated with HEXTRAN-SMABRE (Syrjälahti 2018a).

Essential in this transient are the changing mass flows in the system. Mass flow rates in all primary loops during the transient recorded by ICMS (In-core Monitoring System)

are provided in the Kalinin-3 benchmark data and are presented in Figure 3. After MCP-1 is switched off, the mass flow in loop 1 is reversed. This is compensated by other loops with increased mass flow. Mass flow rate through core decreases similarly to that in loop 1. As seen from the figure, mass flow rate measurement changes abruptly at 40s in loop 1, and the same happens in whole core measurement. This is because the mass flow rate cannot be measured directly and the measurement estimation is based on two algorithms: one for normal use and one for reversed flow only. The algorithm changes 40 seconds after the signal about MCP-1 switching off is received. During the switchover time, both of the algorithms are out of their application range, which makes the measurement unreliable for the first 90 seconds of the transient. (Georgieva 2016)

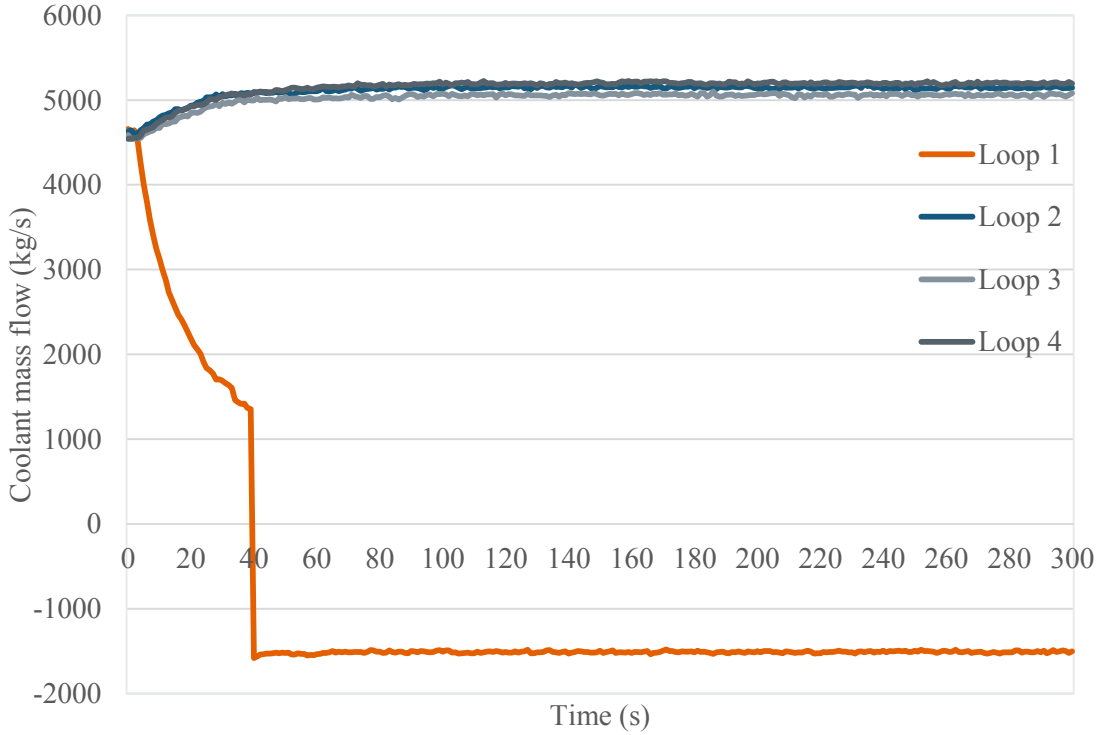

Figure 3. Mass flow rates in all primary loops during the transient recorded by ICMS.

There is always uncertainty in measurements, to which the calculation results are compared. Kozloduy-6 is a NPP unit with the same VVER-1000 design as Kalinin-3. During the plant-commissioning phase a series of start-up tests was performed there that have been modelled before as a part of V1000CT Coolant Transient benchmark (Ivanov et al. 2002). Measurement errors for steady state conditions in Kozloduy-6 NPP at 29 % power with MCP-3 switched off are known and presented in Table 1. The experiment done in Kozloduy-6 is different from this case, so the actual output values should not be

compared, but since the two NPP's have the same design, it can be assumed that the scale of measurement error is the same in both plants. It is worth noting, that the error is several percentages in many of the measured parameters.

Table 1. Measurement uncertainty ranges for Kozloduy-6 NPP steady state at 29 % power with MCP-3 switched off (Ivanov et al. 2002).

Parameter	**Value**	**Accuracy**	**Accuracy (%)**
Core power (MWt)	883.50	±60	±6.8
Primary side pressure (MPa)	15.6	±0.3	±1.9
RCS first cold leg temperature (K)	555.55	±2.0	±0.4
RCS second cold leg temperature (K)	554.55	±2.0	±0.4
RCS third cold leg temperature (K)	554.35	±2.0	±0.4
RCS fourth cold leg temperature (K)	555.25	±2.0	±0.4
RCS first hot leg temperature (K)	567.05	±2.0	±0.4
RCS second hot leg temperature (K)	562.85	±2.0	±0.4
RCS third hot leg temperature (K)	550.75	±2.0	±0.4
RCS fourth hot leg temperature (K)	566.15	±2.0	±0.4
Core flow rate (kg/s)	13611	±800.0	±5.9
First loop flow rate (kg/s)	5031	±200.0	±4.0
Second loop flow rate (kg/s)	5069	±200.0	±3.9
Third loop flow rate (kg/s)	−1544	±200.0	±13.0
Fourth loop flow rate (kg/s)	5075	±200.0	±3.9
Pressurizer level (m)	7.44	±0.15	±2.0
Water level in SG1 (m)	2.30	±0.075	±3.3
Water level in SG2 (m)	2.41	±0.075	±3.1
Water level in SG3 (m)	2.49	±0.075	±3.0
Water level in SG4 (m)	2.43	±0.075	±3.1
Secondary side pressure (MPa)	5.937	±0.2	±3.4
Pressure difference in the reactor (MPa)		±0.02	
Pressure difference in MCP (MPa)		±0.02	

3 UNCERTAINTY AND SENSITIVITY ANALYSIS

The goal of uncertainty and sensitivity analysis is to identify the sources of uncertainty in a complex model and quantify how they affect the model outcome (Marino et al. 2008). Uncertainty analysis provides probability and range for calculation results, whereas sensitivity measures describe the relative contribution of each input variable to output uncertainty. Both uncertainty statements and sensitivity measures are analysed simultaneously for the output of interest. (Glaeser 2008) There are numerous ways to do uncertainty and sensitivity analysis. In the following chapters, different methods and the one used in this thesis are introduced more closely.

3.1 Sensitivity analysis methods

One way to classify the several existing uncertainty and sensitivity analysis methods is to differentiate between local and global methods. In local sensitivity analysis, there is typically only one input parameter varied at a time. Global sensitivity analysis, on the other hand, allows varying several input parameters at the same time and running the simulation with random combination of the variables. (Ikonen & Tulkki 2014)

Another way to group different methods is to divide them into deterministic and statistical methods. Deterministic methods are often also local. (Ikonen & Tulkki 2014) The uncertainty is evaluated with chosen values of input variable with a small range of variation (Marchand 2008). With statistical analysis, the values of the input variables are sampled from a distribution and the output distribution is then analysed statistically (Ikonen & Tulkki 2014). There are also other ways, for example extrapolating the model output uncertainties by comparing the results to experimental data, such as the CIAU method (Glaeser 2013).

For a complex nuclear plant code with a large number of input parameters, a global and statistical method is the best option (Ikonen & Tulkki 2014). The statistical method proposed by GRS (Gesellschaft für Anlagen- und Reaktorsicherheit) is used widely in safety research and licensing in the nuclear energy field (Glaeser 2013). In the GRS method, each input parameter value is selected from a probability distribution randomly, which is called Monte Carlo sampling (Ikonen & Tulkki 2014). The number of samples or calculations is independent of the number of uncertain parameters, and it is

determined with Wilks' formula. Sensitivity measures are then calculated to determine the importance of input uncertainties on the results. (Glaeser 2008) Method used in this thesis follows the GRS method closely.

3.2 Sources of uncertainty

An important part of uncertainty and sensitivity analysis in modelling is to recognize the sources of uncertainty. Uncertainties arise from several different sources, such as measurements, approximations of modelling, imprecise knowledge of initial and boundary conditions, and simplifications. These uncertainties must be considered in simulations when deciding input values, initial conditions, boundary conditions, models, nodalization, geometry, convergence criteria, time step size and so on. (Glaeser 2008) The ability to recognize the sources of uncertainty often requires vast knowledge about the modelled system as well as the used code and model.

Modelling a complex system such as a nuclear power plant requires several steps with many different programs. Uncertainties propagate from one calculation system step to another. Therefore the output uncertainties should be taken into account as input uncertainties in the next calculation step. For example, output uncertainties from the neutronics calculations should be taken into account as input uncertainties in the fuel modelling. (Hou et al. 2019a)

3.3 Monte Carlo simulation

Monte Carlo methods include statistical sampling to obtain random or pseudo-random numbers from the probability distributions of input values (Marino et al. 2008). Once the sources of uncertainty have been identified, each parameter is given a user-defined probability distribution. Usually the distribution is given a range and type (uniform, normal, triangular, discrete, etc.). (Syrjälahti 2005) These decisions are made based on prior information (Marino et al. 2008). It is important that the distribution is realistic in order to give meaningful information about the uncertainties (Syrjälahti 2006).

In traditional Monte Carlo sampling, samples are randomly selected according to the probability distributions (Adams et al. 2018). In other methods, such as Latin hypercube sampling (LHS), different techniques are used in order to acquire random values that

represent the distribution better. LHS is a technique, where the length of the distribution is divided into *N* equal probability intervals, where *N* is the number of samples. One random value is then selected from each interval. This guarantees that there are samples from the outer ranges of the distribution as well. (Marino et al. 2008)

These randomly selected values are then used as input values in simulations. The samples represent the population of all possible values and outcomes. In order for the representation to be accurate, the sample size – or number of calculations – has to be big enough. The number of calculations is determined with the Wilks' formula. (Glaeser 2008)

3.4 Number of calculations

The Wilks' formula is a widely used method for determining a sample size. Because the sample size is limited, the formula includes both the confidence level and probability for the results. There are different formulas for one and two-sided confidence intervals. The formula for a one-sided tolerance interval is:

$$1 - \alpha^n \geq \beta\,, \tag{1}$$

where *n* is the minimum number of code runs required, α × 100 (%) is the tolerance interval and β × 100 (%) the probability level. If α = 95 % and β = 95 %, the amount of required code runs is 59. (Glaeser 2008) This means that the maximum calculated value in the sample is an upper statistical tolerance limit, and that any calculated value is below the tolerance limit with 95 % confidence. According to NEA, the one-sided tolerance limit is enough for regulatory purposes, where the licensing criteria is of primary interest, or when there is only one output parameter of interest. (Glaeser 2013)

The formula for a two-sided tolerance interval is:

$$1 - \alpha^n - \mathrm{n}(1-\alpha)\alpha^{n-1} \geq \beta. \tag{2}$$

If the same tolerance interval and probability as in the previous example are chosen, the required sample size is 93. (Glaeser 2008) This means that with 95 % probability 95 % of the calculated values lie between the smallest and largest value of the sample. (Glaeser 2013) For this thesis' purposes, a two-sided tolerance interval is used, since

there are several output parameters of interest and both lower and upper limits are studied.

At present, international organizations have agreed that the 95%/95% approach is enough, and that is what STUK (Radiation and Nuclear Safety Authority) requires as well (STUK 2019). There is still discussions going on whether it is sufficient for safety purposes, but for now that is the used tolerance limit. Another point of discussion has been the number of calculations, if there are several output parameters of interest. In addition to 59 or 93 calculations, sample sizes of 124, 146 and 221 have been used depending on the order of the Wilks' formula and whether it is intended for one or two-sided tolerance intervals. (Hong et al. 2013) However, it was pointed out that the decided input uncertainty ranges affect the results much more than the increased sample size (Glaeser 2013). Therefore, it was decided to use 93 simulations in this study instead of increasing the sample size, which would have been computationally much heavier.

3.5 Sensitivity measures

The results of uncertainty calculations are usually expressed with an uncertainty range and probability density functions or probability distributions. Sensitivity measures, on the other hand, evaluate the importance of a certain input parameter on calculation results. The influence is expressed with correlation coefficients. (Glaeser 2008)

There are simple correlations, which are calculated using the actual input and output data, and rank correlations, which use ranks of the data (Adams et al. 2018). When the relationship between input and output is non-linear but monotonic, rank transformed sensitivity measures are good measures for correlation (Marino et al. 2008). NPP models are complex, non-linear systems, which means that rank transformed correlations are used. Rank correlation coefficients that are used is this thesis are the Spearman's Rank Correlation Coefficient (RCC) and the Partial Rank Correlation Coefficient (PRCC).

3.5.1 Spearman's rank correlation coefficient

The Spearman's rank correlation coefficient is a widely used sensitivity measure in nuclear engineering field (Ikonen & Tulkki 2014). When calculating RCC, the data is first ranked. Input parameters as well as output variables are sorted to increasing order.

Then a rank number is given to each variable. If there are identical values, an average rank is used. RCC is calculated with the following formula:

$$RCC(y_i, x_j) = \frac{\sum_{irun}\left(R(y_{i,irun}) - \overline{R(y_i)}\right)\left(R(x_{j,irun}) - \overline{R(x_j)}\right)}{\sqrt{\sum_{irun}(R(y_{i,irun}) - \overline{R(y_i)})^2 \sum_{irun}\left(R(x_{j,irun}) - \overline{R(x_j)}\right)^2}}, \quad (3)$$

where x_j signifies the input parameter, y_i signifies the output variable, R is the rank of the given variable, irun is the run number, i is the number of the output variable, and j the number of the input parameter. The correlation coefficient is calculated between all input parameters and output variables. RCC gets values between −1 and 1. A value of 1 means that there is a strong positive correlation between the two variables and −1 that the correlation is negative. A value of 0 signifies that there is no correlation. Student's T-distribution is used to determine whether the correlation is significant. With a 5 % risk, the correlation is significant if the absolute value of RCC is greater than 0.2. (Syrjälahti 2005)

3.5.2 Partial rank correlation coefficient

The partial rank correlation coefficient can be calculated by using RCC. In PRCC, the correlation between one input parameter and an output variable is calculated so that the influence of other input parameters is removed. PRCC between two variables, when the effect of a third variable is removed, can be calculated with the formula:

$$PRCC_{12.3} = \frac{RCC_{12} - RCC_{13}RCC_{23}}{\sqrt{(1 - {RCC_{13}}^2)(1 - {RCC_{23}}^2)}}, \quad (4)$$

where $PRCC_{12.3}$ is the partial correlation between x_1 and x_2 when the effect of x_3 is removed, RCC_{12} is the rank correlation between variables x_1 and x_2, and so on. (Iman & Conover 1982) Equation (4) can be expanded further to consider several variables. For example, in the case of five variables the formula would be:

$$PRCC_{12.345} = \frac{PRCC_{12.45} - PRCC_{13.45}PRCC_{23.45}}{\sqrt{(1 - {PRCC_{13.45}}^2)(1 - {PRCC_{23.45}}^2)}}, \quad (5)$$

where the effect of x_3, x_4 and x_5 is reduced from the correlation between x_1 and x_2. (Iman & Conover 1982) This formula can be expanded further to include an arbitrary amount of variables.

4 MODELLING

VTT has several codes used in different areas of reactor physics and dynamics calculations. Together they form VTT's calculation system for different reactor types, presented in Figure 4. Codes developed at VTT are shown in yellow and external codes in blue. This thesis focuses on three-dimensional reactor dynamics and thermal-hydraulic system codes, from which the reactor dynamics code HEXTRAN was used alone and coupled with the system code SMABRE.

The most essential part relative to three-dimensional transient analysis are HEXBU-3D and SIMULATE, which calculate the nodewise fuel burnup distribution for HEXTRAN, TRAB3D and Apros. They use cross-section libraries with two-group constant data, which CASMO-4/4E or Serpent have compiled from nuclear data. HEXTRAN is used for reactor cores with fuel assemblies in a hexagonal lattice and TRAB3D for square lattice. FINIX is a fuel behaviour module coupled to HEXTRAN, and can be used to calculate thermomechanical behaviour in the fuel rods. Hot channel analyses are usually done with one-dimensional TRAB. There is ongoing work to couple CFD (computational fluid dynamics) codes OpenFOAM and PORFLO with HEXTRAN-SMABRE and TRAB3D-SMABRE for more detailed fluid modelling in the reactor pressure vessel. ENIGMA, FRAPCON, SCANAIR and FRAPTRAN are used in more specific fuel rod behaviour analyses either alone or coupled with thermal-hydraulics code GENFLO.

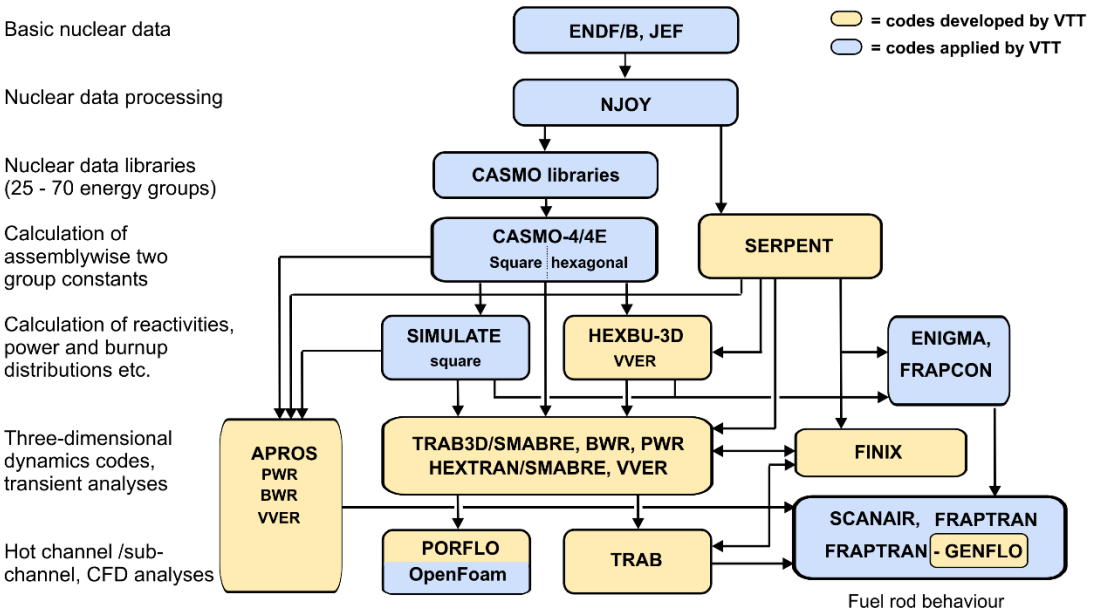

Figure 4. VTT's calculation system (VTT).

In addition to VTT's existing codes, a new system code TRACE was used in this study. It was taken into use as a part of the work done for this thesis. In the future, TRACE will be part of VTT's next generation computational framework, Kraken, presented in Figure 5. Codes marked with yellow are VTT's own codes and red ones are external. The Monte Carlo code Serpent will create cross-section libraries for Ants, which is a nodal neutronics solver module for the core, and other reactor codes. Ants will be coupled with TRACE, which will be used alongside SMABRE and Apros as a system code. The codes and models used in this thesis are introduced more closely in the next chapters.

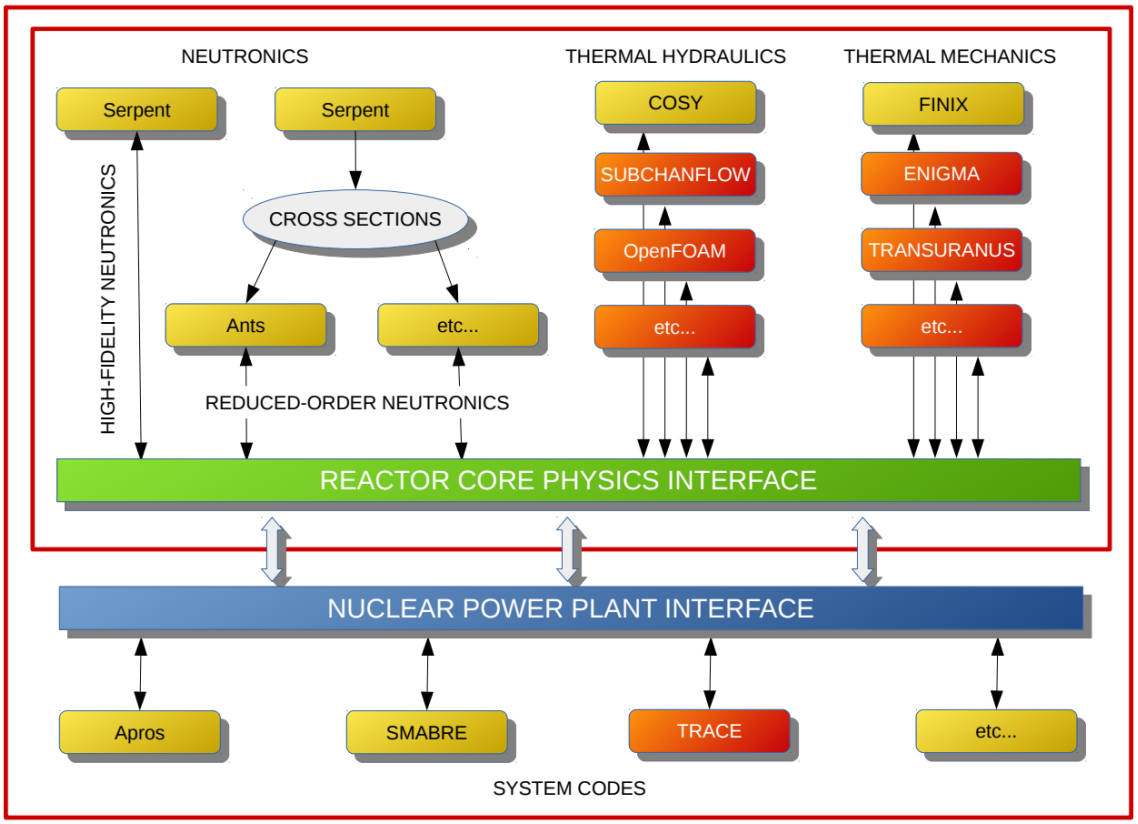

Figure 5. VTT's new computational framework Kraken (VTT).

4.1 HEXTRAN-SMABRE

HEXTRAN (Hexagonal Transient analysis code) is a best-estimate three-dimensional core dynamics code for reactor cores with a hexagonal fuel lattice developed by VTT. It solves coupled reactor neutronics and thermal-hydraulics processes in the core. It has been validated and extensively applied for transient and accident analyses of both

VVER-440 and VVER-1000 type reactors. (Kyrki-Rajamäki 1995) HEXTRAN can be used by itself to model the reactor core or coupled together with SMABRE.

SMABRE (Small Break Accident analysis code) is a thermal hydraulic system code for cooling circuit modelling developed by VTT as well. It was first created to model small break accidents – as the name suggests – but has later been expanded for other type of accidents as well. (Kyrki-Rajamäki 1995) It uses five conservation equations to describe two-phase behaviour in the system: mass equations for steam and water, one mixture momentum equation and energy equations for steam and water. Drift flux correlation is used to calculate phase separation. It is possible to use SMABRE by itself with a point kinetics model for the core, but usually it is used together with a three-dimensional core model. (Miettinen 2000)

For HEXTRAN-SMABRE, both parallel and internal coupling are possible. This determines how information is exchanged and calculation is organised between HEXTRAN and SMABRE. In the parallel coupling model, SMABRE gives the core inlet and outlet pressure, inlet mass flux and enthalpy to HEXTRAN as boundary conditions. HEXTRAN calculates the nodewise power distribution in the core and transfers it to SMABRE. Both codes calculate thermal-hydraulics in the core with their own models and nodalization. In the HEXTRAN model, there is one channel per each fuel assembly, whereas in the SMABRE model the fuel assemblies are grouped together to bigger channels. Each channel is divided axially into nodes. The operations in parallel coupling are illustrated in Figure 6.

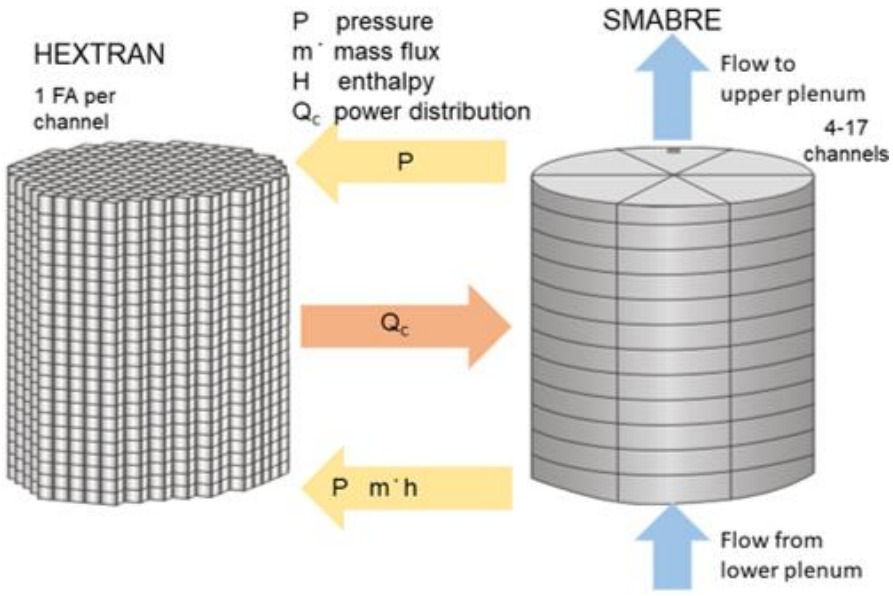

Figure 6. Parallel HEXTRAN-SMABRE coupling (VTT).

In the internal coupling model, information is exchanged between every node in the core. Power and fuel temperature is calculated in the HEXTRAN model and transferred to SMABRE. Nodewise values of mass flux, coolant temperature and heat flux are transferred from SMABRE calculations to HEXTRAN. In the internal coupling, only SMABRE calculates core thermal-hydraulics. These operations are presented in Figure 7.

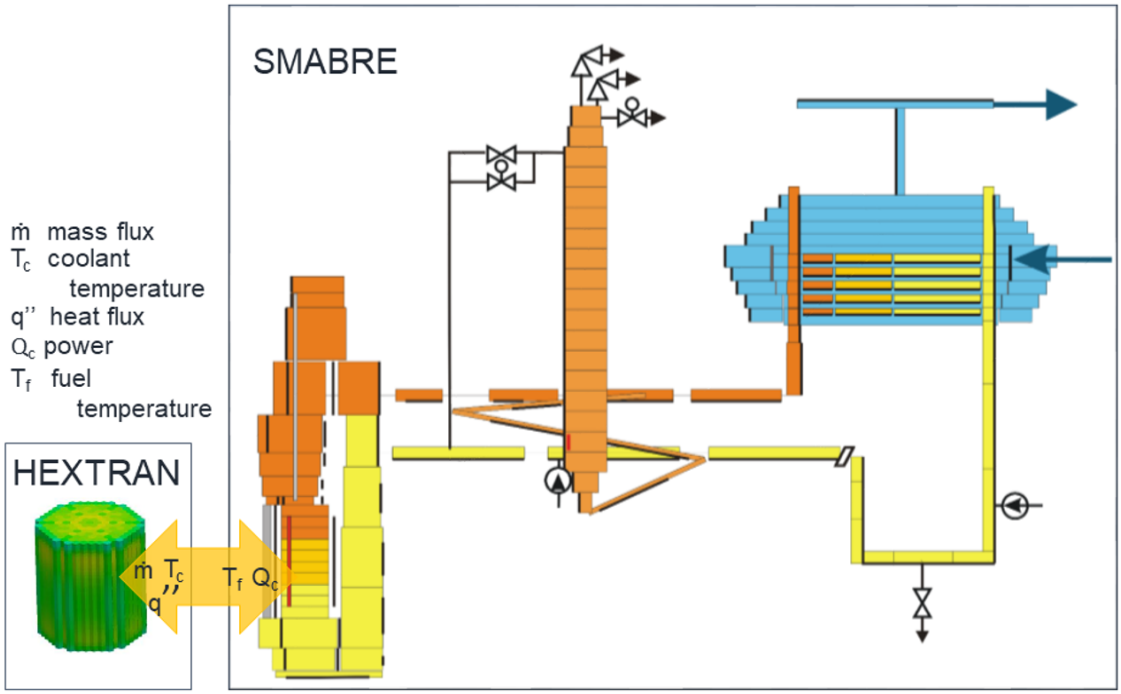

Figure 7. Internal HEXTRAN-SMABRE coupling (VTT).

4.1.1 Kalinin-3 model for HEXTRAN-SMABRE

The Kalinin-3 model for HEXTRAN-SMABRE was created in 2018 by Syrjälahti. It was modified from a Kozloduy-6 NPP model, which has the same VVER-1000 design. The Kozloduy-6 model has been used in, for example, EU projects and V1000CT coolant transient benchmark for VVER-1000 reactors. Preliminary simulations of the main coolant pump switching off transient has been made and the results agree well with the actual plant behaviour. However, there are still some uncertainties concerning the plant data, such as pump curves, fuel assembly details and pressure losses in the primary circuit. Until final information about these issues is received from the benchmark team, the model cannot be fully adjusted to Kalinin-3 pump transient. (Syrjälahti 2018a)

The Kalinin-3 model is made for both parallel and internal coupling mode. In this thesis, the parallel coupling model is used, since it has already been found to model the real power plant behaviour well. (Syrjälahti 2018a) The SMABRE system model includes all four primary coolant loops, the secondary side from steam generators to turbine valves, and all related control systems. The nodalization of one primary circuit loop and the cross-section of the core are depicted in Figure 8. The cross-section depicts the positioning of primary loops in relation to the reactor core. The core model and nodalization of HEXTRAN and SMABRE models are presented in Figure 9. In the HEXTRAN core model, there are 163 fuel assemblies and core channels with 30 axial layers. The core channels are grouped together to 13 bigger channels in SMABRE model.

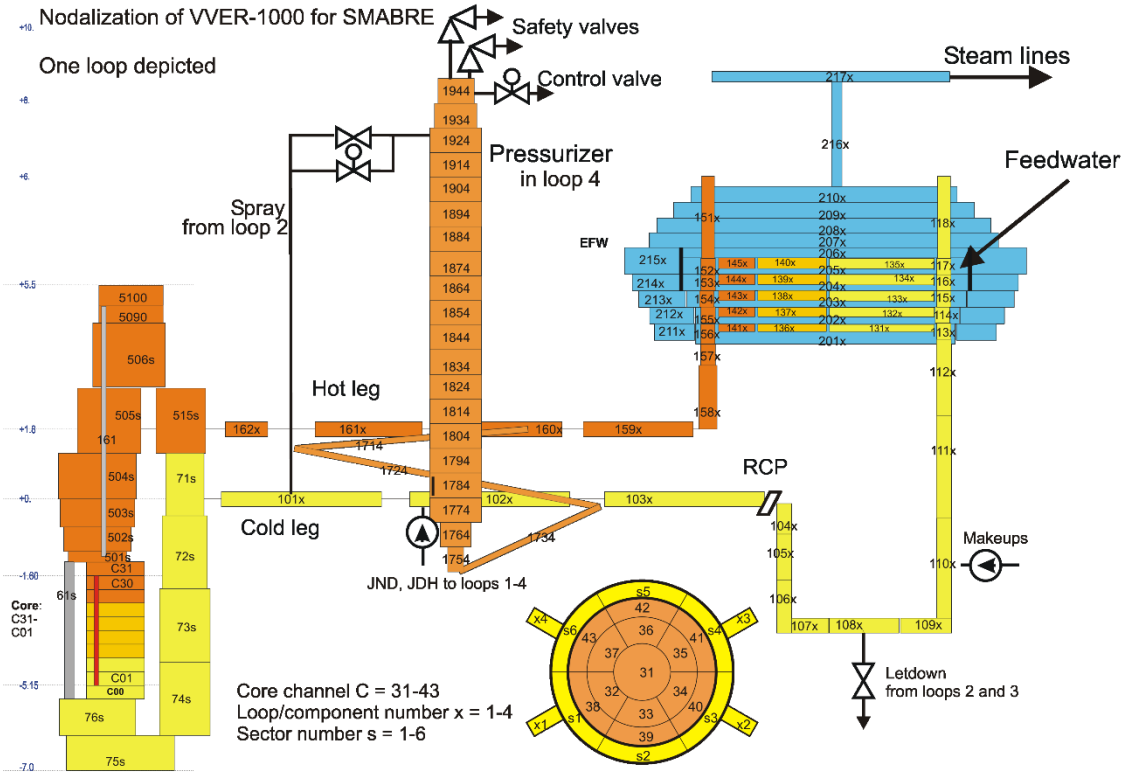

Figure 8. SMABRE nodalization of one VVER-1000 primary circuit loop (Syrjälahti 2018a).

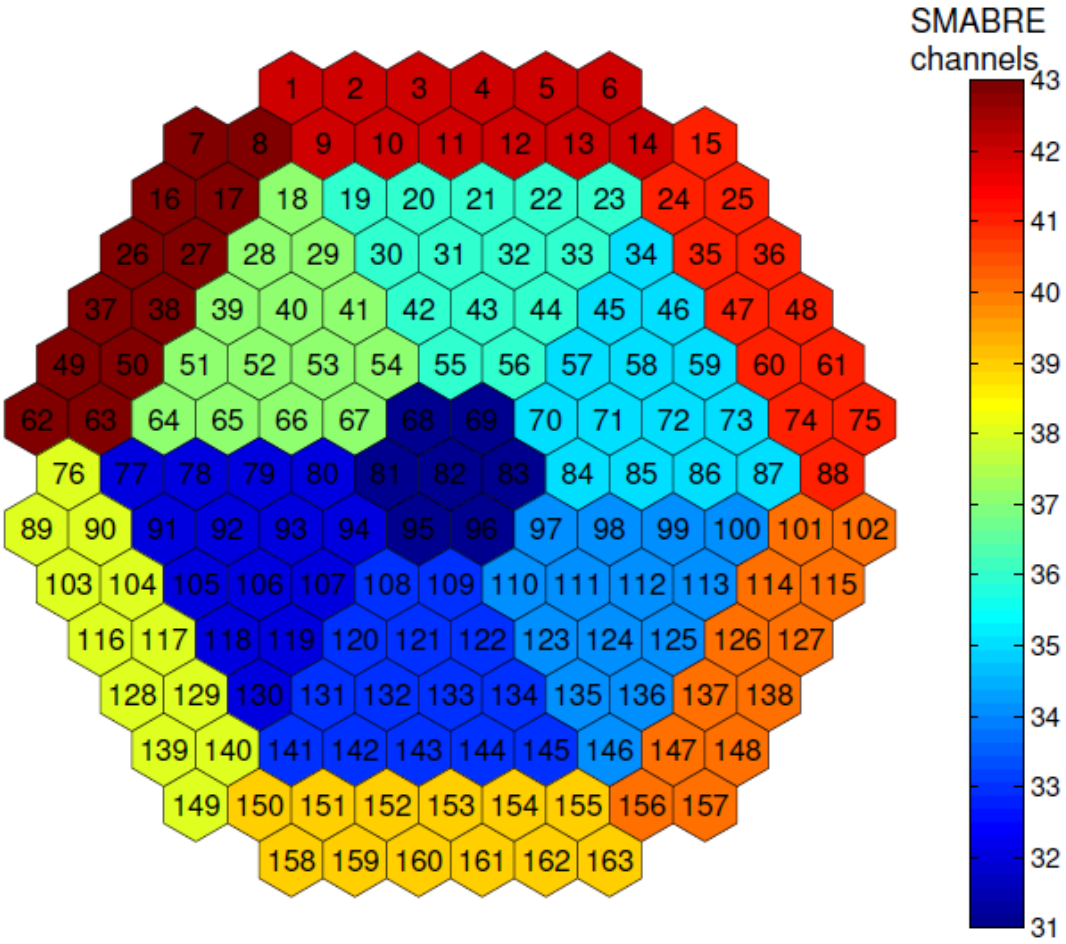

Figure 9. Core channels in HEXTRAN model and their grouping to channels in SMABRE model (Syrjälahti 2018a).

Neutronics data for the HEXTRAN model comes from a separate cross-section library file that contains group constant data for each material composition in the core. The Kalinin-3 benchmark team provided cross-section data for unrodded compositions, Boron carbide rodded compositions, and Dysprosium-Titanium rodded compositions, because the control rods are made of these two materials. In addition, the same files were provided for that sector of the core in which one faulty fuel assembly had been replaced earlier during the fuel cycle. This data was compiled into two cross-section files, one for each control rod material. (Syrjälahti 2018a) The file that contained Dysprosium-Titanium rodded data was used in the base simulation, because the part of the control rods that is inserted is Dysprosium-Titanium.

4.1.2 Kalinin-3 model for HEXTRAN

The HEXTRAN model used in the coupled calculations was modified for stand-alone HEXTRAN. Stand-alone HEXTRAN requires boundary conditions for pressure, enthalpy and mass flow, which are provided in a separate boundary condition file. The 13 thermal-hydraulic channel groups used with SMABRE were separated into 163 channels each with their own boundary conditions. The boundary condition file was compiled from data provided by the Kalinin-3 benchmark team. Only the outlet pressure was provided, so the inlet pressure was calculated by assuming constant pressure difference over the core. With these changes, the results with this model agree well with the HEXTRAN-SMABRE simulations.

4.2 TRACE

TRACE (TRAC/RELAP Advanced Computational Engine) is a general thermal-hydraulics code developed by U.S. Nuclear Regulatory Commission (USNRC). It is a product of combining USNRC's four main system codes: TRAC-P, TRAC-B, RELAP5 and RAMONA. TRACE is used to perform best-estimate analyses of different accidents and transients in NPP's. (U.S. Nuclear Regulatory Commission 2017) It is a well-known and much used code for safety analyses worldwide. Similar to SMABRE, TRACE can be coupled with three-dimensional reactor core models, such as PARCS, but at the moment it is used alone at VTT. In the future, it will be coupled with a new neutronics solver module Ants, that is currently being developed at VTT.

TRACE uses models for multidimensional two-phase flow, nonequilibrium thermo-dynamics, generalized heat transfer, reflood, level tracking, and reactor kinetics. The system is modelled by using components with different properties, for example pipes, heat structures and boundary condition components. The components can be further divided into cells over which the equations are averaged.

TRACE is used through SNAP (Symbolic Nuclear Analysis Package). SNAP provides a graphic user interface for editing and submitting the code and processing the results. SNAP has separate plug-ins for several analysis codes including TRACE as well as a plotting package AptPlot and uncertainty quantification tool DAKOTA, which are both utilized in this thesis. TRACE, SNAP and DAKOTA are all a part of USNRC's CAMP (Code Applications and Maintenance) program, in which VTT is participating.

4.2.1 VVER-1000 model for TRACE

VTT has received a VVER-1000 model for TRACE from Karlsruhe Institute of Technology. This model is modified from an old RELAP5 input and it is based on modelling the Bulgarian Kozloduy-6 NPP, which has the same design as Kalinin-3. Originally, this model was used with a coupled PARCS core model, but it can be used with stand-alone TRACE as well. The results have been compared to reference values given in benchmark specifications and the steady state achieved with the stand-alone TRACE coincides with the plant data. (Tóth 2015) Picture of this model as seen in SNAP is presented in Appendix 2 Figure 48. The figure shows the reactor pressure vessel and primary circuits with steam generators and pressurizer, and their nodalization. In addition to these, the model includes main steam lines out from the secondary side of the steam generators all the way to the turbine valves.

4.2.2 Changes to the model

The first step was to run the model at steady state, and some modifications were needed in order to succeed. The main coolant pumps in the model were not working properly: the code was not reading torque values even though the pumps were on. This caused a decrease in the mass flow through the core resulting in coolant temperature rising to a boiling point. This was corrected by adding the torque values to the input file manually. After this, some oscillation in the secondary circuit of the steam generator was observed. The gas and liquid velocities in some of the pipes were vibrating, which prevented the steady state calculations from converging. This problem was rectified by adding friction to the oscillating pipes: the resistance coefficient, K-factor, was changed from zero to 0.01, which steadied the fluid velocities. With these changes, steady state was reached and it was possible to move on to transient calculations.

This model was made to simulate a massive loss of coolant accident in the steam line of loop 4. Because of this, many changes had to be made in order to simulate the wanted MCP-1 switching off transient. In addition, changes in the reactor power caused by control rod insertion had to be modelled somehow, since there was no reactor dynamics code coupled to TRACE in these calculations.

At first, the break and all the control systems concerning the accident were removed. Subsequently, a trip, which switched off MCP-1 at t = 15s, was added. The starting time

of the transient was set on 15 seconds, allowing for a sufficient time in the beginning of the simulation for the system to stabilize. The ending time of the simulation was then set to t = 315s. When the pump trip is switched on, the motor torque of MCP-1 is reduced to zero, which eventually causes the pump to stop.

The changing power profile can be modelled in TRACE in a few different ways. The first option is to use a table, where power is given as a function of an independent variable, for example time. The second option is to use a point kinetics reactor model. The latter was used in this case. The point kinetics model in TRACE requires reactivity and delayed neutron groups at minimum, which were obtained from the input data for Kalinin-3 benchmark.

TRACE has a reactivity feedback model that calculates feedback reactivity based on fuel temperature, moderator temperature, gas volume fraction (void fraction) and boron concentration, and combines it with inserted control rod reactivity (U.S. Nuclear Regulatory Commission 2017). However, there was not enough information to use that model. Instead, total reactivity values, which have been calculated by the Kalinin-3 benchmark participants, were utilized in the model. The reactivity values were roughly approximated from the participants' results and fed to TRACE in a table. The used values are presented in Table 2. These values resulted in a satisfactory power profile, which was used in developing the model further. The axial power profile was not considered. A more detailed neutronics model is possible to achieve using the stand-alone TRACE, but for this thesis' purposes, a simplified version was enough. The goal was only to achieve a proper power profile in order to simulate the thermal-hydraulic phenomena in the primary circuit. In the future, neutronics and power generation for TRACE are modelled with a separate code and a more detailed core description is used for developing the model further.

Table 2. Used values of total reactivity as function of time.

Time after transient (s)	**Total reactivity**
0	0.0
1	-1.5E-4
10	-3.8E-4
70	-3.8E-4
80	-2.4E-4
90	-1.8E-4
100	-1.4E-4
105	-1.1E-4
120	-9.0E-5
130	-7.0E-5
140	-5.0E-5
150	-4.0E-5
200	-3.0E-5
240	-2.0E-5
290	-1.0E-5

Originally the primary pressure was kept constant in this model with a boundary condition component that was attached to the pressurizer. The pressurizer is depicted in Figure 10 and the pressure boundary condition component, BREAK 506, is attached to the top of the column. However, during this transient, the pressure and pressurizer water level change. The boundary condition can be removed by inserting a valve between the boundary condition component and pressurizer (Tóth 2015). According to the model report there was supposed to be this kind of valve in the model but it was missing. The valve was inserted between the BREAK 506 component and the pressurizer according to the model report parameters, and it was set to close at the beginning of the transient so that the pressure would decrease. When the pressure is low enough, heaters activate thus increasing the pressure again to a normal level. The cooling spray is not used during this transient and therefore it is not modelled.

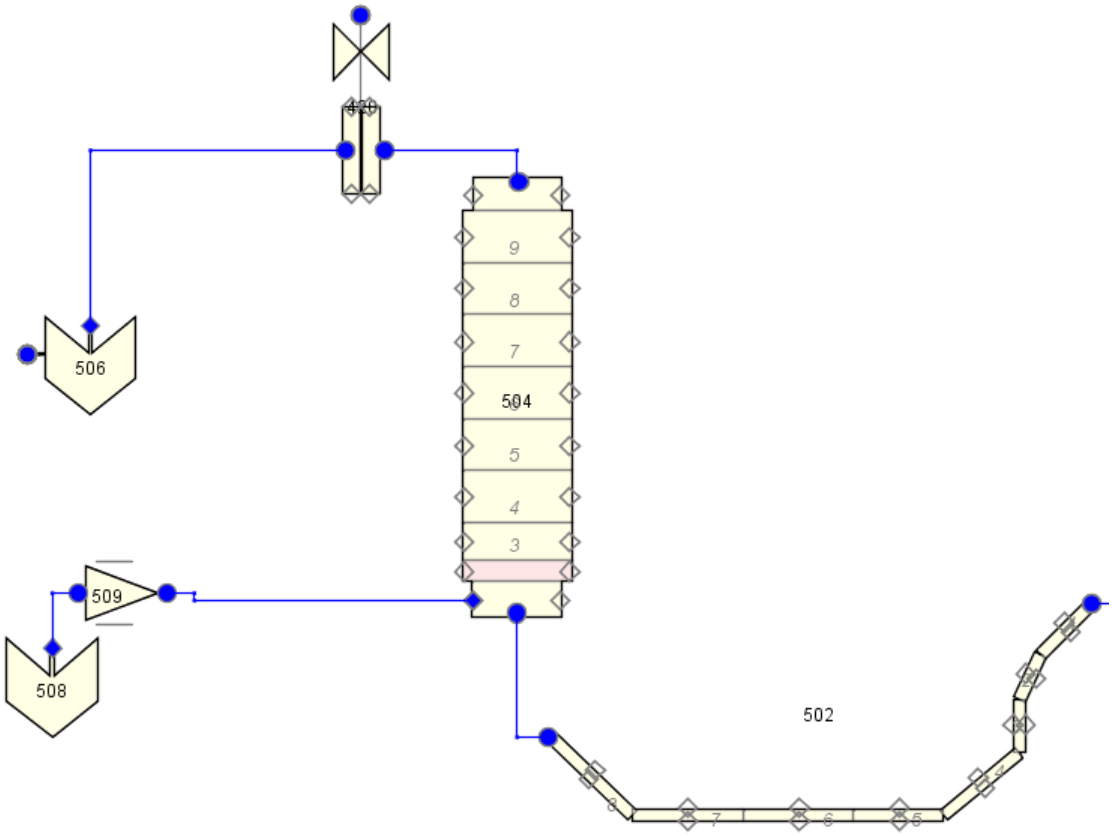

Figure 10. Pressurizer in TRACE model. Attached to the top the pressurizer column is the boundary condition component, BREAK 506, and the inserted valve.

Some modifications were needed in the secondary circuit as well. Pressure in the steam lines and the feedwater flow to steam generators was defined to remain constant with boundary condition components. Similarly to the primary pressure, secondary pressure and feedwater flows change during this transient. Pressure in the secondary loop affects heat transfer in the steam generator, which then again affects temperature in the primary loop. Considering the uncertainty analysis, it was important to remove the boundary conditions and add control systems to the secondary side.

The steam line leading to turbines, depicted in Figure 11, was modified in each loop. As seen from the picture, first, there is a main steam isolation valve, which is not used in this model, and then a turbine valve before the BREAK component. A control system was added to turbine valves so that the valve flow area changes linearly in relation to the pressure of the preceding pipe component. The BREAK component was changed so that instead of setting a boundary condition to the pressure, its pressure changes according to the preceding component.

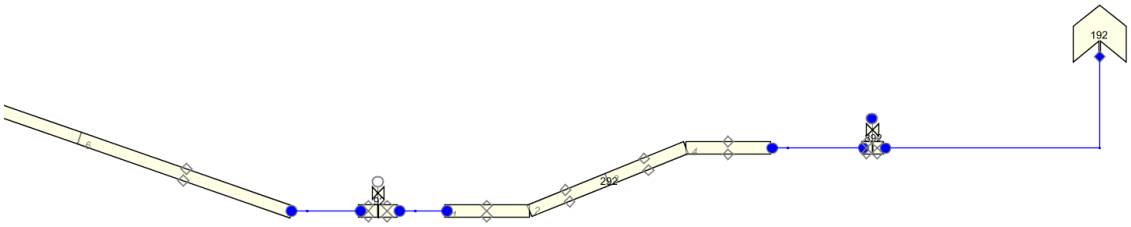

Figure 11. Steam line, main steam isolation valve and turbine valve in one loop of the TRACE model.

The other change on the secondary side considered feedwater flow. Originally, the flow was kept constant, which meant that the water level in the steam generators rose during the transient, which is not realistic behaviour. A control system was added, so that the feedwater flow is controlled by SG water level. With this change, SG water level in loops 2-4 behaved similarly to measurements, but in loop 1 it did not. Finally, loop 1 feedwater flow was set as a boundary condition which changes as a function of time. This enabled the right kind of behaviour in SG 1 water level.

Changes to the secondary side affected pressure in the primary circuit causing it to drop to a much lower level than it is supposed to. Originally, the pressure was adjusted so that the pressure behaviour in the lower plenum of RPV follows the primary pressure given in the Kalinin-3 benchmark specifications. However, the measurement is more likely from the upper plenum of the RPV, which means that the pressure is too low in the TRACE model overall due to the pressure drop over core. This was changed so that the initial pressure in the upper plenum matches the primary pressure given in the benchmark specifications, which increased the pressure overall to a level that matched the measurements better.

The results with these changes were similar to HEXTRAN-SMABRE model and measurements from the actual transient. In Figure 12 is shown the total reactor power calculated with TRACE and HEXTRAN-SMABRE models and measurement from the actual transient. Figure 13 shows the pressure measurement and calculation results from both codes in the pressurizer (PRZ) and above the reactor core. At this point it was decided that the model is good enough for the uncertainty analysis.

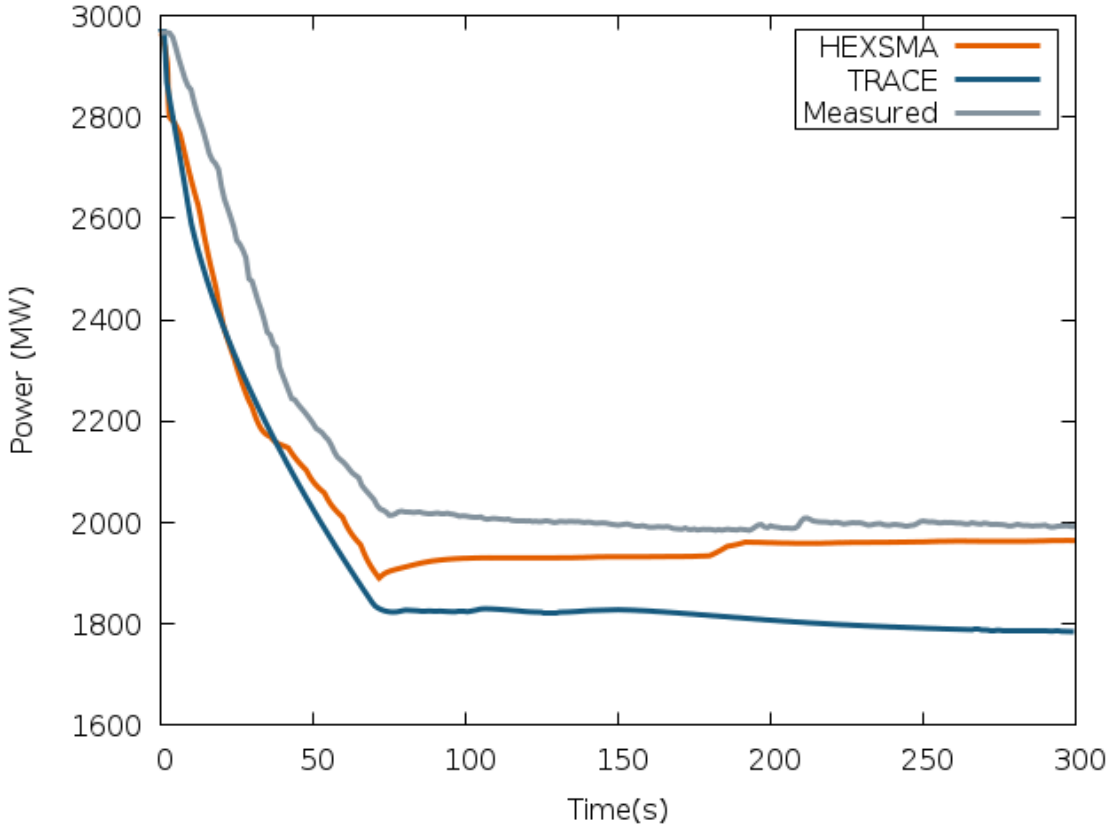

Figure 12. Total reactor power measurement and calculation results with HEXTRAN-SMABRE and TRACE.

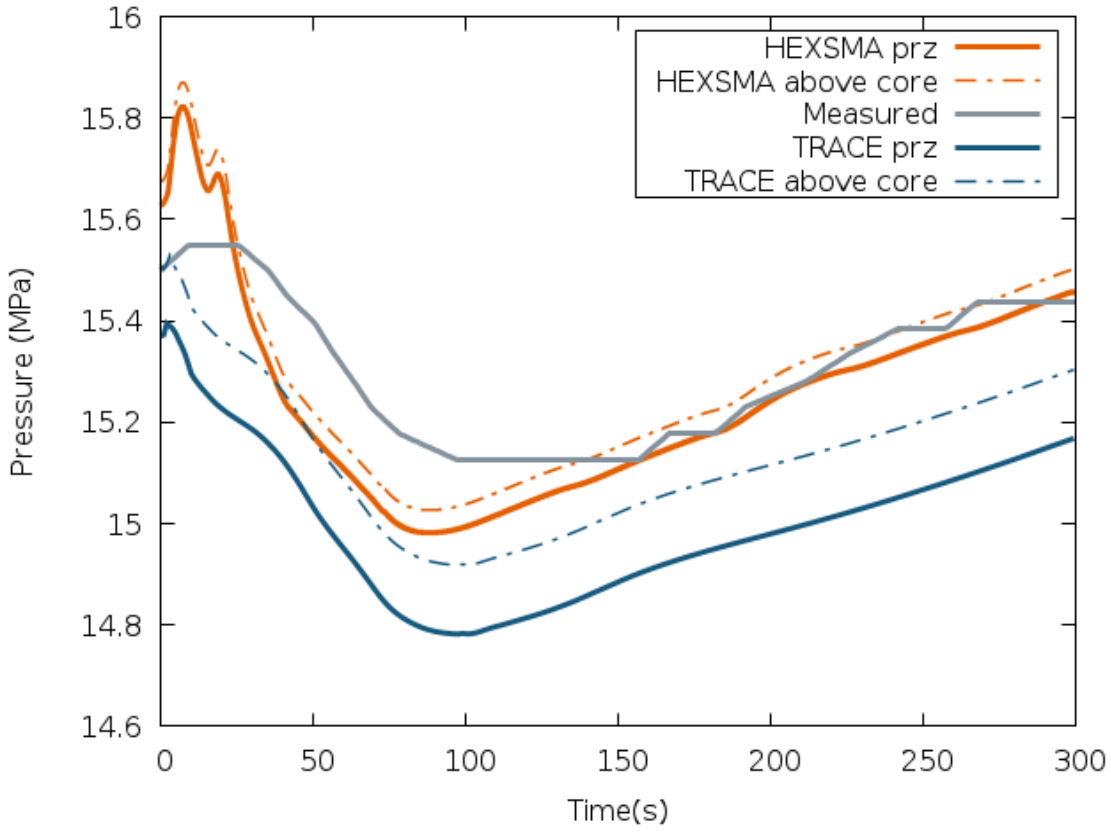

Figure 13. Primary pressure measurement and calculation results from pressurizer and above reactor core with HEXTRAN-SMABRE and TRACE.

5 SENSITIVITY RUNS

In this chapter, the used sensitivity analysis tools and parameter variations for each case are presented. Before the sensitivity analysis runs, it is important to know the capabilities of the used tool. That affects what kind of parameter variations are possible. The UAM benchmark specification worked as a guideline when the parameter variables were decided on. In addition to that, knowledge about the used models and previous studies helped recognizing the sources of uncertainty.

5.1 Tools for sensitivity analysis

Both HEXTRAN-SMABRE and TRACE have their own tools for uncertainty and sensitivity analysis. Both of the tools are introduced more in detail in the following chapters. VTT's own sensitivity analysis tool needed some changes and upgrades, which are described below as well.

5.1.1 VTT's tool for sensitivity analysis

The development of VTT's tool for uncertainty and sensitivity analysis for reactor dynamics codes – a Perl script *sensla_q2_xs2_bc.pl*, later referred to as Sensla – started in 2004. Sensla automatizes doing several calculation runs, which had been laborious before when each run had to be done separately. The program generates input parameter values and inserts them into the input files, thus applying a Monte Carlo method. Once the simulations are completed, the program performs statistical analyses and plots the results. Statistical measurements used are RCC, Kendall's tau and PRCC. (Syrjälahti 2005) Sensla can be used for both TRAB3D-SMABRE and HEXTRAN-SMABRE calculations (Syrjälahti 2008).

Several changes were made to Sensla. Now it can be used for stand-alone HEXTRAN calculations whereas it was before only applied for coupled calculations. For stand-alone HEXTRAN, a separate boundary condition file is needed. The user can choose to use the same file in every run or apply variations, in which case the program generates a separate boundary condition file for each run. At the moment, this feature works only for this Kalinin-3 model, for which a new boundary condition file tool was made. A

Python script *k3bcconv.py* reads values from two separate data files provided by the benchmark team and writes them into one boundary condition file.

In 2018, Sensla was modified so that it was possible to use a different cross-section file in every run. For that, one SMABRE initialization run was done which was then used in all of the simulations. (Syrjälahti 2018b) Now the work was continued and it was made possible to do a separate SMABRE initialization for each run and modify the HEXTRAN and SMABRE input files simultaneously with cross-section file variations. Some changes were needed for the post-processing of SMABRE results, since the programs have changed since the last use. An interactive program *smblist_lin*, which creates an .f17 file that can be used for plotting, was automatized so that it, *smblist_auto*, can be used inside Sensla. Now Sensla also asks whether the SMABRE post-processing is executed in the case that sensitivity measure calculations and plotting is done separately.

PRCC calculation had been added to Sensla earlier but it had not been used or verified. Now the calculation procedure was checked and modified. The formula works, when sample size is big enough and correlations are not too strong ($<|0.8|$). The algorithm loops formula (4) from chapter 3.5.2 until the correlation of all other variables has been reduced from the RCC between analysed output and input variables. The correlation between input variables is not taken into account.

In order to do a sensitivity analysis for coupled HEXTRAN-SMABRE, Sensla needs to be run three times: first the SMABRE initialization, then the coupled HEXTRAN-SMABRE transient calculations, and finally calculating the sensitivity measures and plotting. For stand-alone HEXTRAN two runs are enough. In the future some changes could be made so that only one run is needed. The most time consuming part is the calculation of sensitivity measures and plotting. This can be controlled by managing the amount of output variables that SMABRE writes to the output files. Also plotting for radial values in the .dissla file was coded, but since it takes the most time and brings little value to interpreting of the results, it was left out of the procedure.

5.1.2 DAKOTA

Uncertainty and sensitivity analysis runs for TRACE can be made easily through SNAP, which has a plug-in for the uncertainty analysis tool DAKOTA. DAKOTA (Design and

Analysis Toolkit for Optimization and Terascale Applications) is a toolkit for design optimization, parameter estimation, uncertainty quantification, and sensitivity analysis developed in Sandia National Laboratories (Adams et al. 2018).

The uncertainty and sensitivity analysis runs are defined in SNAP via an Uncertainty job stream, which is presented in Figure 14. The job stream is submitted to a calculation server, where the stream steps are performed in a defined order. The first block, the TRACE model, includes all input files for different runs with varied parameters. The second block does the TRACE steady-state calculations with each input. After that, transient calculations can be made as restart runs from the steady states. In the Extract Data block, selected results are extracted from TRACE output files and fed to DAKOTA uncertainty calculations in the last block. DAKOTA creates a report from the sensitivity calculations with tables and plots about the results. With AptPlot step the wanted results are plotted in a user defined format.

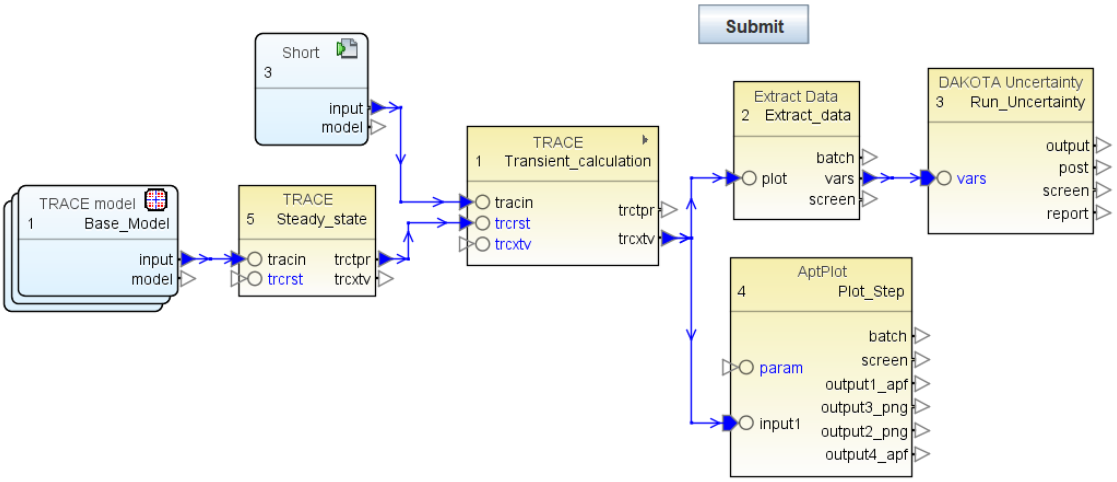

Figure 14. Uncertainty job stream in SNAP.

When defining the Uncertainty stream, the user selects the varied parameters from a list. The possible sources of uncertainty are boundary conditions, general tables, and modelling uncertainties, which includes adding sensitivity coefficients to the model. A distribution is created for each parameter with a user defined variance or minimum and maximum values. The distribution can be normal, lognormal, uniform, loguniform, triangular, exponential, beta, gamma, gumbel, frechet, Weibull or user-defined histogram. DAKOTA uses the Monte Carlo or Latin Hypercube sampling techniques to get values for the variables from the created distributions. The number of samples can be calculated with the Wilks's formula or decided arbitrarily.

The user defines which output parameters are selected for sensitivity calculations. Either the minimum or maximum values or values at a certain time step are used. DAKOTA calculates simple, partial, rank, and partial rank correlation coefficients between these output values and all input variables. The user may select how extensive the report is that DAKOTA writes as an output.

5.2 Uncertainty parameter variations

NEA's UAM benchmark defines three types of input uncertainties for system modelling: neutronics, fuel modelling and thermal-hydraulic input uncertainties. Neutronics uncertainties for these simulations come from two-group cross section libraries provided by the benchmark team. Fuel modelling uncertainties include boundary conditions, fuel rod geometry, and heat transfer parameters from fuel to coolant. Respectively, thermal-hydraulics input uncertainties include boundary conditions, geometry, and modelling uncertainties. (Hou et al. 2019a)

The benchmark team provides some variations for core calculations, but there are yet no specific instructions concerning other variables. At the moment, it is left to participants to decide on the used variations. In this thesis, some variations come from references and others were decided arbitrarily based on knowledge about the code. Sensitivity runs were done for stand-alone HEXTRAN (core multi-physics), HEXTRAN-SMABRE (coupled core/system) and TRACE (system thermal-hydraulics).

5.2.1 HEXTRAN

Input uncertainties for the UAM benchmark Phase III core calculations come from output uncertainties of Phase II. Neutronics uncertainties for HEXTRAN and HEXTRAN-SMABRE simulations come from the cross-section library data provided by the benchmark team. It consists of 500 cross-section files including all neutronics uncertainties calculated in the second phase of the benchmark. A cross-section file for each run was chosen randomly from this library, since the number of files was larger than the number of simulations.

Same variations for the boundary conditions – pressure, flow rate and inlet coolant temperature – were used as given in the UAM benchmark Phase II specification (Hou et al. 2019b, p. 81). Inlet coolant temperature is given as enthalpy in HEXTRAN input, so

the temperature values were converted when making the boundary condition file and uncertainty was added after that. Variations for power and power distribution were given also in the benchmark specification, but because it is not possible to change the power distribution in HEXTRAN input, only the initial power was varied.

Fuel, cladding and gas gap (the space between fuel and cladding) conductance deviations were calculated from the Phase II results and given in the UAM benchmark Phase III specification. Gap conductance uncertainty was said to be 20-22 % (Hou et al. 2019a, p. 6), but even bigger variations have been used before at VTT, for example values between 0.68 and 1.98 by Langenbuch et al. (2005). Geometry variations for the Phase III were not specified, but distributions for fuel and cladding inner and outer radius were used, since there are actual manufacturing tolerance limits to these values. There was also some ambiguity about rod geometry in the benchmark data, and the one differing fuel assembly was not considered in the input file, so the fuel geometry was considered as a one source of uncertainty. Variations for fuel rods were taken from research previously done at VTT by Syrjälahti (2011). In addition to these, control rod worth was selected as one source of uncertainty. Control rod groups 9 and 10 are the ones working during this transient, so their worths were given a distribution according to studies previously done at VTT (Langenbuch et al. 2005).

The varied parameters and their distributions are presented in Table 3. The variable type can be scalar, factor, or additive, depending on whether the initial value is replaced, multiplied, or added to the generated value. In stand-alone HEXTRAN, some of the varied parameters were in the input file and some in the boundary condition file.

Table 3. Varied parameters in the HEXTRAN sensitivity runs.

Parameter name	**File**	**Type**	**Distribution**	**Distribution**	**Reference**
System pressure	bc file	scalar	± 2.0 %	normal	(Hou et al. 2019b)
Flow rate	bc file	scalar	± 4.5 %	normal	(Hou et al. 2019b)
Inlet fluid enthalpy	bc file	scalar	± 2.0 %	uniform	(Hou et al. 2019b)
Power	input	factor	± 0.3 %	normal	(Hou et al. 2019b)
Control rod worth	input	factor	0.8, 1.0, 1.1	triangular	(Langenbuch et al. 2005)
Gas gap conductivity	input	factor	± 22 %	uniform	(Hou et al. 2019a)
Fuel conductivity	input	factor	± 7 %	normal	(Hou et al. 2019a)
Cladding conductivity	input	factor	± 5.5 %	normal	(Hou et al. 2019a)
Fuel outer radius	input	scalar	± 0.01 mm (0.3%)	normal	(Syrjälahti 2011)
Clad inner radius	input	scalar	± 0.0175 mm (0.5%)	normal	(Syrjälahti 2011)
Clad outer radius	input	scalar	± 0.025 mm (0.5%)	normal	(Syrjälahti 2011)
Fuel inner radius	input	scalar	± 0.05 mm (4.3%)	normal	(Syrjälahti 2011)

5.2.2 HEXTRAN-SMABRE

With the coupled HEXTRAN-SMABRE, two scenarios were analysed. In the first considered scenario (Scenario 1), the HEXTRAN input uncertainty parameters for the coupled HEXTRAN-SMABRE runs were the same as in the stand-alone HEXTRAN runs, excluding the boundary condition and power variations. Since there were yet no guidelines in the UAM benchmark specifications about which system code thermal-hydraulic parameters should be varied, expert judgement was used when deciding variations in the SMABRE input.

The most important source of uncertainty in this case is the main coolant pump. Because this is a pump transient, it plays a significant role in the thermal-hydraulic system modelling. The information given about the homologous pump curves, which

define the pump behaviour, in the V1000CT-1 benchmark specifications is ambiguous. There are three different set of values given for the head and torque curves: one in table form, second in figures, and third in example RELAP3 input (Ivanov et al. 2002, p. 93-94, 101-102, 165-171). It is also unclear, how long it takes for the pump to stop, since there was contradictory information about that as well (Ivanov et al. 2002, p. 29, 92). This uncertainty was resolved by using different sets of homologous pump curves as options in the sensitivity runs. In addition to the three pump curves given in the specification, an old curve from the SMABRE input and the one used in TRACE input were used as options as well.

There are no boundary conditions in the SMABRE runs, so it is not possible to add uncertainty to those. However, primary pressure is controlled with a pressurizer, which has several sources of uncertainty. The pressurizer heater power and set point limits were varied using engineering judgement about the possible variation limits. According to Glaeser (2008), uniform distribution should be used unless there is justification why some other distribution should be applied.

After the MCP-1 is switched off, mass flow in loop 1 is reversed, which may cause some modelling errors in, for example, heat transfer in the steam generators. Heat transfer in a SG is affected by the water level, which is again controlled by the feedwater flow to the SG. Since there is no actual water surface because of boiling, the water level measurement is only an approximation based on measured pressure differences. Some uncertainty was added to the feedwater control limits, which may have some effect on the heat transfer and therefore temperature in the whole loop. The pressurizer water level has ±0.15 m tolerance limit in the design values, which was used as the uncertainty range in this case as well (Tóth 2005).

As there are not many input uncertainties in the system model, a more severe scenario (Scenario 2) was developed, where some of the control systems might not be working in addition to the variations in the first scenario. A few control mechanisms were selected to have an option to be on or off during the transient. A lock, which prevents MCP's from rotating backwards, is usually on. If the lock is not working and the pump starts to rotate backwards after the flow is reversed, it has an effect on the mass flow through it. In Scenario 2, this lock has an option to be on or off, as well as the pressurizer cooling spray, which is normally on, and make-up and letdown flows, which are normally off in

this model. The varied parameters and their distributions for both scenarios are presented in Table 4. Scenario 2 includes all the parameters from Scenario 1 in addition to the on/off settings.

Table 4. Varied parameters in HEXTRAN-SMABRE sensitivity runs.

Parameter name	**Input file**	**Type**	**Deviation**	**Distribution**	**Reference**
Scenario 1					
Control rod worth	HEXTRAN	factor	0.8, 1.0, 1.1	triangular	(Langenbuch et al. 2005)
Gas gap conductivity	HEXTRAN	factor	± 22 %	uniform	(Hou et al. 2019a)
Fuel conductivity	HEXTRAN	factor	± 7 %	normal	(Hou et al. 2019a)
Cladding conductivity	HEXTRAN	factor	± 5.5 %	normal	(Hou et al. 2019a)
Fuel outer radius	HEXTRAN	scalar	± 0.01 mm (0.3%)	normal	(Syrjälahti 2011)
Clad inner radius	HEXTRAN	scalar	± 0.0175 mm (0.5%)	normal	(Syrjälahti 2011)
Clad outer radius	HEXTRAN	scalar	± 0.025 mm (0.5%)	normal	(Syrjälahti 2011)
Fuel inner radius	HEXTRAN	scalar	± 0.05 mm (4.3%)	normal	(Syrjälahti 2011)
Pump curve	SMABRE	scalar	5 options	discrete	(Ivanov et al. 2002)
PRZ heater power	SMABRE	scalar	± 8.0 %	uniform	
PRZ heater upper limit	SMABRE	additive	± 0.1 MPa	uniform	
PRZ heater lower limit	SMABRE	additive	± 0.05 MPa	uniform	
Feedwater limits	SMABRE	additive	± 0.15 m	uniform	
Scenario 2					
Pump lock	SMABRE	scalar	on/off	discrete	
PRZ spray	SMABRE	scalar	on/off	discrete	
Make-up	SMABRE	scalar	on/off	discrete	
Letdown	SMABRE	scalar	on/off	discrete	

5.2.3 TRACE

The varied parameters for the TRACE uncertainty runs were selected based on, first of all, which parameters it is possible to vary in TRACE, and secondly, which parameters were varied in the HEXTRAN-SMABRE runs. Pressure boundary condition, initial power, heater power, and gas gap, fuel and cladding conductivity coefficients were varied like in the HEXTRAN and SMABRE models. The other variables were built-in sensitivity coefficients, which were selected based on expert judgement about the case. Liquid-to-wall and vapor-to-wall heat transfer coefficients (HTC) and wall drag are the only ones that affect this case because the transient is mild and there is no boiling in the core. Distributions for these were taken from a thesis by Mui (2015). HTC for heat loss from cold and hot legs was given as a General table in this model, which makes it possible to vary that as well. Accuracy of 24 % was used (Porter et al. 2015). All the varied parameters and their distributions are presented in Table 5.

Table 5. Varied parameters in TRACE sensitivity runs.

Parameter name	**Type**	**Deviation**	**Distribution**	**Reference**
Gas gap conductivity	factor	± 22 %	uniform	(Hou et al. 2019a)
Fuel conductivity	factor	± 7 %	normal	(Hou et al. 2019a)
Cladding conductivity	factor	± 5.5 %	normal	(Hou et al. 2019a)
PRZ pressure	scalar	± 2.0 %	normal	(Hou et al. 2019a)
Liquid-wall HTC	factor	± 15 %	uniform	(Mui 2015)
Vapor-wall HTC	factor	± 20 %	uniform	(Mui 2015)
Wall drag	factor	± 5 %	uniform	(Mui 2015)
Heat loss HTC	factor	± 24 %	normal	(Porter et al. 2015)
Power	factor	± 0.3 %	normal	(Hou et al. 2019a)
PRZ heater power	factor	± 8.0 %	uniform	

The options for variations in the TRACE model were limited. Variations to the input file can be done only through boundary conditions (BREAK and FILL components), numerics and general tables. Since there are not many of those in this model, most of the used variables were sensitivity coefficients. Traditional Monte Carlo sampling was used, so that the method is as similar to Sensla as possible.

6 RESULTS

Two runs were made for each HEXTRAN and coupled HEXTRAN-SMABRE calculations: one where the cross-section file was varied from the cross-section library files and one with the same cross-section file for all runs. In this way the correlation coefficients of parameter variations could be calculated without the influence of cross-section variations, since the changes caused by them could not be calculated numerically. Lower and upper limits and standard deviations were taken from cross-section runs because they cause a much higher variance in the results. The effect of cross-section files can be quantified by comparing the standard deviations between runs with and without them. The plots are all from runs with the varied cross-section files.

In the next chapters, results from all the runs are presented in outline. The exact values for the minimum and maximum values, standard deviations, and sensitivity measures are tabulated in Appendix 3. The values are from last calculated time step, when the system has usually been stabilized. Standard deviation for HEXTRAN and HEXTRAN-SMABRE runs are given for both runs with and without the cross-section file variations for comparison. The sensitivity measures used in the results are RCC for HEXTRAN, SMABRE and TRACE calculations and PRCC only for TRACE. Kendall's tau was calculated in all Sensla calculations, but because the results are the same as RCC, they are not discussed further. The number of simulations with HEXTRAN and HEXTRAN-SMABRE was 95, which is slightly more than needed in case some of the runs fail. The number of simulations with TRACE was 93.

6.1 HEXTRAN

In this chapter the results from the stand-alone HEXTRAN runs are discussed. The exact values for mean, minimum, and maximum values and standard deviations (SD) for all output variables are gathered in Appendix 3 Table 6 and RCC values in Table 7. If the results from runs with and without the cross-section (XS) file variations are compared, it can be seen that SD is more or less the same or higher with the cross-section file variations in all outputs. The maximum values are the same or higher in the cross-section file variation runs in every output.

The distribution in the time-dependent fission power results in the stand-alone HEXTRAN runs was quite wide but the behaviour stayed the same in all runs with the power decreasing to 74-81 % of its initial value. Total fission power throughout the transient from all runs is presented in Figure 15 along with lower and upper limits inside which 95 % of the runs fall into with 95 % confidence. The rank correlation coefficients for total power are shown in Figure 16. Inlet water temperature had the strongest correlation with total power, RCC being close to -1. Also the gas gap conductance and cladding inner radius had a significant correlation with the power output.

The maximum assembly-wise peaking factor – meaning the highest power output in a fuel assembly in relation to the average power output in all assemblies – stayed roughly the same throughout the transient (Figure 17). RCC's for the maximum assembly-wise peaking are presented in Figure 18. The maximum fuel temperature decreased as the power decreased during the transient (Figure 19). RCC values for fuel temperature are shown in Figure 20. Both fuel temperature and assembly-wise peaking had the strongest correlation with inlet water temperature and gas gap conductance.

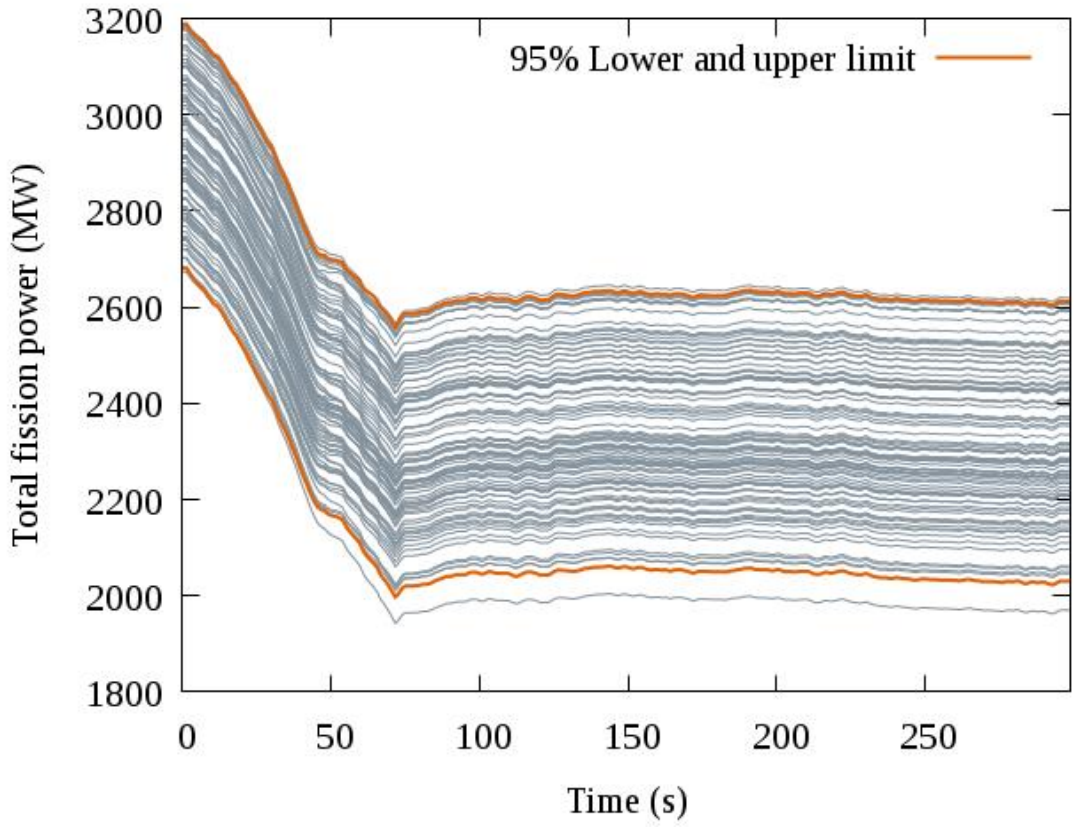

Figure 15. Total fission power in all HEXTRAN runs and 95 % lower and upper limits.

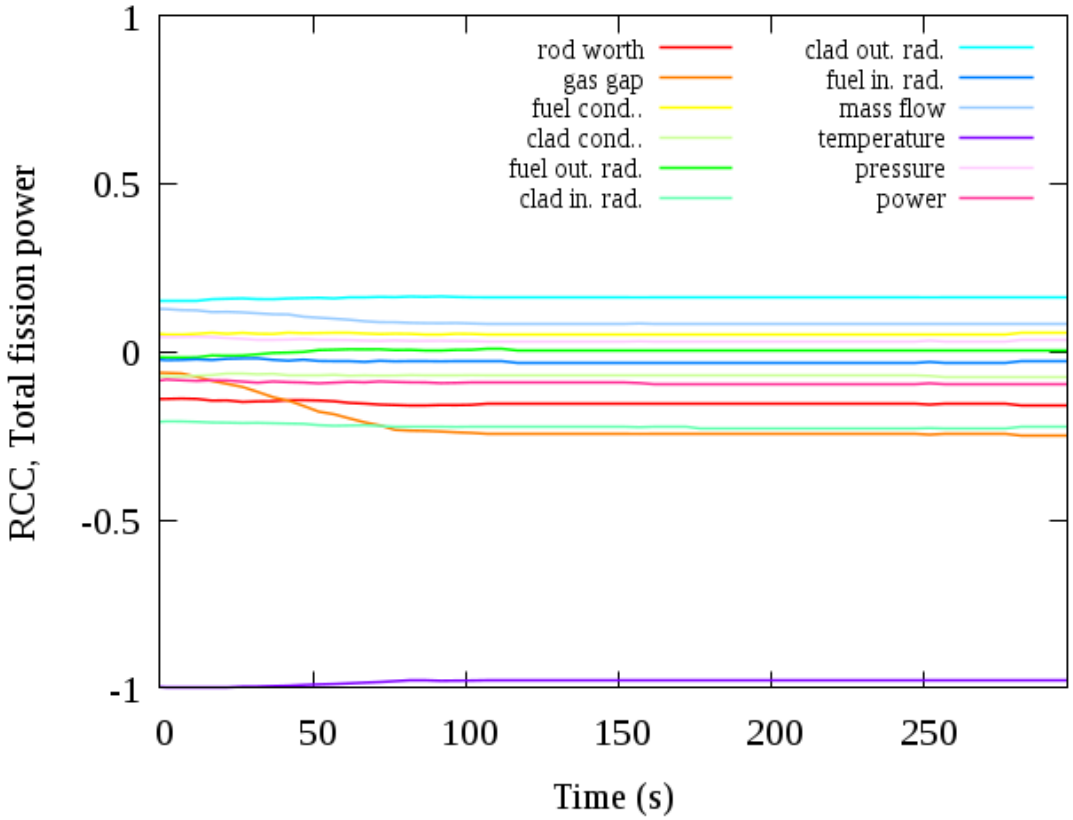

Figure 16. Rank correlation coefficients for total fission power during the transient in HEXTRAN simulations.

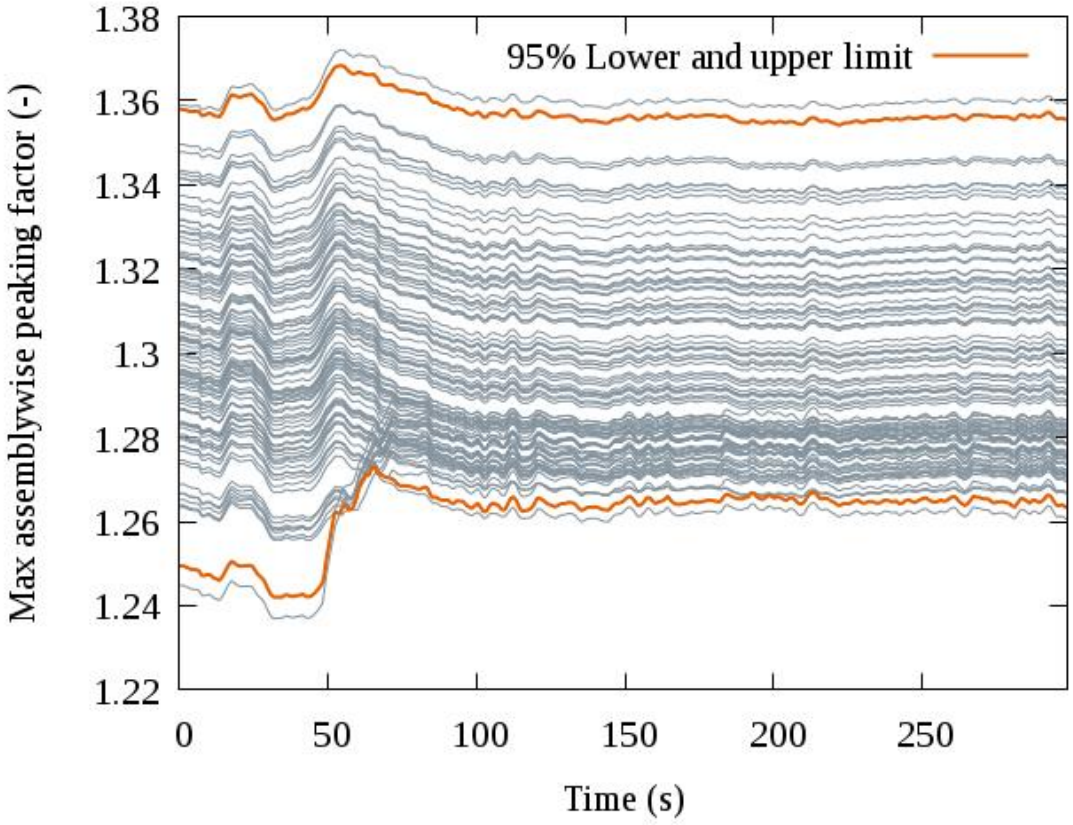

Figure 17. Maximum assembly-wise peaking factor in HEXTRAN simulations.

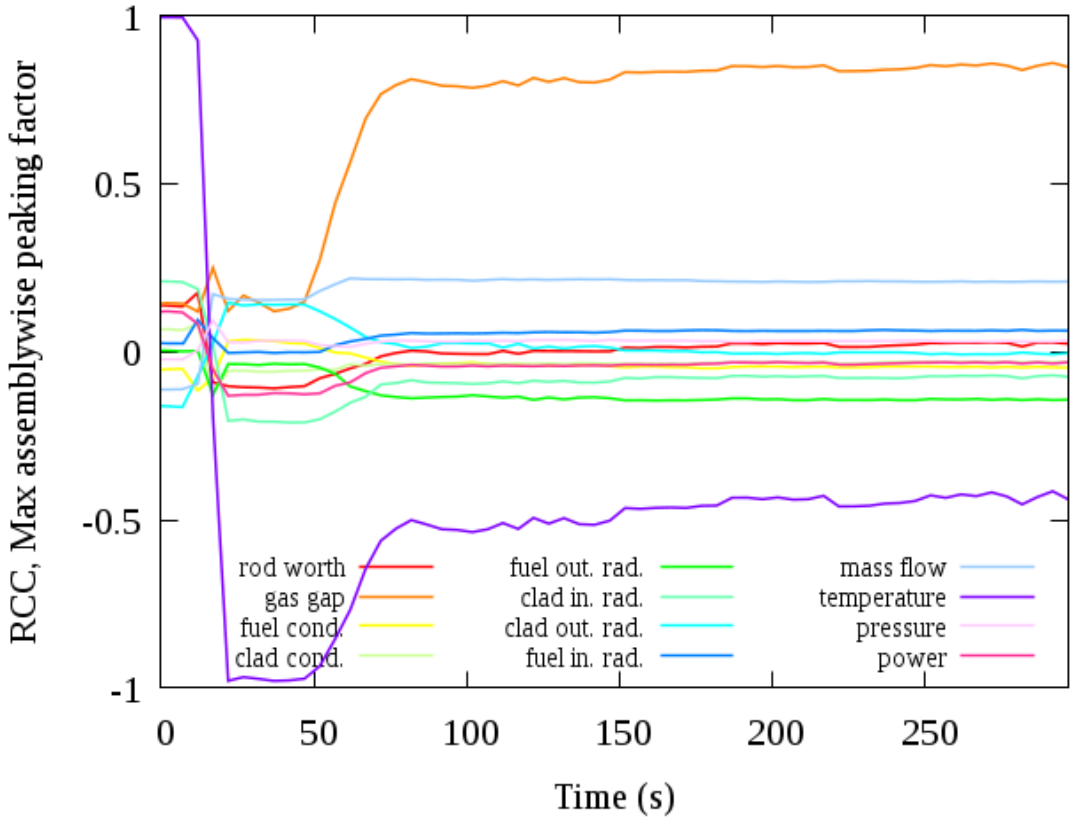

Figure 18. Rank correlation coefficients for maximum assembly-wise power peaking in HEXTRAN simulations.

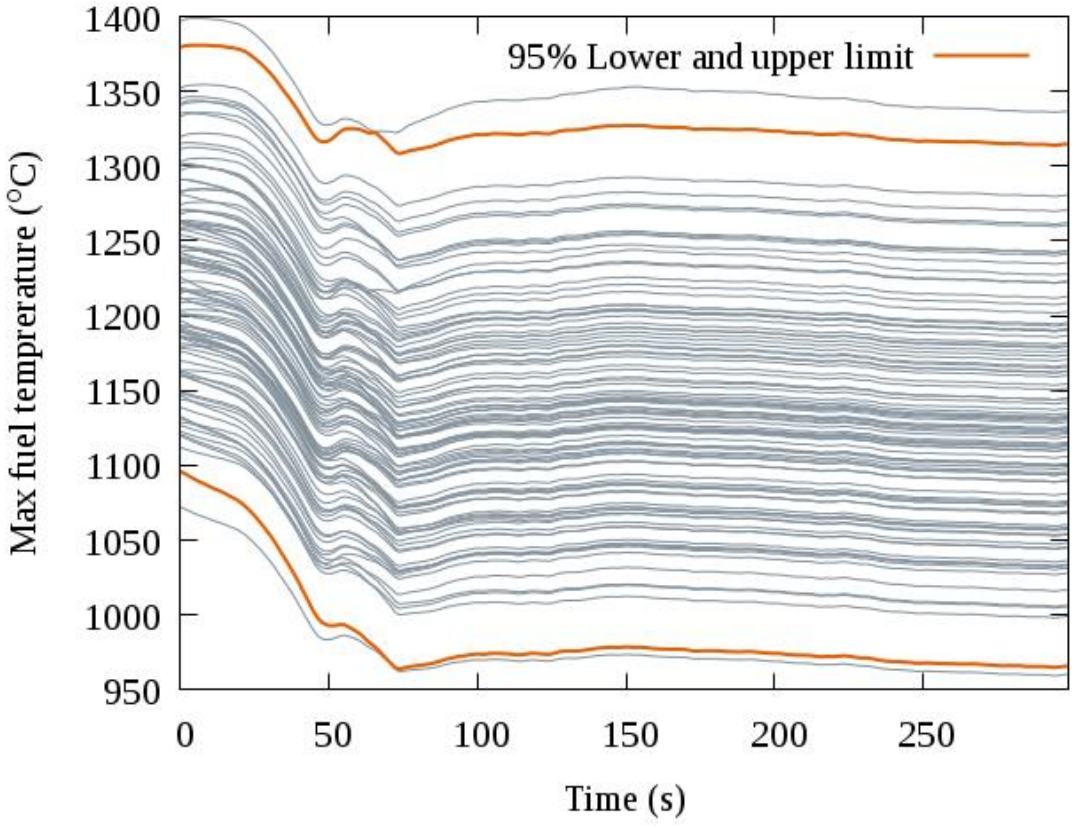

Figure 19. Maximum fuel temperature during transient in HEXTRAN simulations.

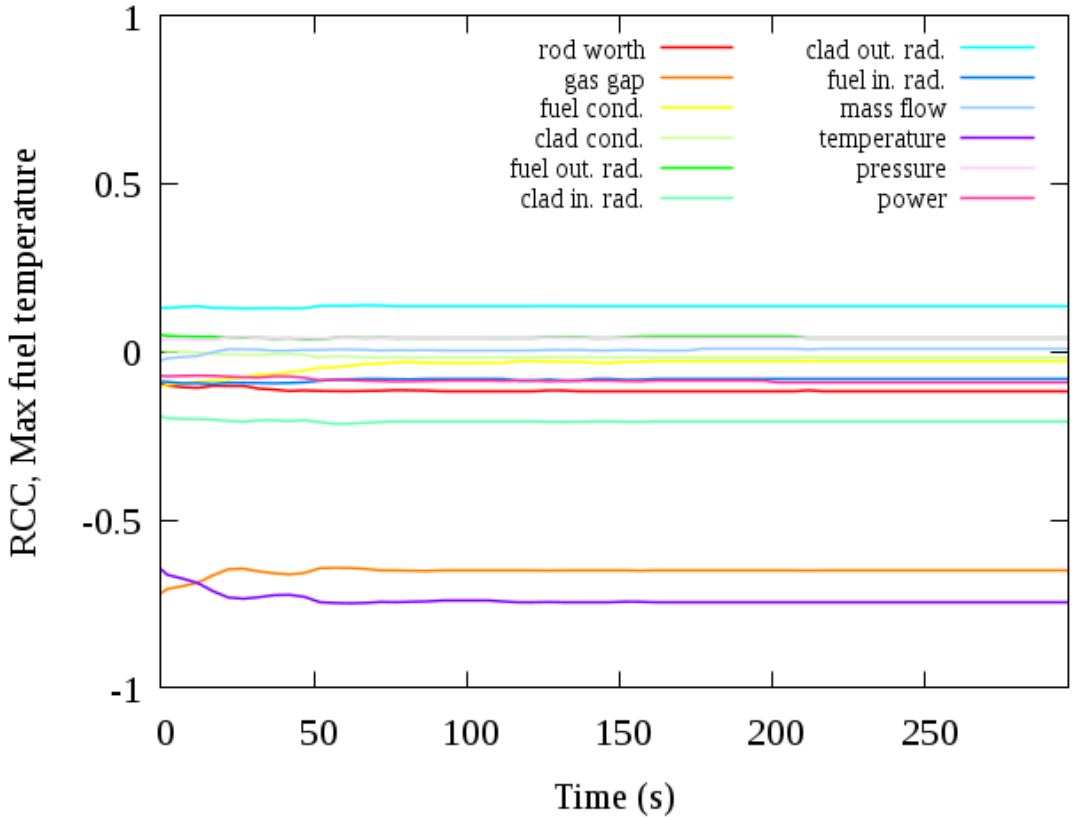

Figure 20. Rank correlation coefficients for maximum fuel temperature in HEXTRAN simulations.

Whole core mass flow, inlet water temperature, and pressure were given to HEXTRAN in a boundary condition file, so their behaviour was not calculated. Therefore the parameter variations affected directly the corresponding output. Core mass flow, mean water temperature, and outlet pressure during the transient are presented in Figures 21, 22 and 23, respectively. After MCP-1 is switched off, core mass flow as well as the water temperature naturally decreases. Pressure first decreases and then increases again close to its initial level.

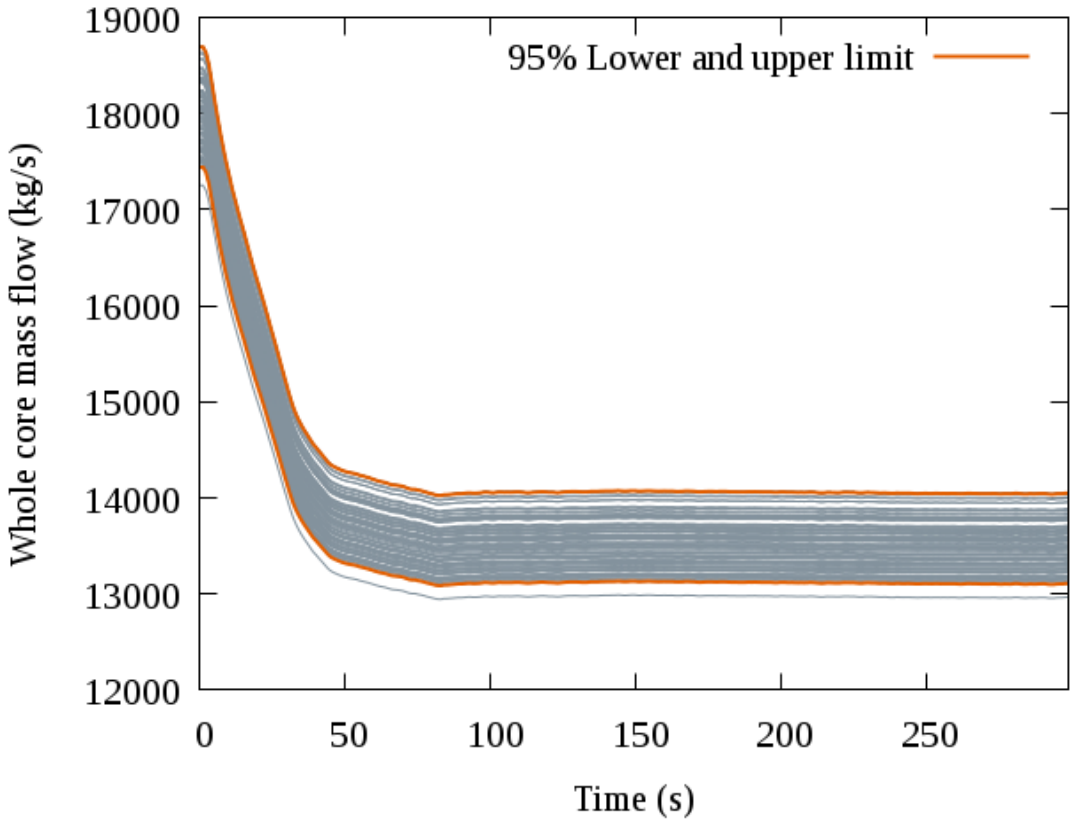

Figure 21. Mass flow through reactor core in HEXTRAN simulations.

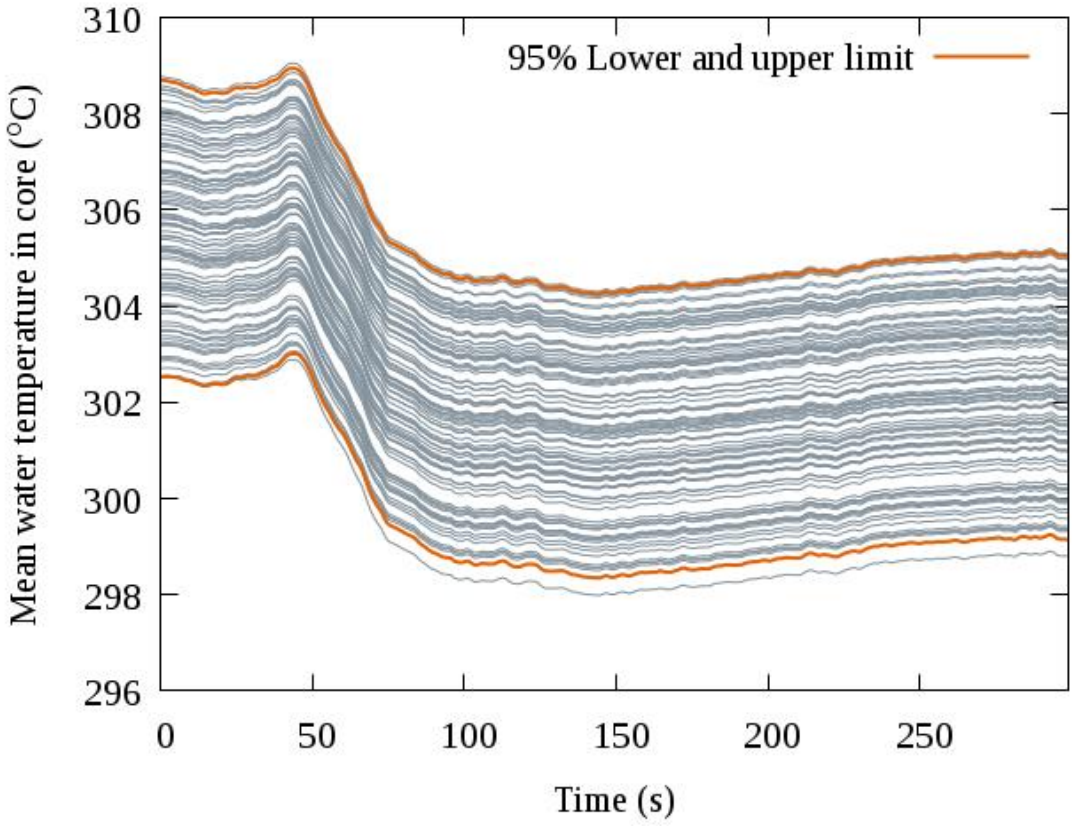

Figure 22. Mean water temperature in reactor core in HEXTRAN simulations.

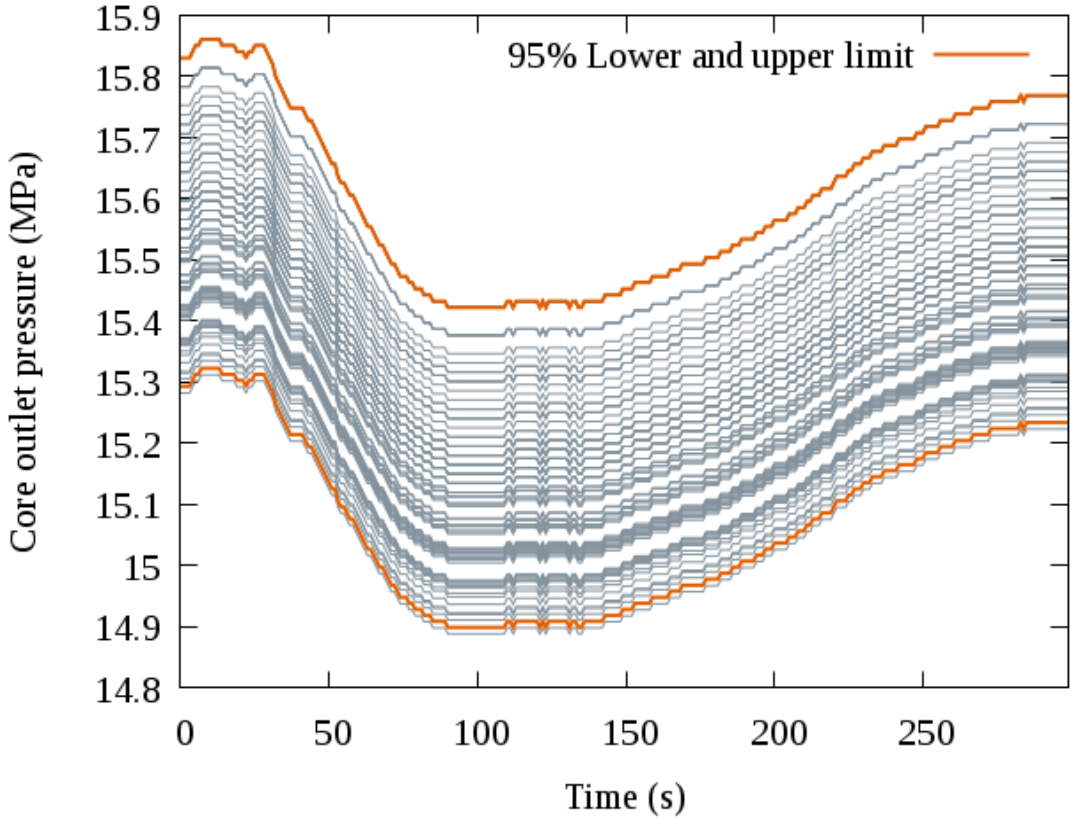

Figure 23. Core outlet pressure in HEXTRAN simulations.

6.2 HEXTRAN-SMABRE

Compared to the stand-alone HEXTRAN, the coupled HEXTRAN-SMABRE calculations had much less variation in the core output values, such as power, moderator temperature and density, core mass flow, and pressure. However, important output values, such as maximum fuel temperature and peaking factor results, were approximately the same in both cases. All results for the HEXTRAN-SMABRE calculations are presented in Appendix 3 – scenario 1 in Tables 8 and 9, and scenario 2 in Tables 10 and 11. Standard deviations and maximum values were bigger in the runs with varied cross-section files than without in all HEXTRAN-SMABRE runs.

6.2.1 Scenario 1

As seen from Figure 24, total fission power had much less variance in the coupled HEXTRAN-SMABRE runs than in the stand-alone HEXTRAN. In the coupled runs the power dropped to 68-72 % of its initial value, which was the same in all runs. The maximum assembly-wise peaking factor and fuel temperature are presented on Figures

25 and 26, respectively. In the coupled runs the variance is slightly smaller when compared to stand-alone HEXTRAN calculations but the results are otherwise similar. All of these parameters had the strongest correlation with gas gap conductance. In addition, fuel conductivity had a significant correlation with the maximum fuel temperature.

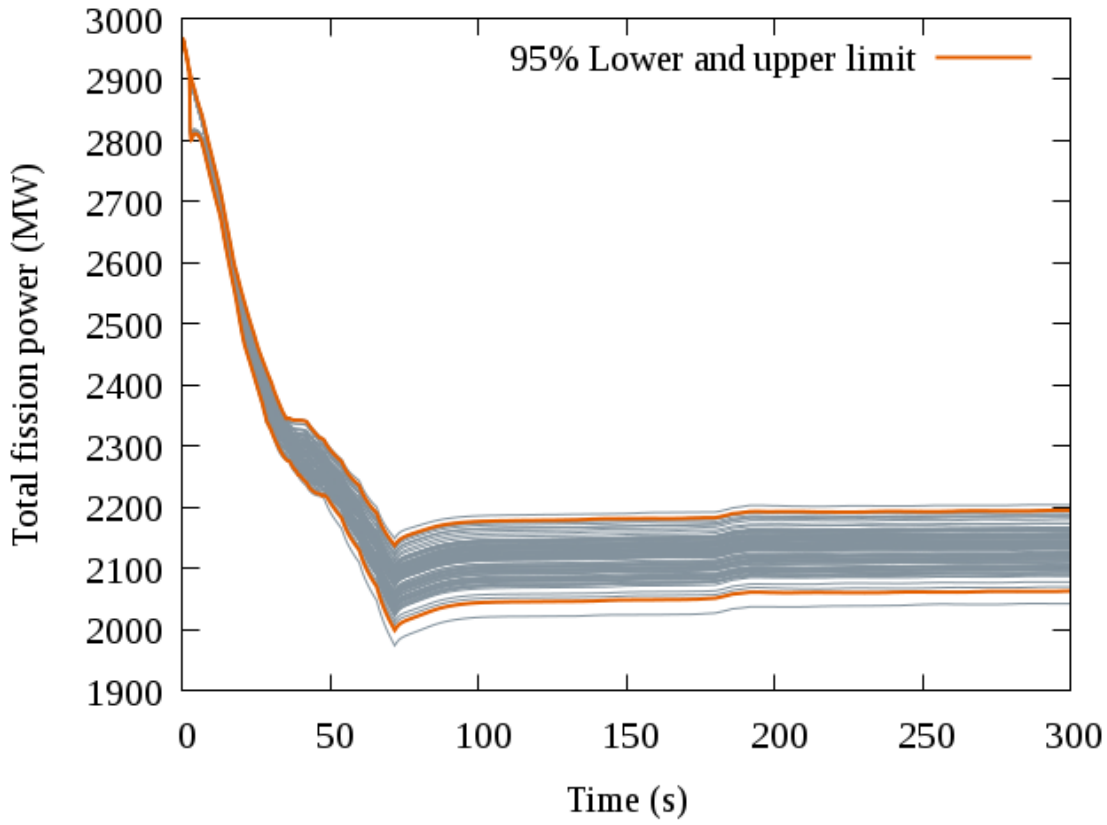

Figure 24. Total fission power in HEXTRAN-SMABRE Scenario 1 with 95 % lower and upper limits.

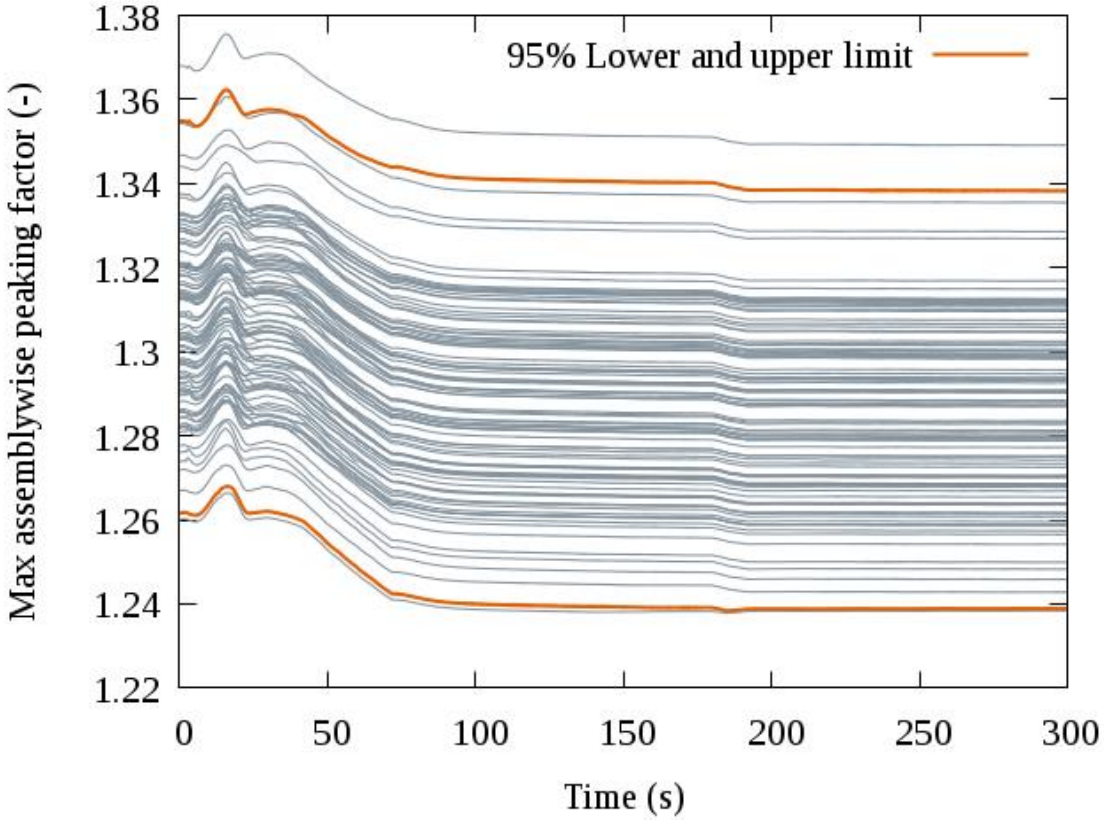

Figure 25. The maximum assembly-wise peaking factor in HEXTRAN-SMABRE Scenario 1.

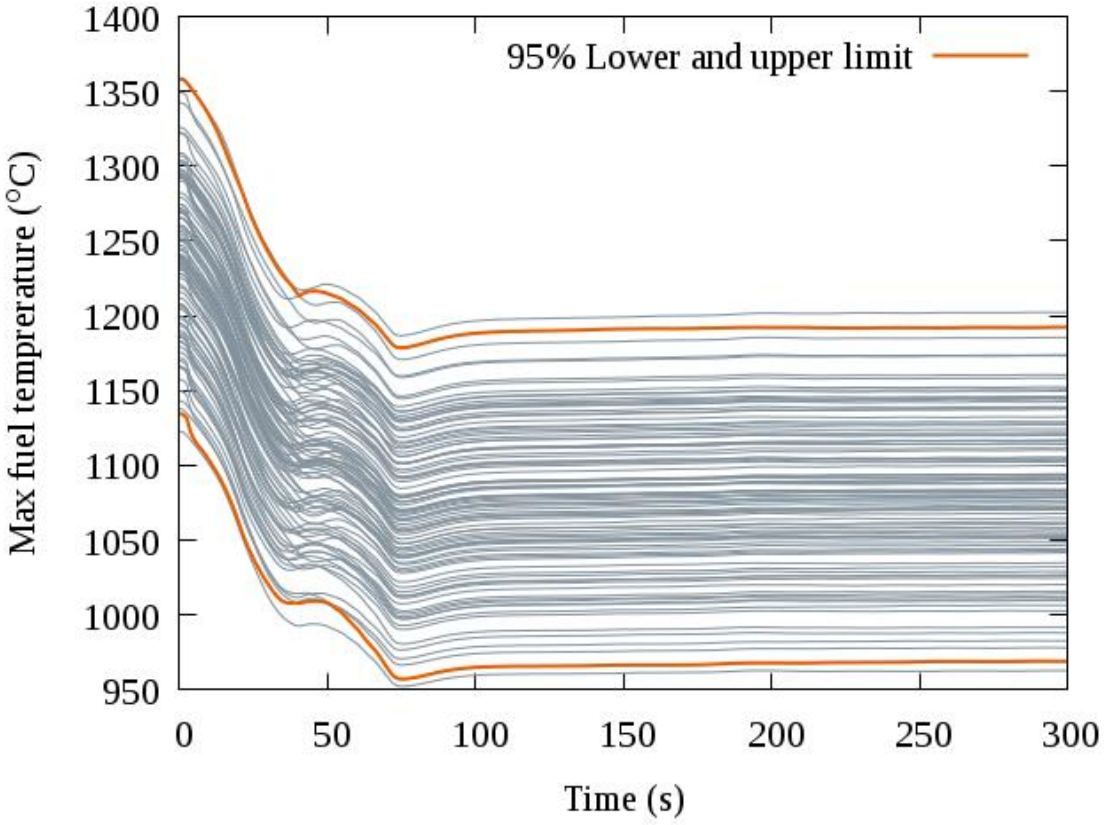

Figure 26. Maximum fuel temperature in HEXTRAN-SMABRE Scenario 1.

The five different pump curve options caused differences in pump speeds. MCP-1 had three different coast down times, whereas MCP2-4 had five different final speeds depending on the pump curves. The MCP pump speeds are shown in Figure 27. The mass flows overall follow closely a few different curve bundles depending on the pump speed. The core mass flow and cold leg mass flows are presented in Figures 28 and 29. The total mass flow through core decreases like in the stand-alone HEXTRAN calculations. Coolant flow in cold leg 1 is reversed, and the mass flows in other loops increase slightly. In loops 2-4, the mass flow increases notably more with one of the pump curve options. According to the sensitivity measures, fuel outer radius and heater upper limit had the strongest correlation on cold leg mass flows along with pump curve, but the results are questionable since it can be clearly seen that the biggest variation in all mass flows is caused by the different pump curves. Because the curves are divided into few different bundles based on that one option, the order is mixed up which again messes up with the rank correlation calculations. RCC cannot be calculated to pump curves at all, because the curves do not have an actual value that could be ranked, only a number from 1 to 5. Because of the nature of the results, they must be interpreted only from the plots.

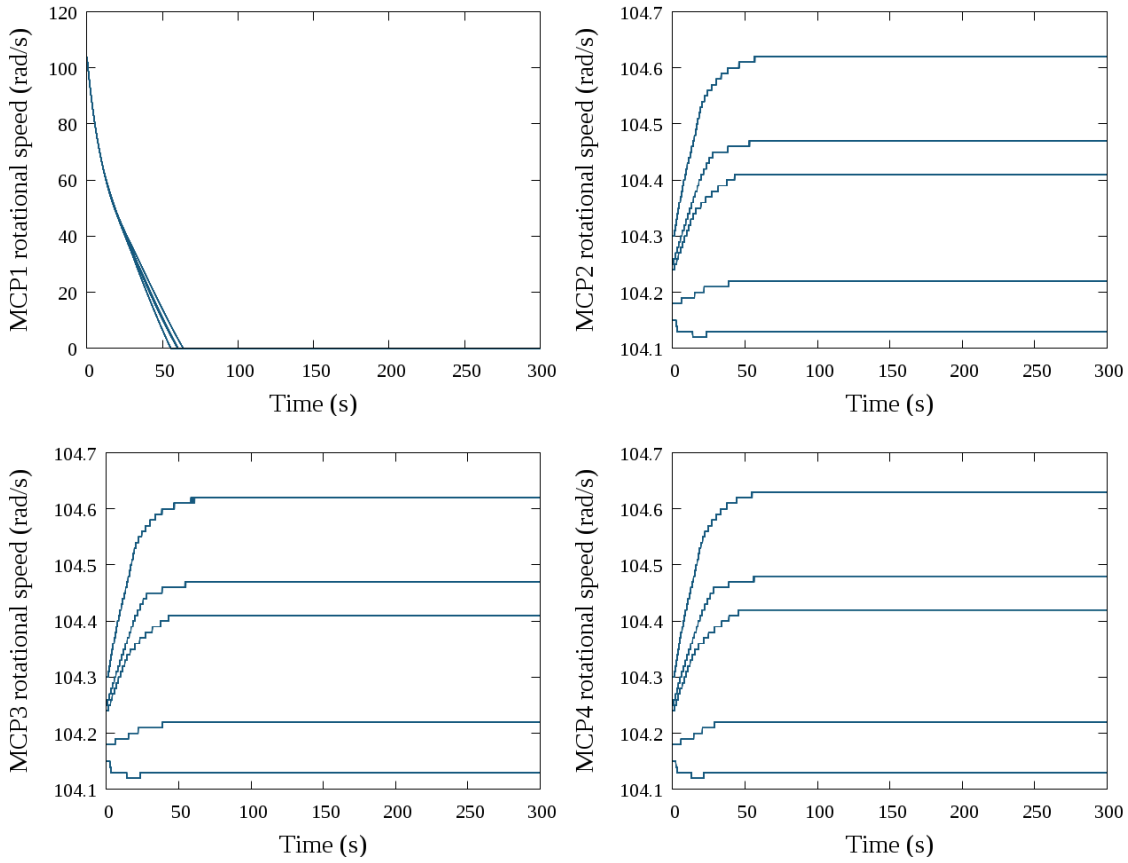

Figure 27. Main coolant pump rotational speeds in all loops in HEXTRAN-SMABRE Scenario 1.

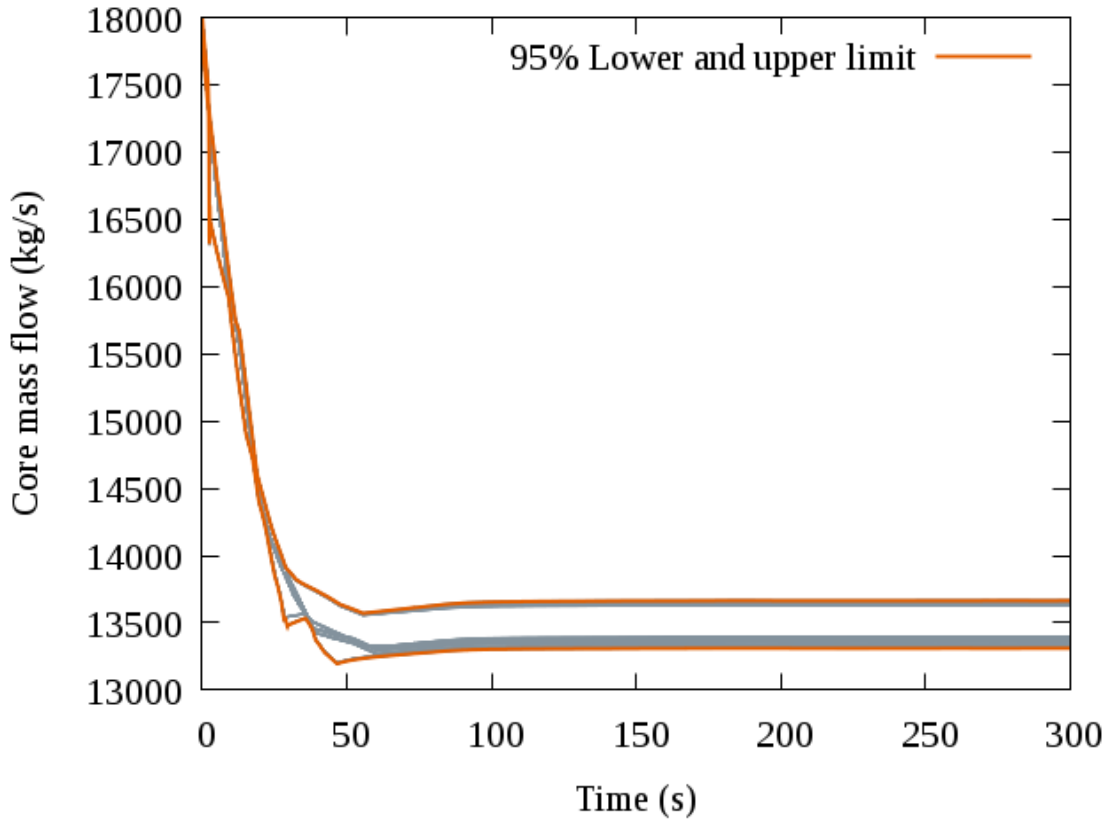

Figure 28. Mass flow through reactor core excluding by-pass flow in HEXTRAN-SMABRE Scenario 1.

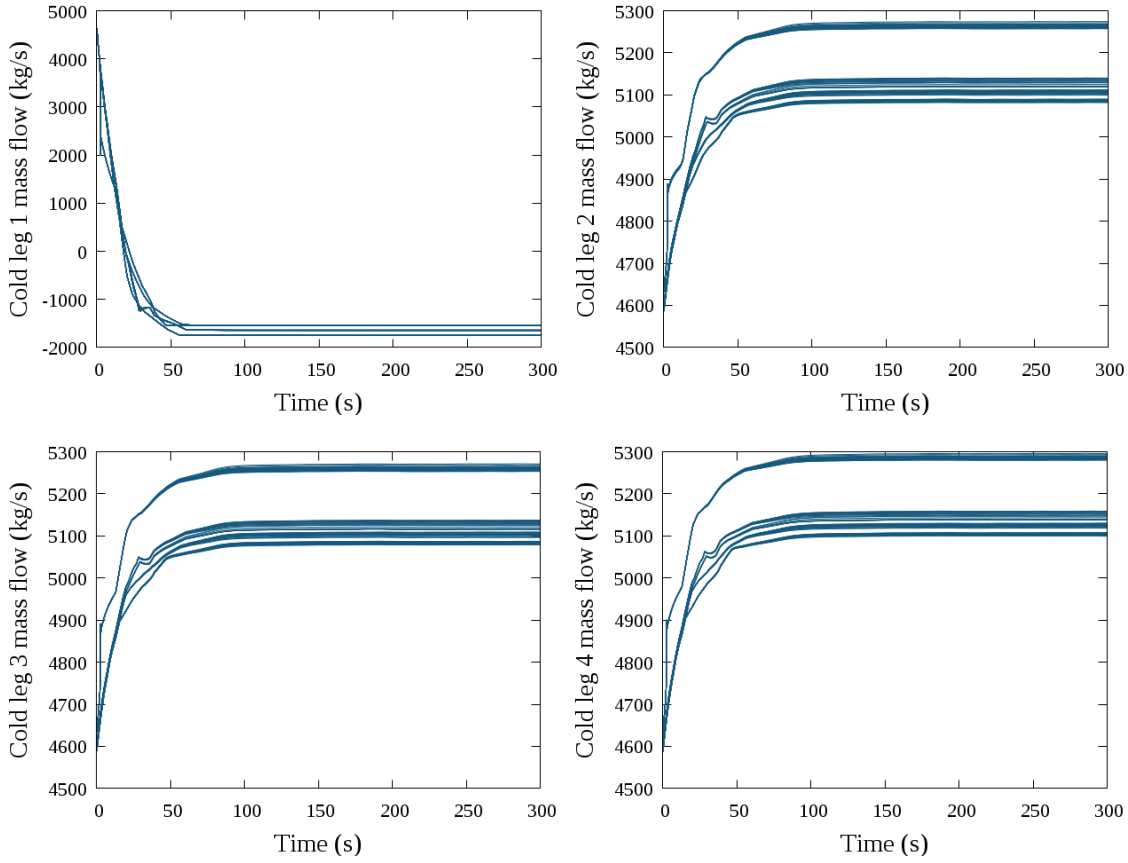

Figure 29. Cold leg mass flows in all primary loops in HEXTRAN-SMABRE Scenario 1.

Mean water temperature in the core is shown in Figure 30. The variance is smaller than in the stand-alone HEXTRAN calculations, where the output distribution was determined by boundary condition variations. Additionally, the temperature behaves a bit differently throughout the transient increasing more in the beginning. Water temperature in the core had the strongest correlation with gas gap conductance.

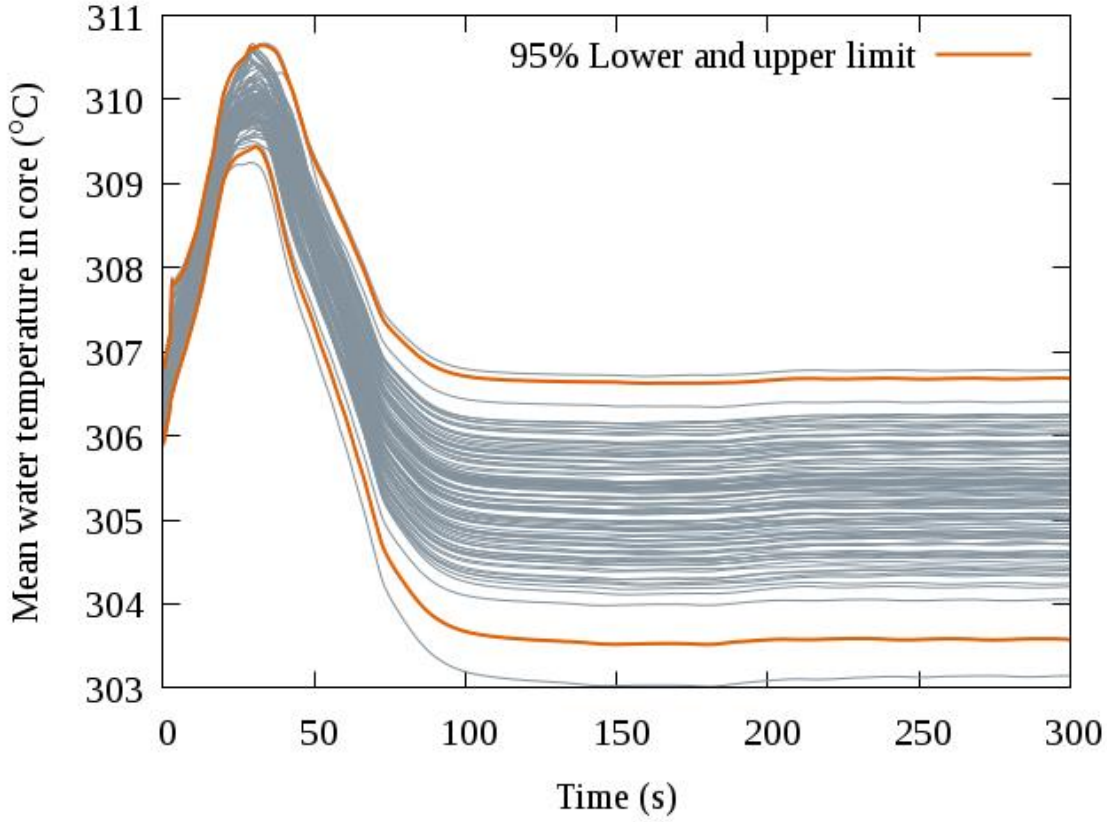

Figure 30. Mean water temperature in reactor core in HEXTRAN-SMABRE Scenario 1.

Figures 31 and 32 show hot and cold leg temperatures, respectively, in all primary loops. Temperature in hot leg 1 decreases dramatically when the flow in loop 1 is reversed. In other hot legs temperature decreases after increasing slightly, most in hot leg 4, which is closest to loop 1. Temperature in cold legs 2-4 decreases similarly, whereas cold leg 1 temperature decreases when the pump is slowing down and then starts to increase, when the flow in loop 1 is reversed, before settling to the same temperature as the other loops. Gas gap conductivity had the strongest correlation with all of these temperatures, RCC being close to -1. The only exception was hot leg 1 temperature, where the results were fuzzier, probably due to much smaller variance.

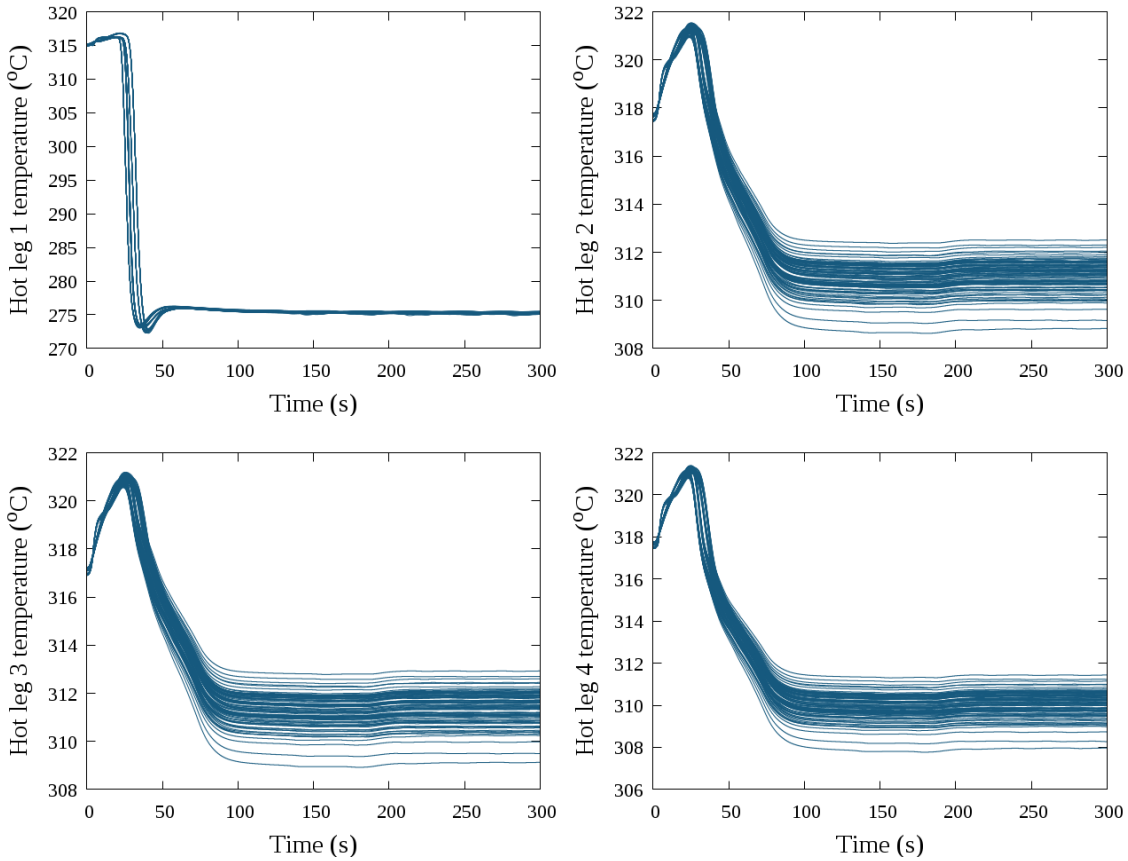

Figure 31. Hot leg temperatures in all primary loops in HEXTRAN-SMABRE Scenario 1.

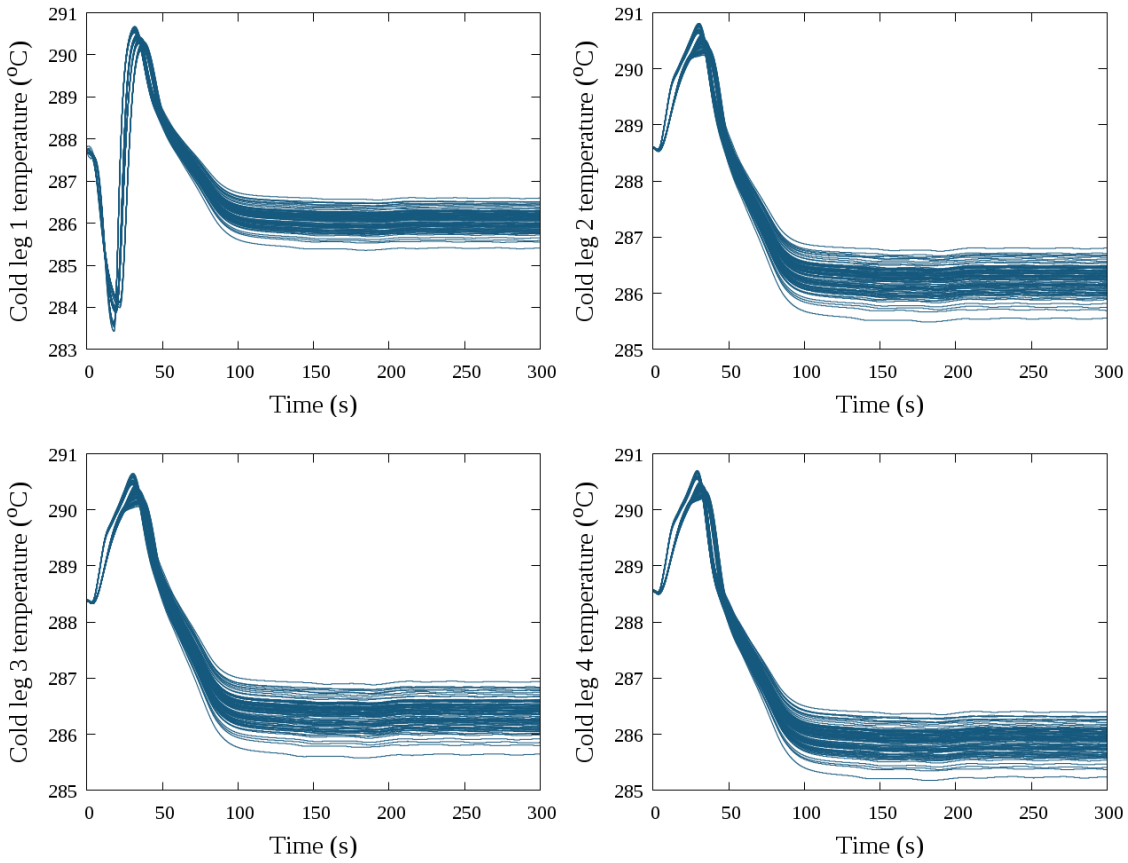

Figure 32. Cold leg temperatures in all primary loops in HEXTRAN-SMABRE Scenario 1.

Calculation results for pressure in the upper plenum of the reactor pressure vessel are shown in Figure 33 and RCC's in Figure 34. At first, the pressure incerases slightly, then it drops as the mass flow through the core decreases. After that, the heaters are activated and pressure starts to increase again. The parameter correlation most with pressure varies throughout the transient. In earlier stages, gas gap conductance has the highest correlation, but its meaning decreases later on. Naturally, parameters affecting the pressurizer heaters have a high correlation with system pressure. Earlier in the transient, when pressure decreases, the lower limit of the heater has a high positive correlation. As the pressure starts to increase, heater power and the upper limit of the heater has more impact.

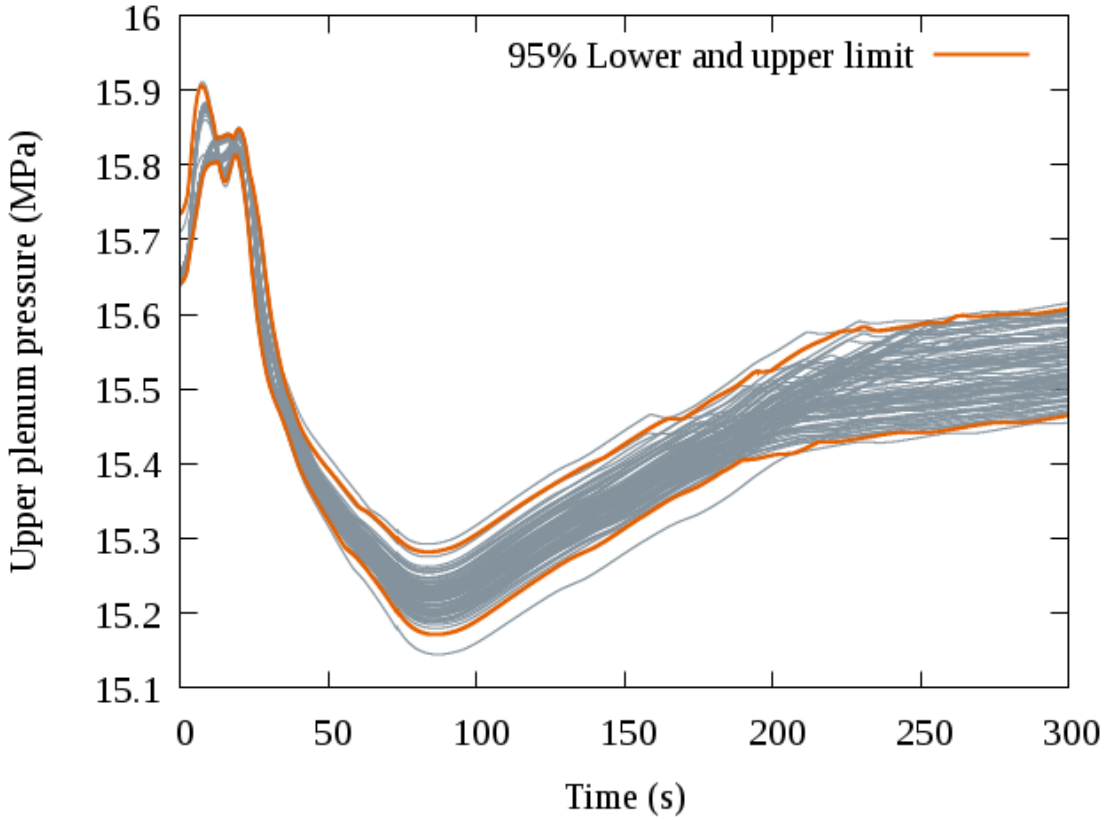

Figure 33. Upper plenum pressure in HEXTRAN-SMABRE Scenario 1.

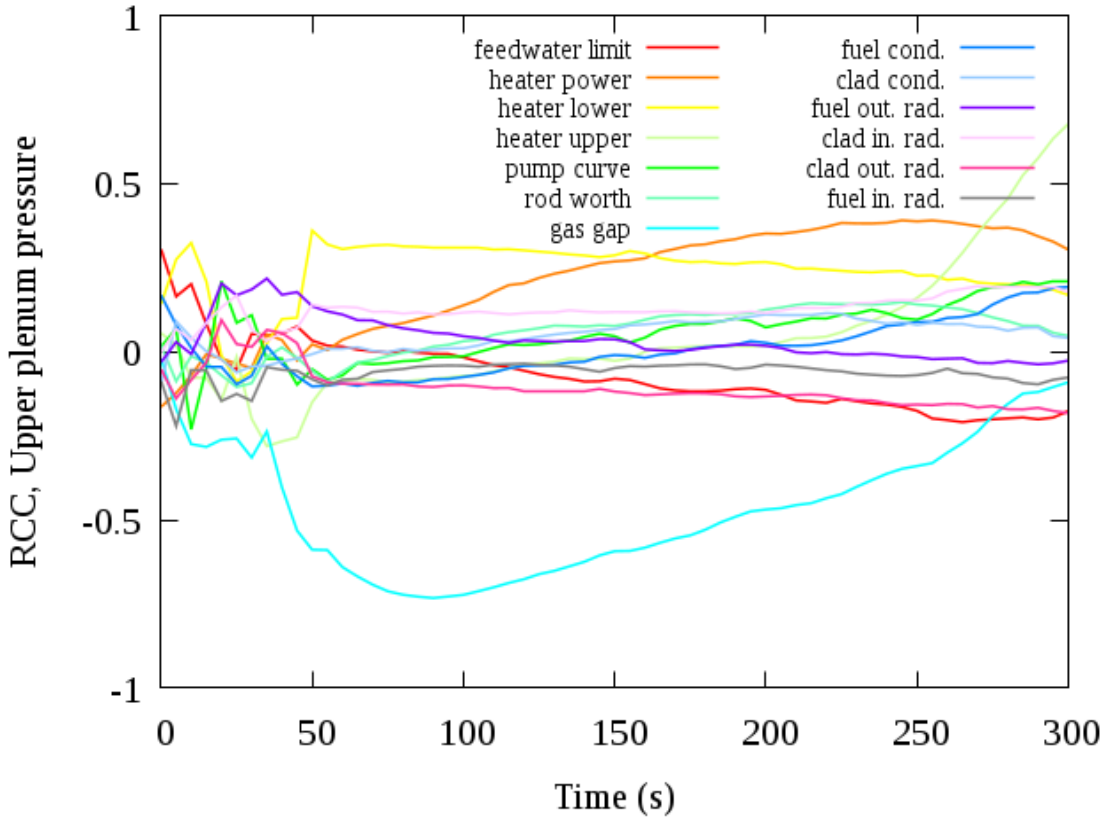

Figure 34. Rank correlation coefficient for upper plenum pressure in HEXTRAN-SMABRE Scenario 1.

6.2.2 Scenario 2

The results from Scenario 2 were substantially the same as from Scenario 1. The biggest difference was seen in the mass flows, where the variance in Scenario 2 was larger than in Scenario 1. This was caused by the pump lock option, which changed the pump speeds, shown in Figure 35. The biggest difference can be seen in MCP-1, which starts to rotate backwards in some cases.

The results for mass flows in the core and cold legs can be seen in Figures 36 and 37. The results are similar as in Scenario 1 but with slightly wider variance and more curve bundles. In addition to the pump curves, the pump lock option had the biggest influence on the mass flow results, because the backwards rotating MCP-1 enabled a higher mass flow in loop 1 thus affecting the other loops as well. Again, the sensitivity measures for mass flows are incorrect, as discussed in the previous chapter, but it can clearly be seen from the figures that pump behaviour affected the mass flow results the most while the variance caused by other input parameters is small in comparison.

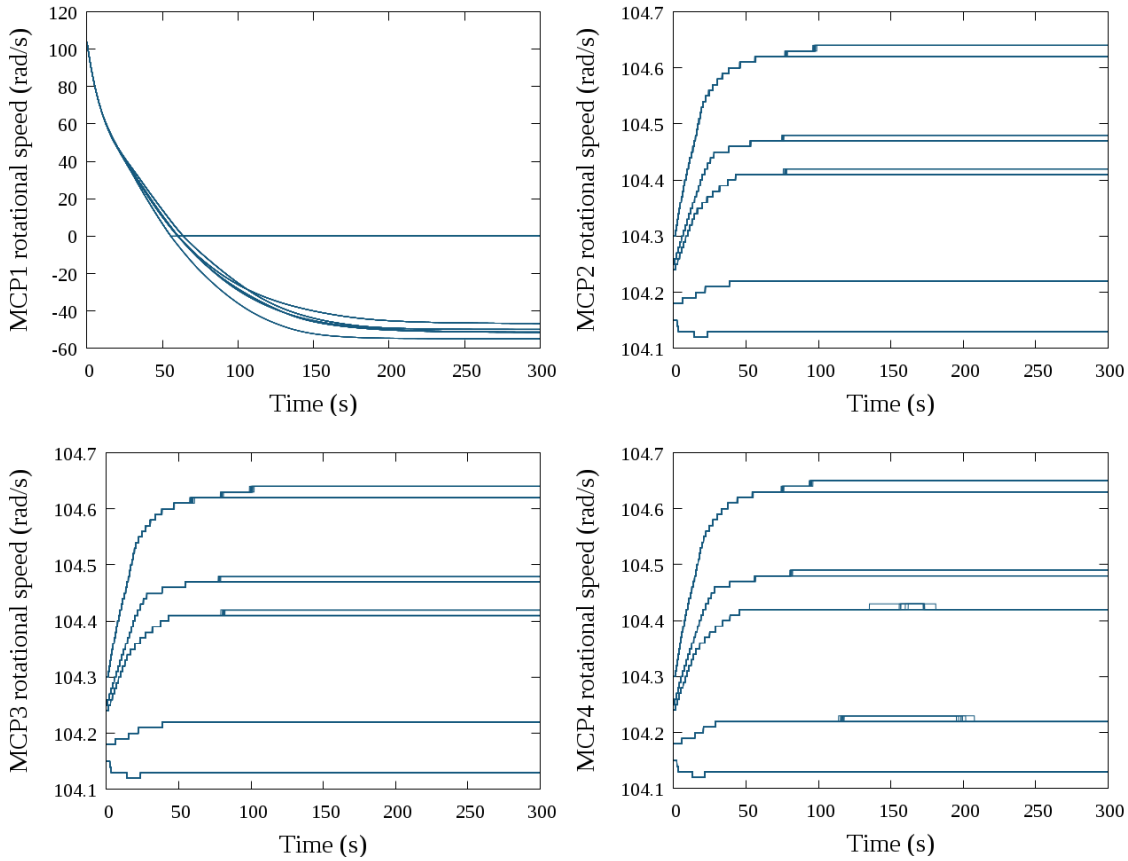

Figure 35. MCP rotational speeds in all primary loops in HEXTRAN-SMABRE Scenario 2.

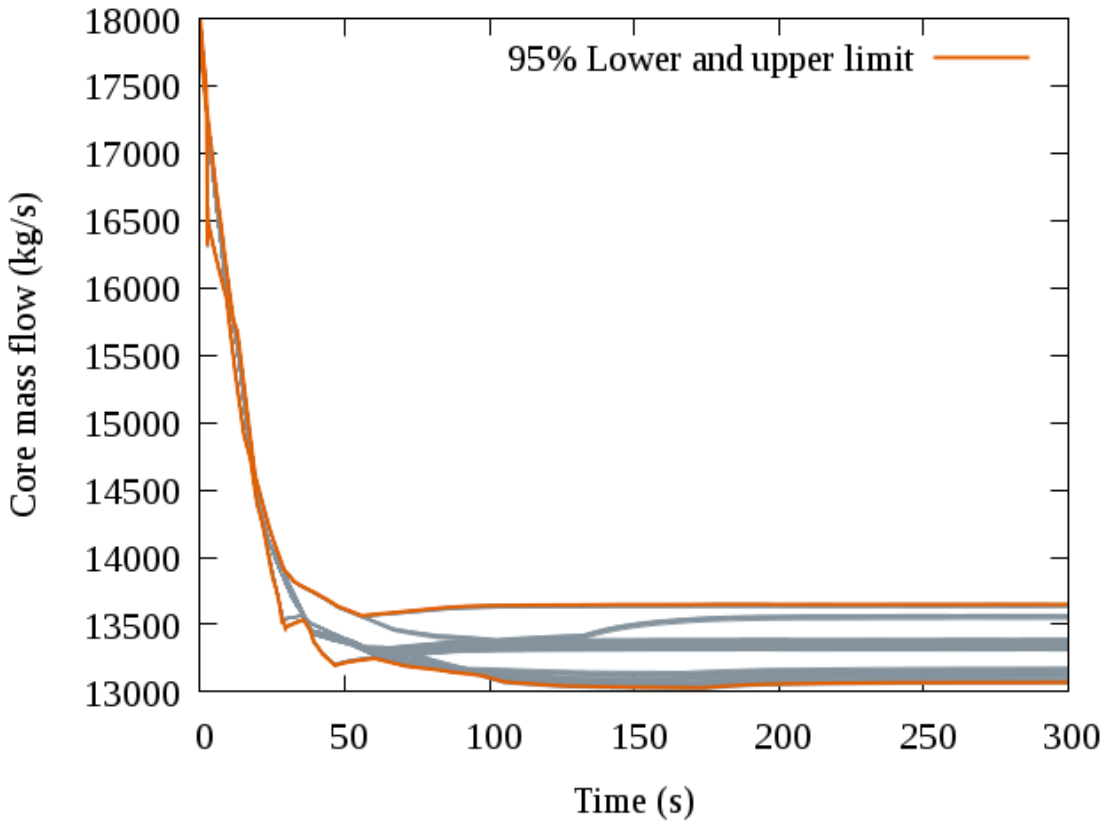

Figure 36. Mass flow through reactor core excluding by-pass flow in HEXTRAN-SMABRE Scenario 2.

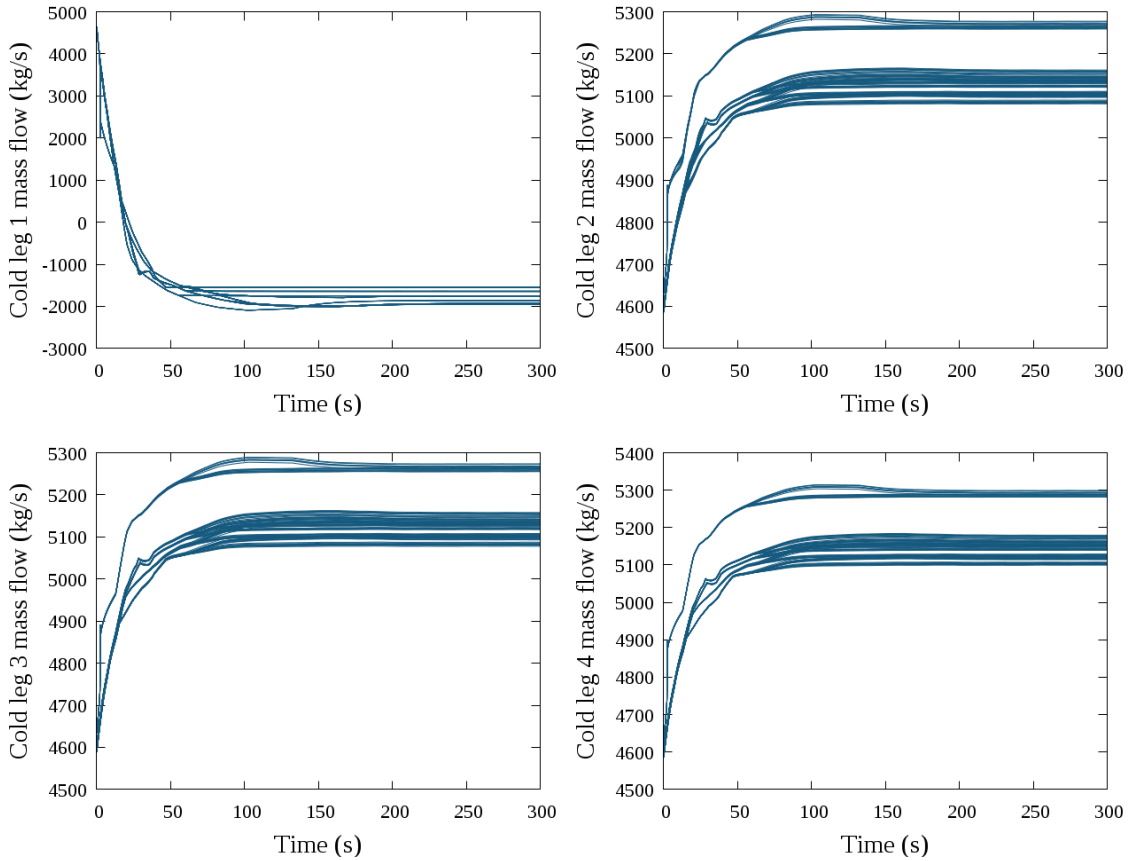

Figure 37. Cold leg mass flows in all primary loops in HEXTRAN-SMABRE Scenario 2.

In Scenario 2, pressure varied slightly more and in the early stages of the transient is increases to a higher level than in Scenario 1. Pressure in the upper plenum of the reactor pressure vessel is presented in Figure 38. Many of the input parameters had a meaningful correlation with pressure, Figure 39. In the early stages, during the pressure increase, cooling spray and letdown had a strong negative correlation with pressure, whereas the correlation with feedwater limit was positive. After that, during decreasing pressure, the heater lower limit, gas gap, and fuel inner radius had more significant correlation. Finally, as the pressure increases, the heater upper limit and make-up flow begin to have a stronger correlation, much like in scenario 1. Other results from Scenario 2, such as temperatures, were roughly the same as from Scenario 1 and are not discussed in more detail.

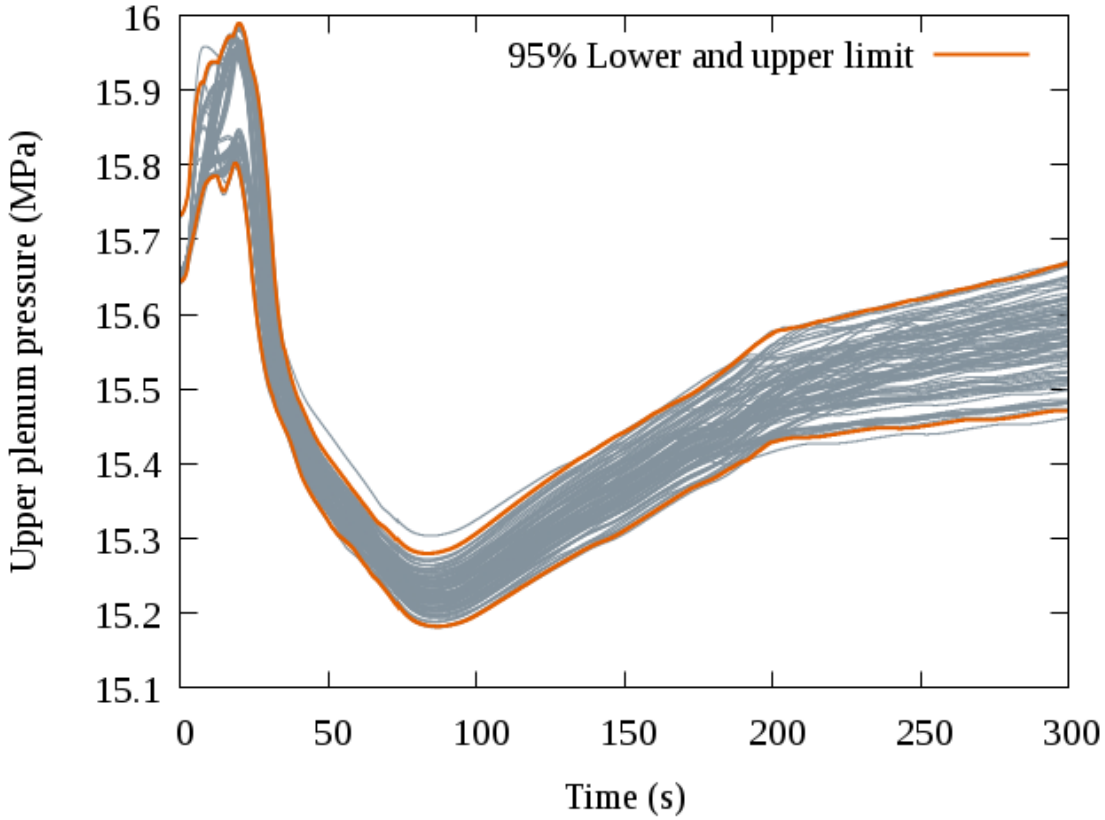

Figure 38. Upper plenum pressure in HEXTRAN-SMABRE Scenario 2.

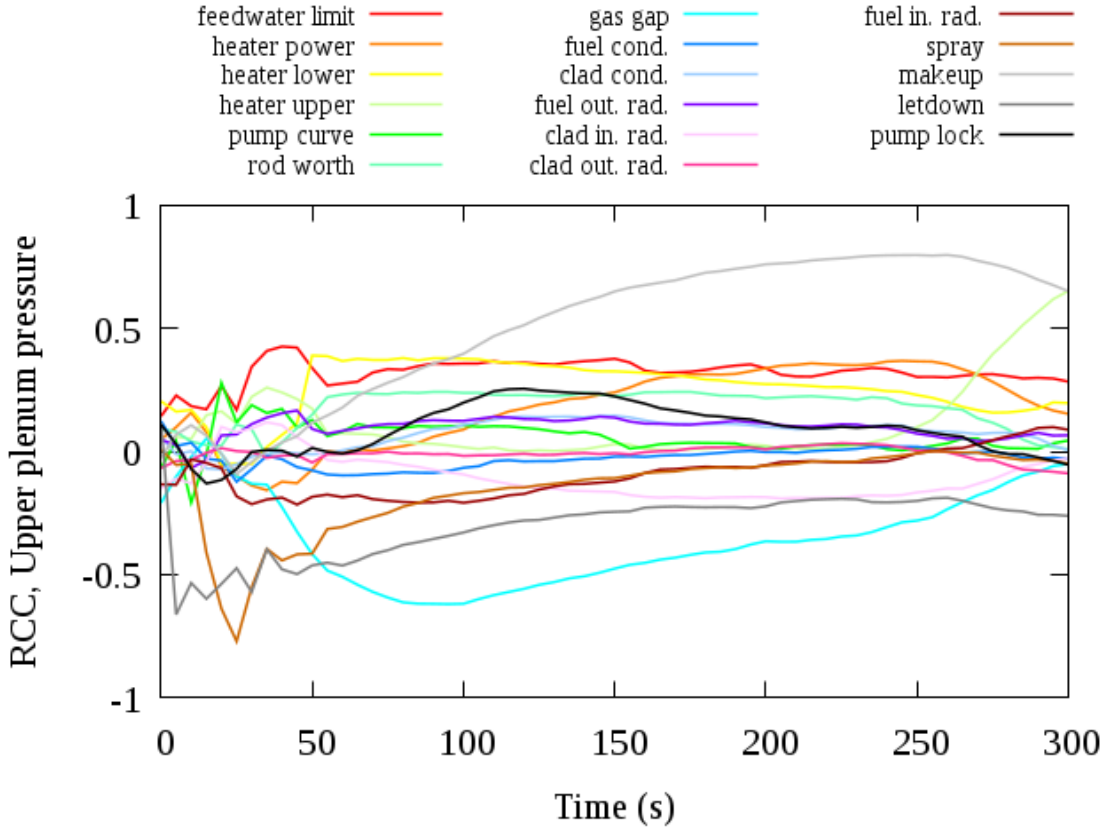

Figure 39. Rank correlation coefficients for upper plenum pressure in HEXTRAN-SMABRE Scenario 2.

6.3 TRACE

In this chapter, results from the TRACE calculations are outlined. It is not meaningful to analyse results concerning the reactor core, such as fuel temperature or peaking factors, since there was no detailed core model. More important are the thermal-hydraulic outputs from the primary circuit. All mean, maximum, and minimum output values are presented in Appendix 3 Table 12. All rank correlation and partial rank correlation coefficients from the last calculated time step are collected in Tables 13 and 14, respectively. Standard deviations in the results are much smaller than in the HEXTRAN-SMABRE results, which could be a sign that the uncertainty limits are not very realistic. The model is probably still too defined by its boundary conditions and needs more control systems.

The core power was modelled with point-kinetics by using total reactivity values. There was no reactivity feedback, which means that for example temperature did not affect reactivity. Due to this simplification there was no variance in the total fission power apart from the power input parameter variations, Figure 40.

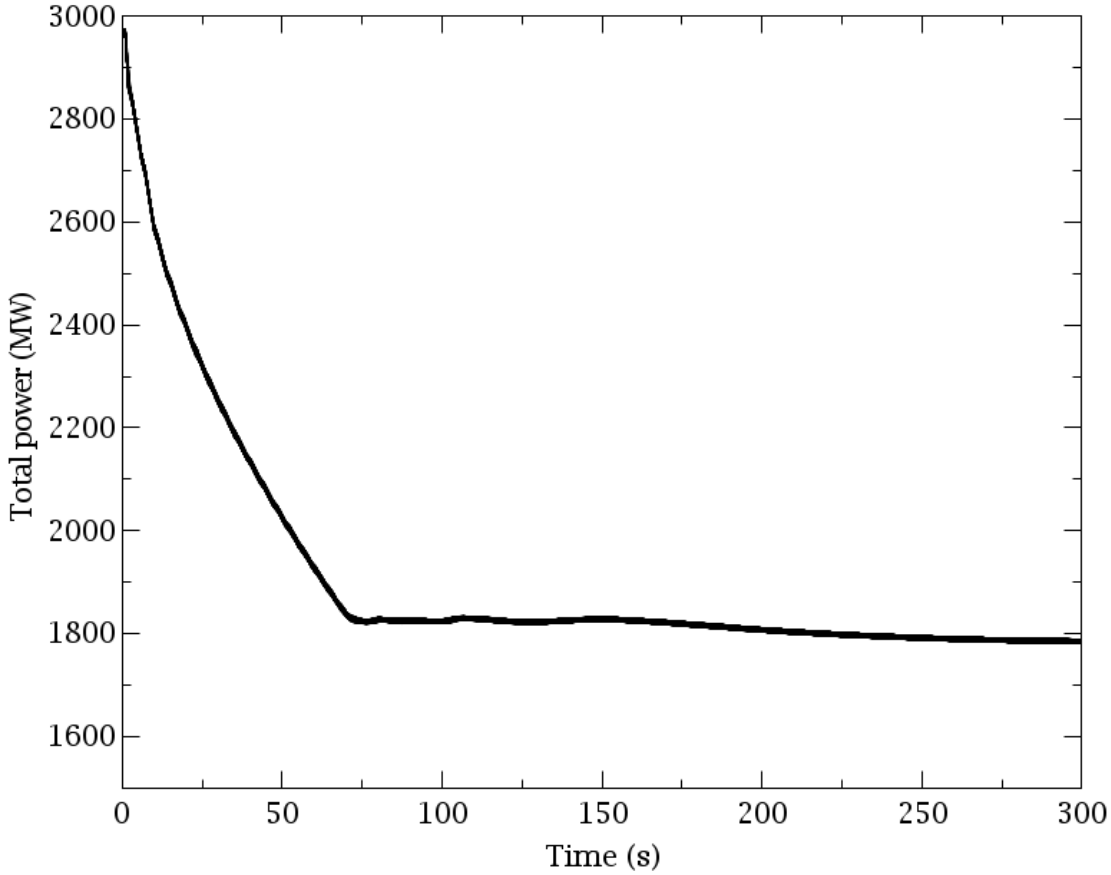

Figure 40. Total fission power during TRACE transient calculations.

The pressure boundary condition was varied two percentages, which directly affected pressure overall in the primary circuit. Upper plenum pressure is presented in Figure 41. The results are similar to HEXTRAN-SMABRE runs except here pressure rises much less during the first 20 seconds of the transient. Apart from pressure input variations, gas gap, liquid to wall HTC and wall drag had significant correlation with pressure.

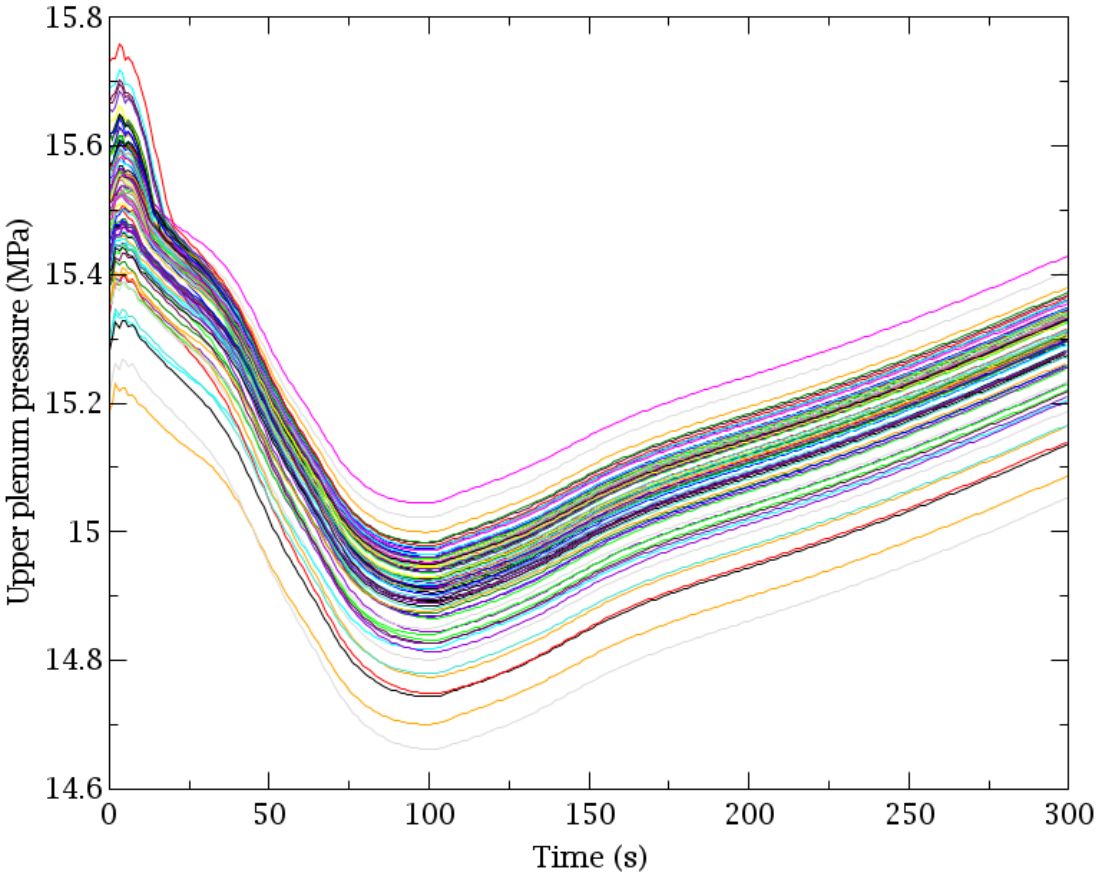

Figure 41. Upper plenum pressure in all TRACE sensitivity runs.

There was some variance in the rotational speeds of MCP's, Figure 42. The coastdown time of MCP-1 was almost the same in every run, but speeds in loops 2-4 varied and behaved differently than in the HEXTRAN-SMABRE runs. At first the speed increased like in HEXTRAN-SMABRE, but then decreased until finally settled on a slightly descending curve. MCP-1 stopped about 20 seconds later than it should. Mass flow through the core and cold legs are presented in Figures 43 and 44, respectively. Compared to the HEXTRAN-SMABRE calculations, the results are similar except that in the cold legs 2-4 variance is higher in the TRACE runs. The strongest correlation with these results was with the wall drag coefficient. Pressure and liquid-to-wall heat transfer coefficient had significant PRCC values with mass flows overall.

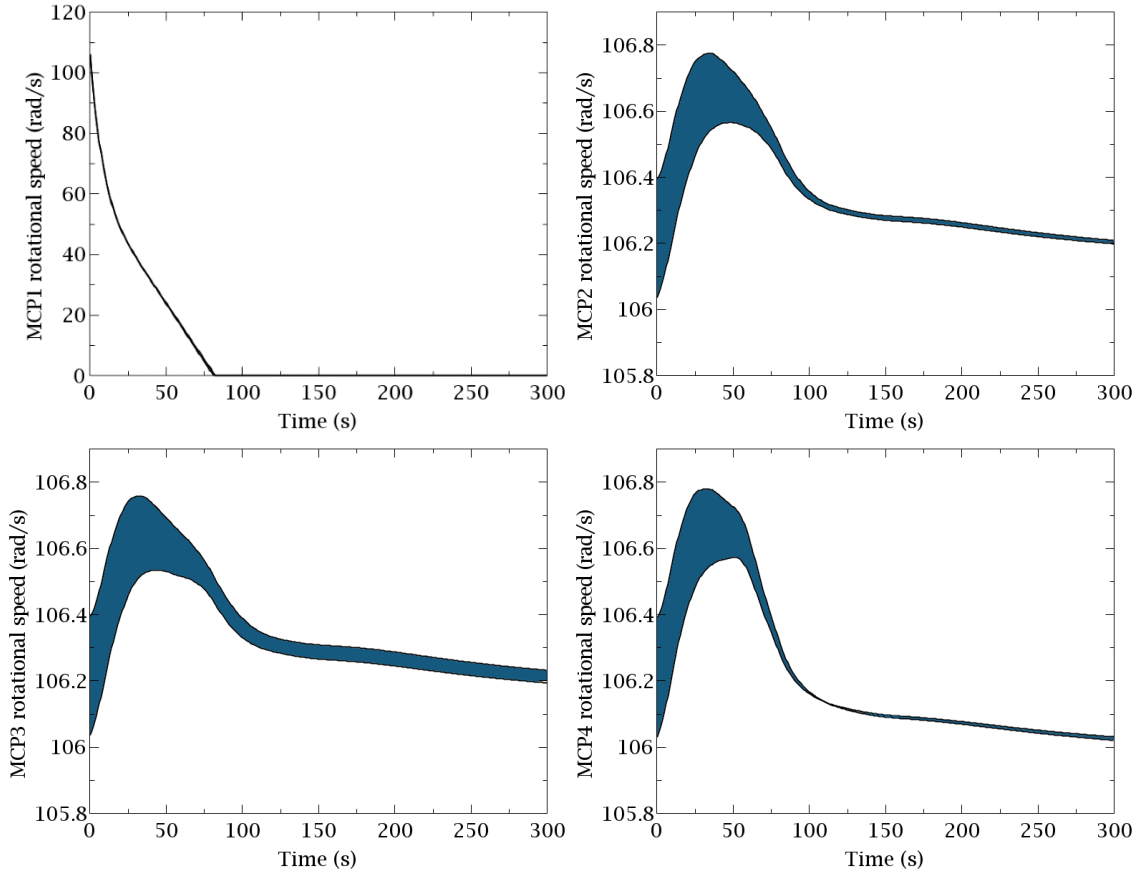

Figure 42. Main circulation pump rotational speeds in all primary loops in TRACE simulations.

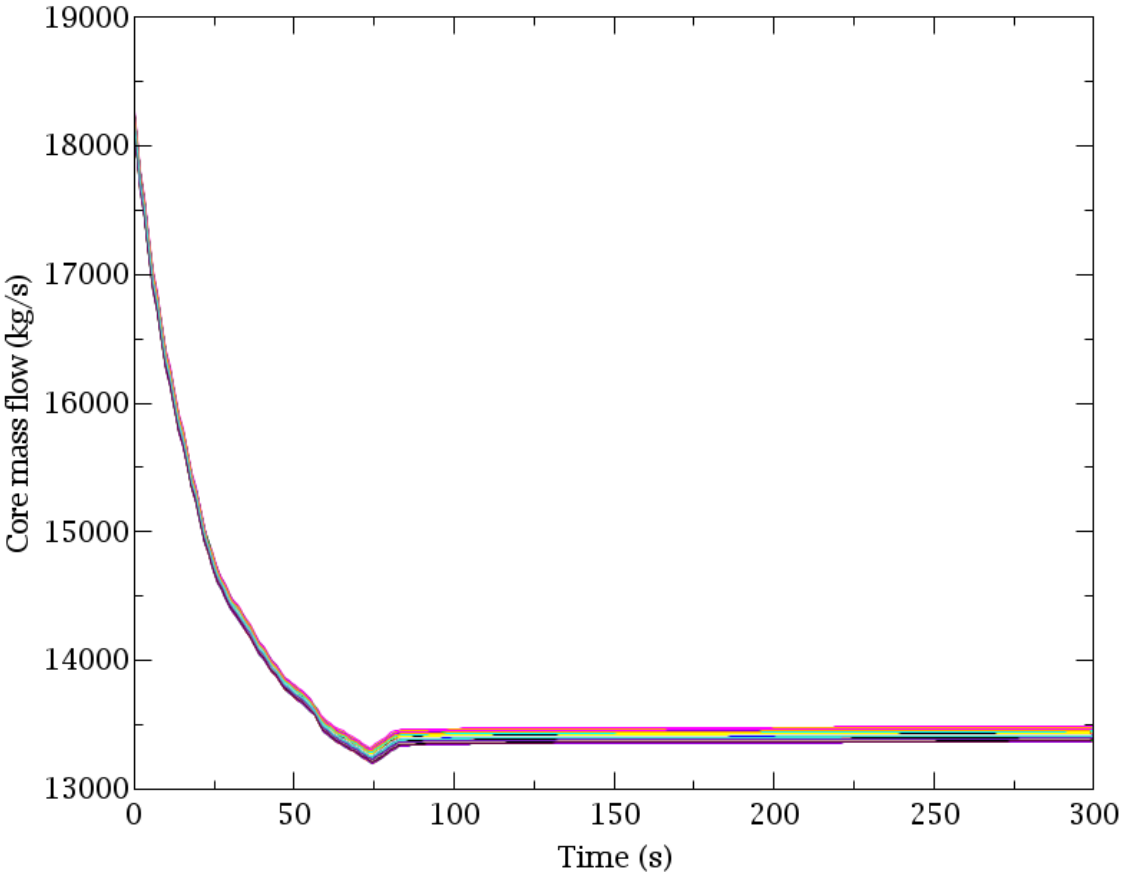

Figure 43. Whole core mass flow in TRACE simulations.

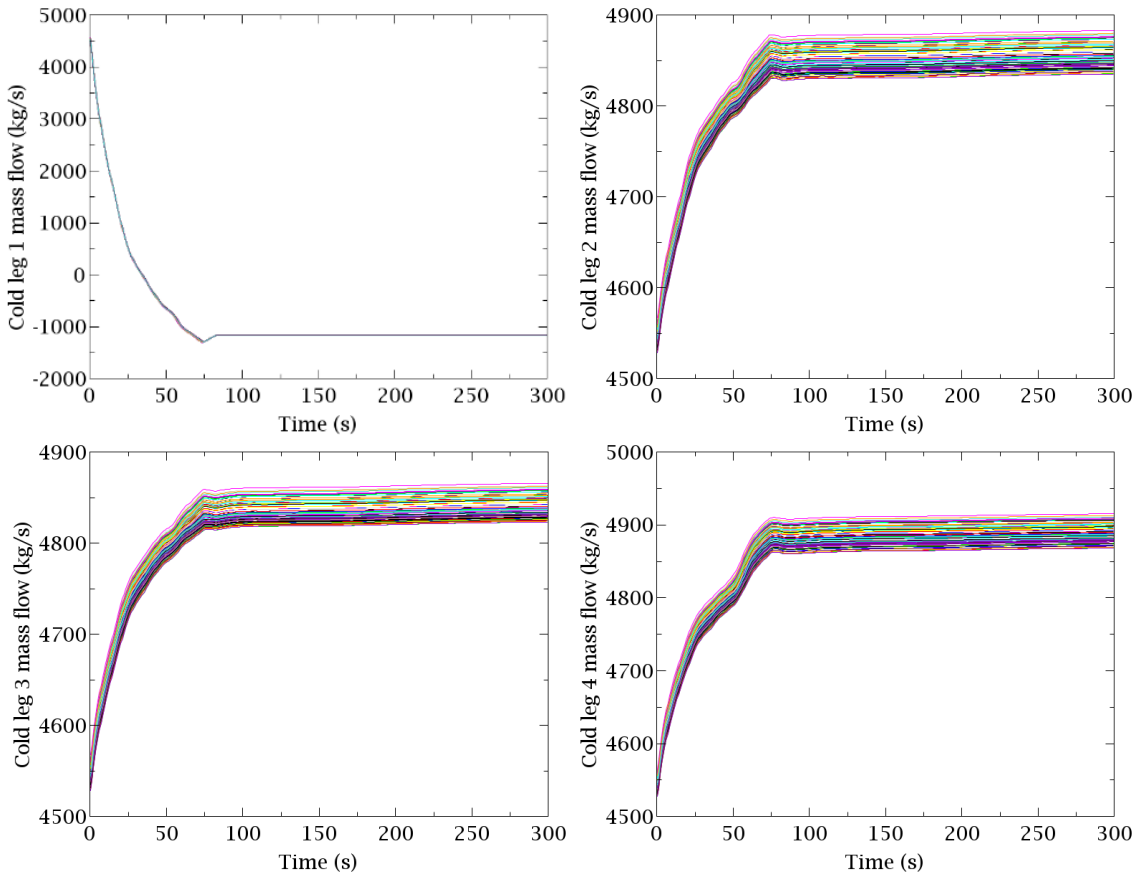

Figure 44. Cold leg mass flows in all primary loops in TRACE simulations.

Hot leg temperatures from all loops are presented in Figure 45 and cold leg temperatures in Figure 46. They behaved similarly than in the HEXTRAN-SMABRE calculations, except in loops 2-4 the temperatures did not increase as much in the beginning of the transient, barely at all in the hot legs. Temperature outputs had a strong rank correlation with liquid-to-wall heat transfer coefficient and partial rank correlation was significant with power, wall drag, clad conductivity and heat loss.

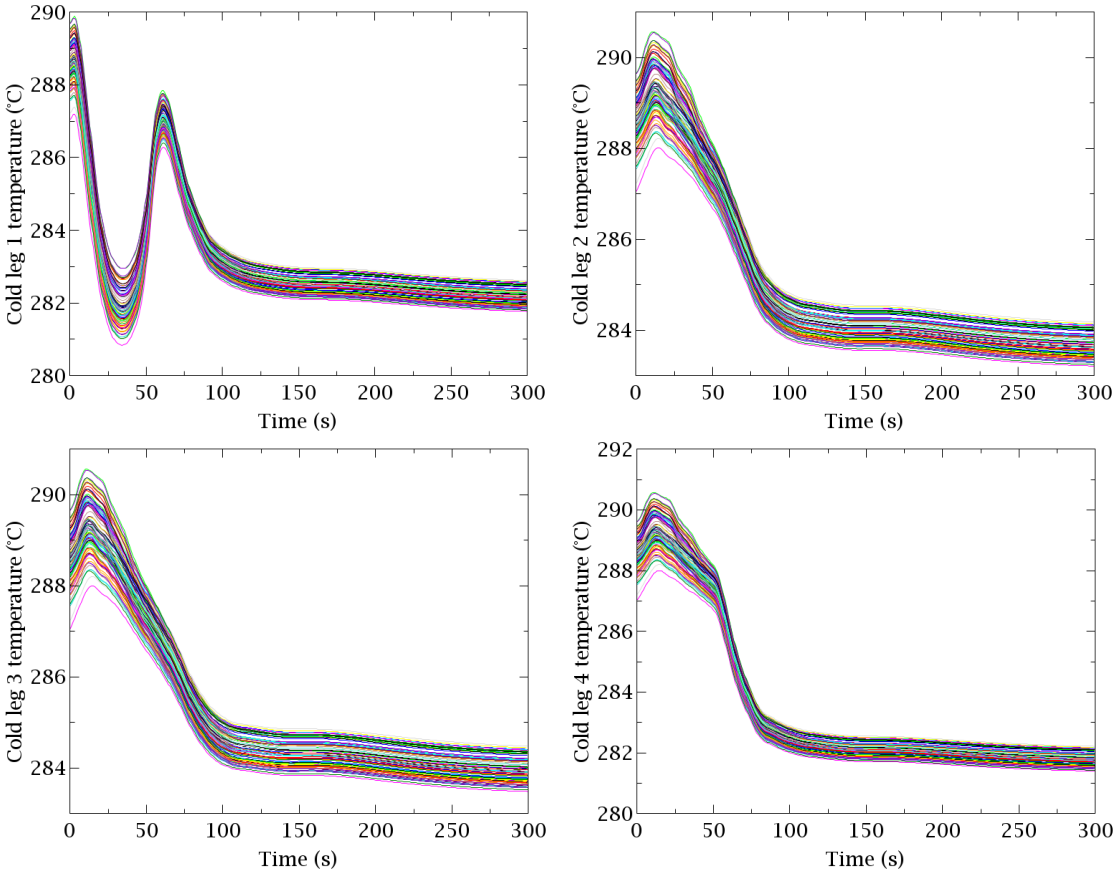

Figure 45. Cold leg temperatures in all primary loops in TRACE simulations.

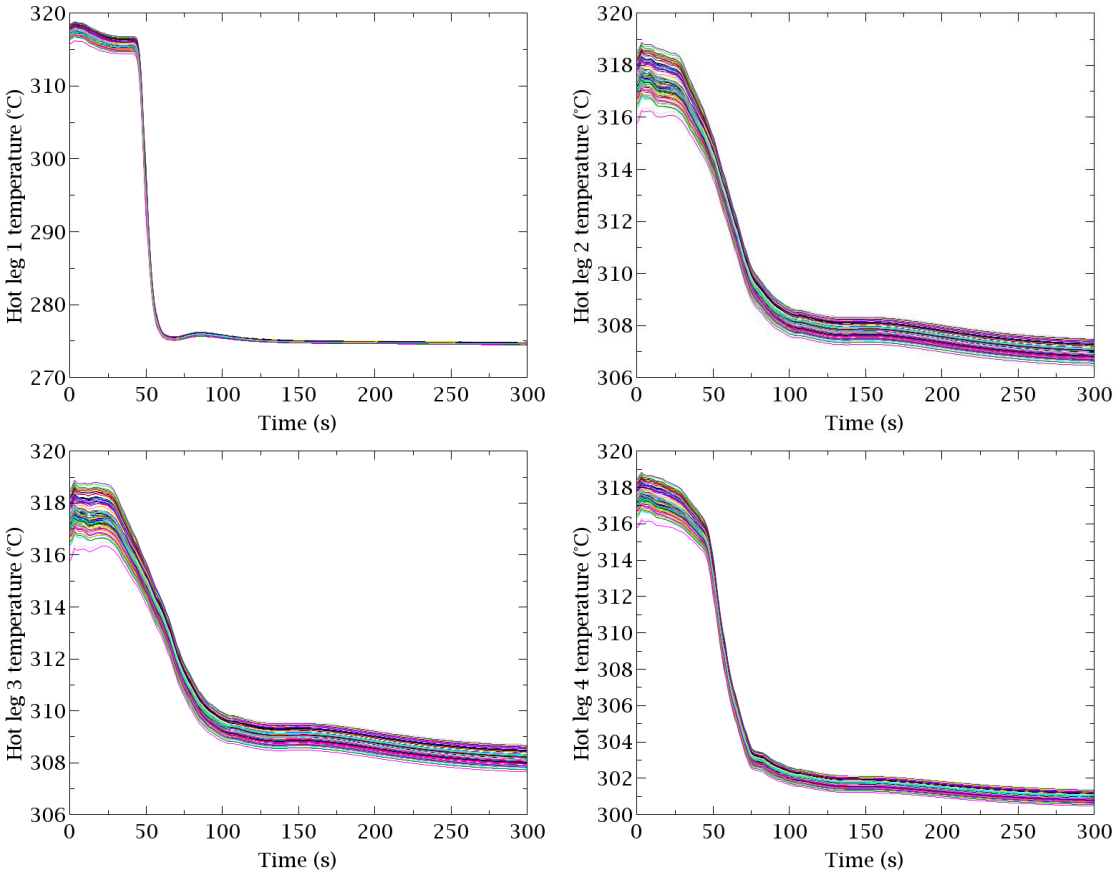

Figure 46. Hot leg temperatures in all primary loops in TRACE simulations.

7 DISCUSSION

One purpose of this thesis was to recognize the most important sources of uncertainty in reactor core, thermal-hydraulic system and coupled core-system models. For reactor core models, the gas gap conductance is a recognized source of uncertainty. The results of this study support that with the gas gap conductivity having a strong effect on power, peaking factors and fuel temperature. Salah et al. (2005) found the gas gap conductivity to be among the most important input variables in a similar pump transient case with the control rod bank course and control rod worth affecting the results most. That is probably because scram was activated in that case, unlike in this transient, where control rods are inserted only slightly, and therefore do not affect the results much. Also in a VVER-440 transient study by Langenbuch et al. (2005) control rod insertion and worth had the biggest effect on the results. In that case, the insertion depth of the control rods was uncertain, which explains the results.

The boundary condition for inlet coolant temperature was another input parameter that affected strongly the fuel temperature, reactor power and power peaking in the separate core model. Coolant temperature has a negative correlation with reactivity, which explains the changes in the power output. Porter et al. (2015) found similarly that inlet temperature affected the fuel bundle thermal-hydraulics the most out of the boundary condition variations. Discussing the sensitivity results on pressure, moderator temperature and mass flow in the separate core is not meaningful, since their output distribution was determined by the boundary condition variations. Out of the geometry variations the cladding inner radius had a significant correlation with water and fuel temperatures and power. This was seen in the separate core but not in the coupled core-system calculations.

In the coupled code calculations, the effect of the temperature boundary condition was not present. Therefore the gas gap conductance was the sole most important source of uncertainty for the power output and peaking, water temperature throughout the whole system, and fuel temperature. It can be seen from the standard deviation results that neutronics uncertainties have a big effect on the output uncertainty limits in the core and the coupled core-system simulations, but the effect cannot be quantified in relation to other input parameters.

In this Kalinin-3 transient case, parameters concerning pumps, such as the homologous pump curve, were other important source of uncertainty affecting mass flows and pressure in the thermal-hydraulic system. In the benchmark specification alone, there were three different sets of homologous pump curves, and so far there is no information about which is the right one. Until the final specifications are received that remains a great source of uncertainty in this system model. For example, the amount of core by-pass flow must be adjusted again once the final information is received, since the mass flows are dependent on pump curves. The pumps in SMABRE and TRACE models behaved differently even though same pump curve was used. It seems that in SMABRE, pump behaviour determines other outputs, such as mass flow, whereas in TRACE model other outputs affect pump speed. However, the differences in pump speeds caused by this are negligible small and the mass flows behaved similarly in both models, which is more important. The coastdown time of MCP-1 in TRACE model was too long and should be adjusted to a wanted level once the right pump curve is known.

The correlation coefficients could not be calculated for the pump curves or mass flows in the HEXTRAN-SMABRE simulations. The pump curve options do not have an actual value that could be used in the ranking of the results, only a random number from 1 to 5. The mass flow values were grouped into a few curve bundles depending on the pump curve, which means that the influence of other input parameters cannot be seen with rank correlations. The effect of other input parameters on mass flows could be quantified by doing the sensitivity runs again without the pump curve option. This was however deemed unnecessary since it was clearly seen that the pump curve single-handedly defined the mass flows throughout the system while the variance caused by other parameters was negligible small in comparison.

In the thermal-hydraulic systems models, sources of uncertainty were harder to recognize, partly because of the mildness of this transient. The varied parameters in the SMABRE model were input variables, whereas in TRACE they were mostly sensitivity coefficients affecting the physical models inside the code. Because of this, there were no identical parameters which could have been varied and results compared, but on the other hand, now the results complement each other. In SMABRE, pressure was affected by the heater set point limits and power. The effect of changing pressure on the thermal-hydraulic system could not be quantified with SMABRE calculations but it was possible

with TRACE, where the pressure boundary condition was varied. Pressure had a significant partial rank correlation with mass flows and hot leg temperatures.

Inputs related to steam generators were recognized as a possible source of uncertainty due to the modelling of reversed flow and heat transfer in that area. Feedwater flow, which is controlled by SG water level, is a real source of uncertainty in the thermal-hydraulic system since the water level does not actually exist. Feedwater flow, however, had little effect on the SMABRE calculation results. Liquid to wall HTC, on the other hand, impacted the system much more in the TRACE calculations. It had a strong rank correlation with the hot and cold leg temperatures and a strong partial rank correlation with mass flows as well. Another important variable in the TRACE model was wall drag, which had high PRCC with all output parameters. Hu (2015) had similar findings in an uncertainty quantification study of TRACE physical models. Even though the studied case was different, liquid to wall HTC and wall drag impacted the results most, along with a few other physical models that are not relevant in this case.

There were differences in SMABRE and TRACE models when it comes to mixing in the reactor pressure vessel. Loop 1 is closest to loop 4, as seen from Figure 8, which means that the mixing of flows between these loops is strong. It could be seen from the plant measurements that especially the temperature in hot leg of loop 4 decreased the most after the flow in loop 1 was reversed compared to hot legs 2 and 3 (Tereshonok et al. 2008). This behaviour was seen with TRACE, which calculates three-dimensional thermal-hydraulics, but not so much in SMABRE. SMABRE calculates one-dimensional thermal-hydraulics, and flow mixing in the reactor pressure vessel is determined by setting mixing coefficients between nodes. It requires more studies, whether these coefficients should be adjusted to simulate the plant behaviour better.

Differences between the results of the HEXTRAN-SMABRE Scenarios 1 and 2 were small apart from the pump speeds and mass flows, even though Scenario 2 was designed to be much harsher. Cooling spray, make-up and letdown systems had the biggest effect on pressure during the first 40 seconds of the transient but little to no effect other than that. The pressure rise, which SMABRE predicts but is not present in measurements and TRACE calculations, is slightly higher in scenario 2. This is probably due to the missing cooling spray, which normally activates in the SMABRE simulation in order to keep the increase in control.

When the results are compared to the uncertainty range of the measurements as shown in Table 3, it can be seen that the calculated standard deviations are much smaller than the measurement errors in all of the output parameters. The core mass flow measurement, for example, which, as discussed in Chapter 2.3, is unreliable for the first 90 seconds of the transient, and after that is in the range of ±800 kg/s. Compared to the simulations with HEXTRAN-SMABRE in scenario 1 and 2 and with TRACE, where the standard deviations were 101, 168 and 34 kg/s, respectively, it is possible to see how large the difference is. Additionally, the used variations, which could be considered quite realistic, did not lead into unexpected results or new scenarios in any of the sensitivity runs. Consequently there are not much uncertainties in this case. Partly this can be explained by the mildness of the transient, for example, there is no boiling in the core, which would multiply the amount of uncertainties in the model. On the other hand, this could also be a sign that the selected uncertainty variations were too narrow or that all sources of uncertainty were not included in the analysis.

Based on the results some improvements to the models can be made. The primary element that needs confirmation for the system models are the homologous pump curves. Once final information about that is received, the models can be updated so that the pump coastdown times and mass flows correspond to the measured values. In addition, there are some uncertainties which were not quantified in this study, such as pressure losses, for which more information is needed from the benchmark team. The TRACE model needed a lot of modifying before any uncertainty runs could be made. Some boundary conditions were removed and control systems added, but further improvements are still needed before the model can be validated. Langenbuch et al. (2005) point out that the plant model should be as complete as possible and include all control and safety systems in order to reveal all possible transient evolutions in the uncertainty and sensitivity analysis. Also, a more detailed core model is needed for further development, for example coupling with the three-dimensional nodal PARCS model.

Another goal of this thesis was to evaluate the capabilities of DAKOTA and Sensla and how they could be improved. With DAKOTA it was not possible to affect many TRACE input file parameters through the SNAP uncertainty stream. Such parameters as geometry, set points or anything that is in table form in TRACE input cannot be affected. This is a clear deficiency in a sensitivity analysis tool. Jeager et al. (2013a) had

similar findings when they compared two sensitivity analysis tools for TRACE. With Sensla it is possible to vary any parameter in the used files, whereas with DAKOTA the options are much more limited. However, it was possible and easy to vary model coefficients inside the code, such as heat transfer coefficients, which would have required modifying the source code in the HEXTRAN-SMABRE calculations. Using Sensla requires some programming skills, whereas DAKOTA was easy to use through the graphical user interface. There were also problems concerning the reporting of the results with DAKOTA. The results in the uncertainty report were not orderly displayed, requiring extra work to obtain the desired results from the DAKOTA output files. Only the output file from the last calculated time step remained, so the results throughout the transient calculation were lost. In the future, the DAKOTA integrated with SNAP will be developed further, which hopefully solves the present problems with TRACE/DAKOTA (Jeager et al. 2013b). Unfortunately, the program cannot be modified without the source code, which VTT does not currently have.

PRCC proved to be a useful sensitivity measure especially when the correlation with one variable was much stronger than with the others. PRCC removes the effect of other variables and shows the correlation between one input variable and output parameter, which revealed some correlations that would have been invisible with just RCC. Unfortunately, the PRCC calculations with Sensla failed. Formula 5 from Chapter 3 was expanded for n variables, but the calculations gave absolute values bigger than one. If one of the RCC values was one, the calculation faced a problem with division with zero. Because of this, PRCC values for HEXTRAN and HEXTRAN-SMABRE had to be rejected. In the future, some other method for PRCC calculation could be programmed to Sensla or it could be calculated with some other code.

Uncertainty and sensitivity analysis requires a lot of experience and knowledge about the codes and the analysis methods. For example, setting too narrow uncertainty ranges for the input parameters does not lead to good quality results. (OECD/NEA/CSNI 2011) The effects of variables, which are not included in the analysis, are not seen and cannot be quantified, which makes the recognising the sources of uncertainty one of the most important steps. The analysis tool and its capabilities also affect the outcome for the same reason. It also complicates the comparison of sensitivity analysis results, when every study is done with different parameter variations. Therefore it is good that in UAM benchmark the variations are given and the goal is that every participant should

try to use the same variations. Salah et al. (2005) proposes that statistical methods should be complemented with deterministic methods, such as the CIAU method, in order to reduce the influence of expert judgement and to get more realistic error bands for the results. This could prove to be a very effective approach if the aim is to get conservative limits for a certain output parameter. However, as seen from the TRACE simulations, which were done with no prior knowledge about the code or the sensitivity analysis tool, the results still gave meaningful information about the greatest sources of uncertainty even though the output uncertainty limits were not necessarily realistic.

TRACE is a new code for transient analysis at VTT, and the work for this thesis gave valuable information about its usability. TRACE and other USNRC CAMP codes are ready code packages, which are easy to take into use. It was easy to use the code through the graphical user interface and the learning curve was not as steep as with VTT's reactor analysis codes. The graphical interface also brings other possibilities, such as animation, which is a useful tool for the interpreting of the results and can be exploited further in the future. However, using SNAP had limitations and some changes to the model had to be made through a text version of the input file. Job stream building in SNAP automatizes the process of running calculation steps sequentially (compare to Sensla, which had to be run manually three times). On the other hand, it remained unclear if it is possible to repeat latter calculation steps, for example the plotting step, without running the whole job stream again. That would be a significant downside, especially now when TRACE is not connected to VTT's Linux cluster and it takes a lot of time to run the simulations. Connecting TRACE to the cluster is another thing that could be studied in the future. Updates and bug fixes for CAMP codes are provided constantly, which could help fixing the current problems, and if VTT received the source codes for the codes, it would enable solving the problems without delay and modifying the codes for VTT's special needs.

8 CONCLUSIONS

In this thesis uncertainty and sensitivity analyses were done for the Kalinin-3 main coolant pump switching off transient, which is a part of OECD/NEA's UAM benchmark. Analyses were done for a separate core model (HEXTRAN), a separate thermal-hydraulic system model (TRACE), and two scenarios for a coupled core-system code model (HEXTRAN-SMABRE). Sources of uncertainty in each model were recognized and uncertainty parameters were given a range and probability distribution using the benchmark specification, previous studies and expert knowledge about the codes as reference. Monte Carlo sampling was applied and the results were analysed statistically. One purpose of this thesis was to quantify the most important sources of uncertainty in the used models, and recognize how the models could be improved by using the knowledge gained from the analyses.

It has been a trend to rank the input uncertainties based on their importance on the system. However, it depends on the output in question, which variable affects it the most, and in this thesis the number of studied outputs was quite large. Nevertheless, in each sensitivity analysis case, a few input uncertainties stood out that had a strong correlation with almost every considered output parameter. Gas gap conductivity was the greatest source of uncertainty in HEXTRAN and the coupled HEXTRAN-SMABRE runs affecting the core thermal output and therefore the whole thermal-hydraulic system. In the separate core calculations, also the core inlet temperature affected most of the output parameters significantly. Neutronics uncertainties caused wide uncertainty limits to the outputs in the separate core and coupled core-system calculations, which shows that neutronics are a great source of uncertainties in a calculation chain like this and should be taken into account in later calculation steps. In the TRACE thermal-hydraulic model liquid to wall heat transfer coefficient and wall drag were the most important sensitivity variables affecting mass flows and temperatures throughout the system. Also the homologous pump curves are a great source of uncertainty in the system models, since the actual curves that should be used are not yet known, and the pump curve determines the mass flows completely. There are no uncertainty studies done for this particular case yet, but studies for different cases have shown similar results.

Simulations done in this study did not lead to unexpected events or different scenarios. That may be due to the fact that this transient is quite mild and there are not many uncertainties in this case. It is also possible that all sources of uncertainty were not recognized or they were given too narrow uncertainty ranges, which leads to unrealistic results. Uncertainty and sensitivity analysis requires a lot of experience and knowledge about the used codes and models. In the future, the effect of user judgement on the results should be mitigated somehow.

In the future, the TRACE model needs to be validated and a three-dimensional core model is needed for that, for example coupling with PARCS. There are still some boundary conditions that should be removed and control systems added. Both TRACE and SMABRE model need some adjustments after the final information about pump curves is received. The coastdown time of pumps has to be fixed in TRACE model and mass flows tuned in both models. Mixing coefficients in SMABRE model need more investigation whether they should be adjusted. One consideration for the future is to connect TRACE to VTT's Linux cluster for faster simulations.

Sensitivity analysis tools used in this thesis were Sensla for the HEXTRAN-SMABRE simulations and DAKOTA for the TRACE simulations. Both of these tools used a statistical method, which is widely used and recognized as good method for complex systems such as nuclear power plant models. There were, however, differences in their capabilities and reporting of results. Uncertainty parameters used in DAKOTA were mainly physical models inside the code, whereas Sensla enabled variations for every input parameter. Enabling physical model variations in HEXTRAN and SMABRE requires modifying their source codes, but it could be a good feature to have for the future sensitivity analyses.

Both programs used RCC as a sensitivity measure and DAKOTA calculated PRCC in addition to that. There was an attempt to code PRCC calculation into Sensla as well, which unfortunately failed. RCC and PRCC are good sensitivity measures for models like these, where the relationship between input and output parameters is usually monotonic but non-linear. PRCC reveals correlations that are not necessarily seen with just RCC. Therefore it is important to include it in Sensla in the future as well. There were several problems with reporting the results with DAKOTA, which require

notifying the code developers or access to the source codes, so that the bugs can be fixed.

Due to this thesis, VTT's sensitivity analysis tool was modified so that it can be used for separate HEXTRAN core models in the future, and its features for the Kalinin-3 model were broadened. Once the UAM benchmark team provides the final specifications, these uncertainty and sensitivity studies can be done again with the suggested parameter variations for HEXTRAN and HEXTRAN-SMABRE, and the results can be compared and discussed with other benchmark participants. TRACE was introduced to VTT's Reactor analysis team as a new code for safety analyses, and the development of Kalinin-3 model for TRACE was started. TRACE, DAKOTA and SNAP are all extensive codes, which is why their all features could not be explored in such a short time, but they seem to be a promising addition to VTT's calculation system.

9 REFERENCES

Adams, B. M., Ebeida, M. S., Eldred, M. S., Geraci, G., Jakeman, J. D., Maupin, K. A., Monschke, J. A., Stephens, J. A., Swiler, L. P., Vigil, D. M., Wildey, T. M., Bohnhoff, W. J., Dalbey, K. R., Eddy, J. P, Frye, J. R., Hooper, R. W., Hu, K. T., Hough, P. D., Khalil, M., Ridgway, E. M., Winokur, J. G. & Rushdi, A., 2010. DAKOTA. A Multilevel Parallel Object-Oriented Framework for Design Optimization, Parameter Estimation, Uncertainty Quantification, and Sensitivity Analysis: Version 6.8 User's Manual. Albuquerque: Sandia National Laboratories. SAND2010-2185. 386 p.

Georgieva, E. L., 2016. Development of a Cross Section Methodology and a Real Time Core Model for VVER 1000 Simulator Application. Karlsruhe: Karlsruhe Institute of Technology. Dr.Tech. Thesis. 125 p. + app. 53 p.

Glaeser, H., 2008. GRS Method for Uncertainty and Sensitivity Evaluation of Code Results and Applications. Science and Technology of Nuclear Installation, 2008, 798901, 7 p.

Glaeser, H., 2013. Summary of existing uncertainty methods. In: OECD/CSNI Workshop on Best Estimate Methods and Uncertainty Evaluations, Workshop Proceedings Barcelona, Spain, 16-18 November 2011. OECD Nuclear Energy Agency.NEA/CSNI/R(2013)8/PART2. p. 5-15.

Hong, I. S., Oh, D. Y. & Kim, I. G., 2013. Generic Application of Wilks' Tolerance Limit Evaluation Approach to Nuclear Safety. In: OECD/CSNI Workshop on Best Estimate Methods and Uncertainty Evaluations, Workshop Proceedings Barcelona, Spain, 16-18 November 2011. OECD Nuclear Energy Agency. NEA/CSNI/R(2013)8/PART2. p. 16-25.

Hou, J., Avramova, M., Ivanov, K., Royer, E., Jessee, M., Zhang, J., Wieselquist, W., Pasichnyk, I., Zwermann, W., Velkov, K., Kozlowski, T. & Le-Pallec, J-C., 2019a. Benchmark for Uncertainty Analysis in Modelling (UAM) for Design, Operation and Safety Analysis of LWRs. Volume III: Specification and Support Data for the System Cases (Phase III). Version 1.2. OECD Nuclear Energy Agency. NEA/NSC/DOC(2019). 82 p.

Hou, J., Blyth, T., Porter, N., Avramova, M., Ivanov, K., Royer, E., Sartori, E., Cabellos, O., Feroukhi, H. & Ivanov, E., 2019b. Benchmark for Uncertainty Analysis in Modelling (UAM) for Design, Operation and Safety Analysis of LWRs. Volume II: Specification and Support Data for the Core Cases (Phase II). Version 1.9. OECD Nuclear Energy Agency. NEA/NSC/DOC(2014). 124 p.

Hu, G., 2015. Inverse uncertainty quantification of TRACE physical model parameters using Bayesian analysis. Urbana: University of Illinois. Master's thesis. 57 p.

Ikonen, T. & Tulkki, V., 2014. The importance of input interactions in the uncertainty and sensitivity analysis of nuclear fuel behaviour. Nuclear Engineering and Design, 275, p. 229-241.

Iman, R. L. & Conover, W. J., 1982. Sensitivity Analysis Techniques: Self-Teaching Curriculum. Albuquerque: Sandia National Laboratories. NUREG/CR-2350 SAND81-1978, 146 p.

Ivanov, B., Ivanov, K., Groudev, P., Pavlova, M. & Hadjiev, V., 2002. VVER-1000 Coolant Transient Benchmark Phase I (V1000CT-1) Vol. I: Main Coolant Pump (MCP) Switching On - Final Specifications. OECD Nuclear Energy Agency. NEA/NSC/DOC/(2002)6. 171 p.

Jaeger, W., Sánchez Espinoza, V. H., Montero Mayorga, F. J., & Queral, C., 2013a. Uncertainty and Sensitivity Studies with TRACE-SUSA and TRACE-DAKOTA by Means of Steady State BFBT Data. Science and Technology of Nuclear Installations, 2013.11 p.

Jaeger, W., Sánchez Espinoza, V. H., Montero Mayorga, F. J., & Queral, C., 2013b. Uncertainty and Sensitivity Studies with TRACE-SUSA and TRACE-DAKOTA by Means of Transient BFBT Data. Science and Technology of Nuclear Installations, 2013. 9 p.

Kyrki-Rajamäki, R., 1995. Three-dimensional reactor dynamics code for VVER type nuclear reactors. Espoo: VTT Technical Research Centre of Finland. VTT Publications 246. Dr.Tech. Thesis. 51 p. + app. 80 p.

Langenbuch, S. Krzykacz-Hausmann, B. Schmidt, K.-D. Hegyi, G. Keresztúri, A. Kliem, S. Hadek, J. Danilin, S. Nikonov, S. Kuchin, A. Khalimanchuk, V. Hämäläinen, A., 2005. Comprehensive uncertainty and sensitivity analysis for coupled code calculations of VVER plant transients. Nuclear Engineering and Design, 235(2–4), p. 521-540.

Marino, S., Hogue, I. B., Ray, C. J. & Kirschner, D. E., 2008. A methodology for performing global uncertainty and sensitivity analysis in systems biology. Journal of Theoretical Biology, 254(1), p. 178-196.

Marchand, E., Clément, F., Roberts, J. E. & Pépin, G., 2008. Deterministic sensitivity analysis for a model for flow in porous media. Advances in Water Resources, 31(8), p. 1025-1037.

Miettinen, J., 2000. Thermohydraulic model SMABRE for light water reactor simulations. Helsinki: Helsinki University of Technology. Licentiate thesis. 151 p.

Mui, T. C., 2015. TRACE code validation of boiling water reactor spray cooling injection into a SVEA fuel assembly [web]. Urbana: University of Illinois. Master's thesis. 63 p. Available: http://hdl.handle.net/2142/89030 [accessed 18.10.2019]

OECD/NEA, 2016. Expert Group on Uncertainty Analysis in Modelling (UAM-LWR) [web page]. Available: https://www.oecd-nea.org/science/wprs/egrsltb/UAM/index.html [accessed 27.11.209]

OECD/NEA/CSNI, 1994. Report of a CSNI Workshop on Uncertainty Analysis Methods. CSNI report. NEA/CSNI/R(94)20/Part.1. 56 p.

OECD/NEA/CSNI, 2011. BEMUSE Phase VI Report - Status report on the area, classification of the methods, conclusions and recommendations. CSNI report. NEA/CSNI/R(2011)4. 122 p.

OECD/NEA/CSNI, 2013. OECD/CSNI Workshop on Best Estimate Methods and Uncertainty Evaluations. Workshop Proceedings Barcelona, Spain, 16-18 November 2011. OECD Nuclear Energy Agency. NEA/CSNI/R(2013)8/PART2. 326 p.

Peltokorpi, L., 2009. Developing of Uncertainty Analysis System for APROS Safety Simulation Environment. Helsinki: Helsinki University of Technology. Master's thesis. 70 p.

Porter, N., Avramova, M. & Ivanov, K., 2015. Uncertainty and sensitivity analysis of COBRA-TF for the OECD LWR UAM benchmark using Dakota. International Topical Meeting on Nuclear Reactor Thermal Hydraulics NURETH, 6, p. 4894-4906.

Rosenergatom, 2018. Nuclear Power Plants, Kalinin NPP [web]. Available: https://www.rosenergoatom.ru/en/npp/kalinin-npp/ [accessed 16.10.2019].

Salah, A., Kliem, S., Rohde, U., D'Auria, F. & Petruzzi, A., 2006. Uncertainty and sensitivity analyses of the Kozloduy pump trip test using coupled thermal-hydraulic 3D kinetics code. Nuclear Engineering And Design, 236(12), p. 1240-1255.

Sandberg, J. (edit.), 2018. Ydinturvallisuus. 3rd edition. Helsinki: Säteilyturvakeskus. 418 p. ISBN 951-712-500-3

STUK, 2018. Radiation and Nuclear Safety Authority Regulation on the Safety of a Nuclear Power Plant. STUK Y/1/2018 [web]. Available: https://www.stuklex.fi/en/maarays/stuk-y-1-2018 [accessed 14.11.2019]

STUK, 2019. YVL B.3 Deterministic safety analyses for a nuclear power plant [web page]. Available: https://www.stuklex.fi/en/ohje/YVLB-3 [accessed 27.11.2019]

Syrjälahti, E., 2005. New sensitivity analysis tool for the reactor dynamic codes. Espoo: Technical Research Centre of Finland. PRO1/1016/05, 9 p. + app. 26 p.

Syrjälahti, E., 2006. New sensitivity analysis tool for VTT's reactor dynamic codes. Espoo: Technical Research Centre of Finland. Conference paper IYNC 2006. Paper No. 181. 11 p.

Syrjälahti, E., 2008. Development of sensitivity and uncertainty analysis tool for reactor dynamics codes. Espoo: Technical Research Centre of Finland. VTT-R-00843-08, 15 p.

Syrjälahti, E., 2011. Characterization of a representative VVER-440 fuel rod with the statistical ENIGMA. Espoo: Technical Research Centre of Finland. VTT-R-08464-11, 18 p.

Syrjälahti, E., 2018a. Kalinin-3 – Model report and simulation of the benchmark problem. Espoo: VTT Technical Research Center of Finland. Research report VTT-R-06914-18. 29 p.

Syrjälahti, E., 2018b. Preliminary simulations of the Kalinin-3 benchmark problem for uncertainty and sensitivity analyses. Espoo: VTT Technical Research Center of Finland. Research report VTT-R-06972-18. 16 p.

Tereshonok, V.A., Nikonov, S.P., Lizorkin, M.P., Velkov, K., Pautz, A. & Ivanov, K., 2008. Kalinin - 3 Coolant Transient Benchmark - Switching-off of One of the Four Operating Main Circulation Pumps at Nominal Reactor Power. OECD Nuclear Energy Agency. NEA/NSC/DOC(2009)5. 95 p.

Tereshonok, V.A., Nikonov, S.P., Lizorkin, M.P., Velkov, K., Pautz, A. & Ivanov, K., 2019. International benchmark for coupled codes and uncertainty analysis is modelling: Switching-off of one of the four operating main circulation pumps at nominal reactor power at Kalinin unit 3 [web document]. Available: https://inis.iaea.org/collection/NCLCollectionStore/_Public/40/059/40059709.pdf?r=1&r=1 [accessed 20.11.2019]. 14p.

Tóth, B., 2015. Development of an integral VVER- 1000 Plant Model for the best-estimate code system TRACE. Karlsruhe: Karlsruhe Institute of Technology. Internship report. 44 p.

USDOE Assistant Secretary for Nuclear Energy, 1987. Overall Plant Design Descriptions VVER Water-Cooled, Water-Moderated Energy Reactor. Washington D.C.: U.S. Department of Energy. Technical report. DOE/NE-0084 Revision 1.

U.S. Nuclear Regulatory Commission, 2017. TRACE V5.0 Patch 5 User's Manual Volume 1: Input Specification. Washington DC: U.S. Nuclear Regulatory Commission.

Appendix 1. Figure of the Kalinin-3 fuel assembly layout in the reactor core.

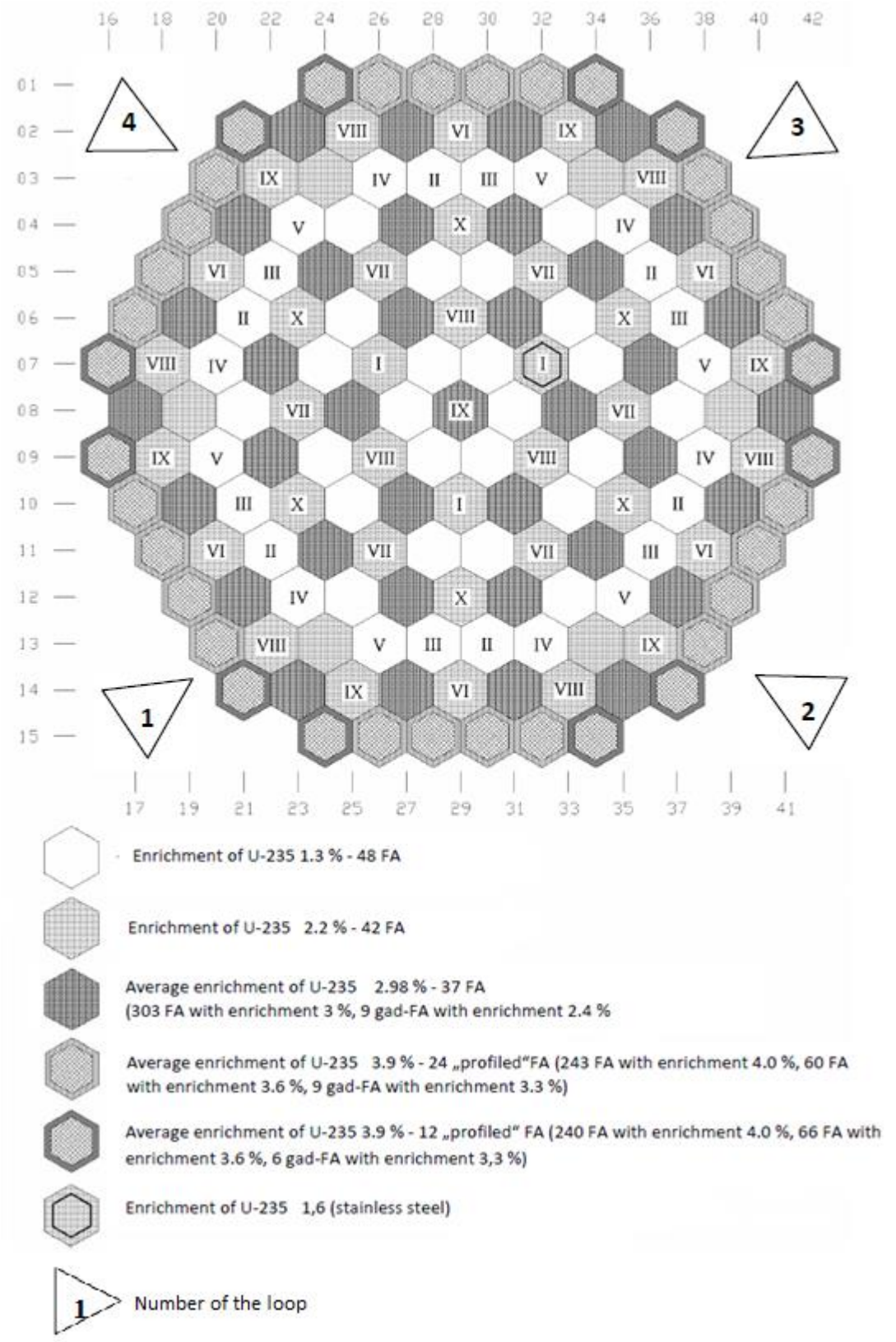

Figure 47. Kalinin-3 fuel assembly layout in the reactor core and locations of control rod groups I-X (modified from Tereshonok et al. 2019).

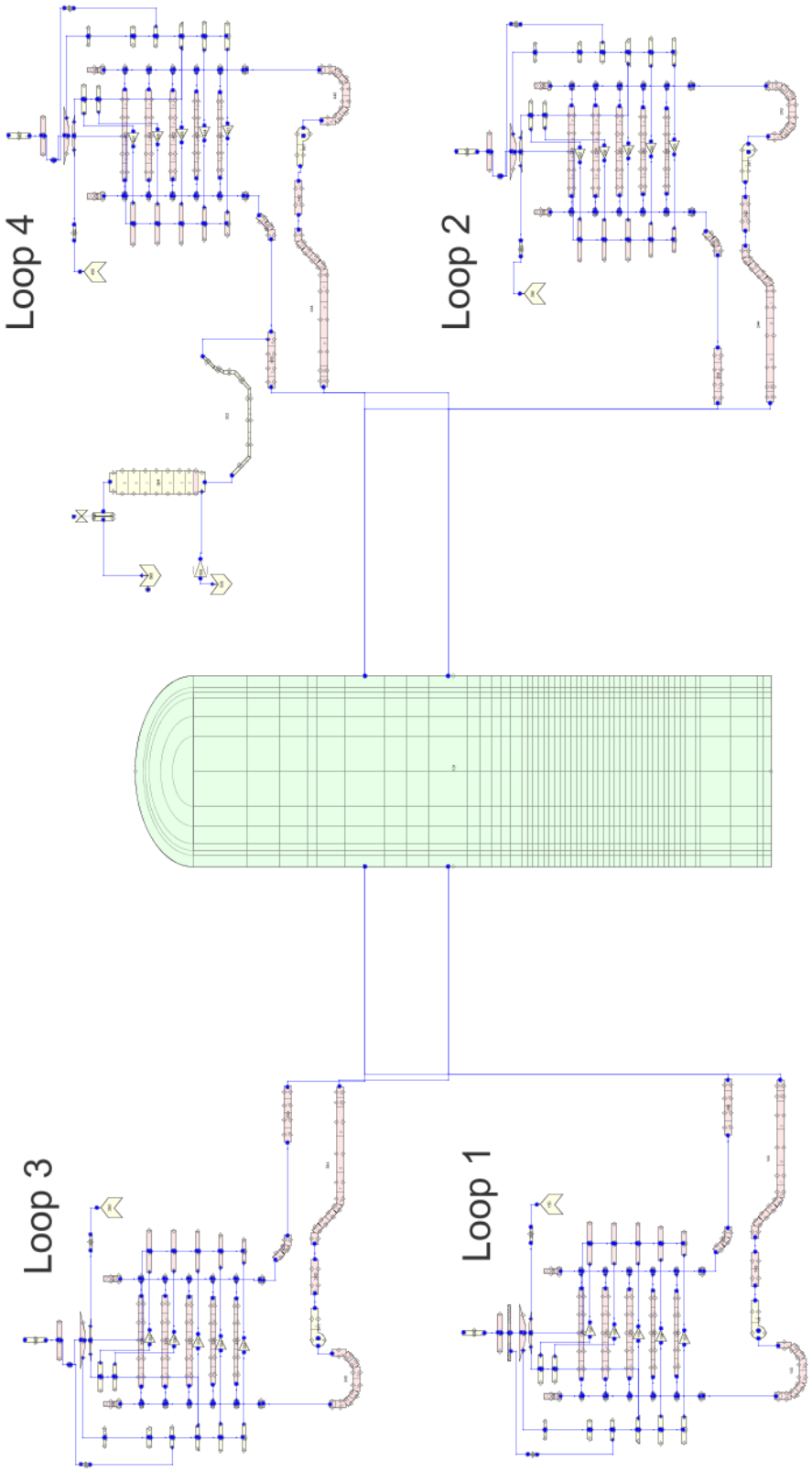

Figure 48. The Kalinin-3 TRACE model reactor, primary loops, steam generators and pressurizer as seen in SNAP.

Table 6. The minimum, maximum and mean values and standard deviations (SD) with and without cross-section file variations (XS) of output parameters in stand-alone HEXTRAN at the end of the simulations.

Output parameter	**Mean**	**Minimum**	**Maximum**	**SD (XS)**	**SD (without XS)**
Power (MW)	2329	2029	2611	161	149
Core mean density (kg/m3)	720.8	714.6	727.5	3.6	3.8
Mean fuel temperature (°C)	506.1	465.9	557.1	20.7	19.7
Core outlet pressure (MPa)	15.50	15.23	15.77	0.15	0.16
Mean water temperature (°C)	302.2	299.2	305.1	1.7	1.8
Max peaking factor	2.47	2.35	2.56	0.04	0.01
Max assembly-wise peaking factor	1.30	1.26	1.36	0.02	0.00
Core mass flow (kg/s)	13541	13109	14049	267	267
Press. difference over core (MPa)	0.141	0.1401	0.1411	0.0003	0.0026
Max fuel temperature (°C)	1128.6	965.9	1314.8	76.3	52.8

Table 7. The rank correlation coefficients from stand-alone HEXTRAN at the end of the transient.

	CR worth	gas gap	fuel cond.	clad cond.	fuel out. rad.	clad in. rad.	clad out. rad.	fuel in. rad.	mass flow	inlet water temp.	pressure	power
power	-0.157	-0.248	0.055	-0.073	0.005	-0.226	0.163	-0.030	0.084	-0.976	0.033	-0.095
water density	-0.123	0.013	0.048	-0.065	-0.010	-0.214	0.152	-0.010	0.135	-0.994	0.039	-0.117
mean fuel temp.	-0.134	-0.860	0.111	-0.003	0.091	-0.139	0.132	-0.065	-0.059	-0.525	0.020	-0.141
core outlet pressure	-0.036	0.000	0.056	0.135	-0.069	-0.120	0.010	0.122	0.116	0.012	1.000	-0.025
mean water temp.	0.119	-0.008	-0.036	0.072	0.008	0.201	-0.146	0.017	-0.124	0.996	0.043	0.120
max peak.	0.044	0.960	-0.084	-0.018	-0.132	-0.007	-0.045	0.047	0.182	-0.166	0.012	0.085
max assemb. peak.	0.014	0.836	-0.046	-0.033	-0.144	-0.078	-0.002	0.064	0.210	-0.457	0.032	-0.036
core mass flow	0.037	0.169	-0.050	0.150	-0.121	0.118	-0.019	0.010	1.000	-0.125	0.116	-0.129
press diff.	0.110	-0.165	-0.024	0.057	0.033	0.218	-0.127	0.004	-0.158	0.968	-0.037	0.085
max fuel temp.	-0.116	-0.650	-0.026	-0.016	0.042	-0.207	0.137	-0.082	0.009	-0.746	0.043	-0.091

Table 8. The minimum, maximum and mean values and standard deviations (SD) with and without cross-section file variations (XS) of output parameters in HEXTRAN-SMABRE Scenario 1 at the end of simulations.

Output parameter	**Mean**	**Minimum**	**Maximum**	**SD (XS)**	**SD (without XS)**
Power (MW)	2137	2073	2194	27.47	22.49
Core mean density (kg/m^3)	713.7	710.9	716.7	1.43	0.65
Mean fuel temperature (°C)	497.7	470.3	526.0	15.63	15.50
Mean water temperature in core (°C)	305.3	303.9	306.5	0.63	0.30
Max peaking factor	2.523	2.441	2.582	0.033	0.010
Max assembly-wise peaking factor	1.285	1.238	1.340	0.023	0.002
Core mass flow (kg/s)	13438	13311	13654	136.09	101.23
Press. difference over core (MPa)	0.945	0.938	0.957	0.007	0.006
Max fuel temperature (°C)	1080.5	986.5	1160.4	47.64	33.28
Upper plenum pressure (MPa)	15.53	15.47	15.61	0.04	0.04
PRZ press (MPa)	15.49	15.42	15.57	0.04	0.04
CL1 temperature (°C)	286.1	285.6	286.5	0.20	0.16
CL2 temperature (°C)	286.3	285.8	286.7	0.21	0.16
CL3 temperature (°C)	286.4	285.9	286.9	0.22	0.17
CL4 temperature (°C)	285.9	285.4	286.3	0.20	0.16
HL1 temperature (°C)	275.3	275.1	275.5	0.09	0.07
HL2 temperature (°C)	311.0	310.0	312.3	0.63	0.43
HL3 temperature (°C)	311.4	310.3	312.7	0.64	0.43
HL4 temperature (°C)	310.0	309.1	311.3	0.59	0.41
CL1 mass flow (kg/s)	-1629	-1751	-1541	87.7	70.0
CL2 mass flow (kg/s)	5153	5082	5267	73.4	53.8
CL3 mass flow (kg/s)	5150	5079	5264	73.1	53.6
CL4 mass flow (kg/s)	5173	5100	5289	75.2	55.1

Table 9. The rank correlation coefficients from HEXTRAN-SMABRE Scenario 1 at the end of the simulations.

	FW limit	heater power	heater lower	heater upper	pump curve	CR worth	gas gap	fuel cond.	clad cond.	fuel out. rad.	clad in. rad.	clad out. rad.	fuel in. rad.
Power	0.036	-0.137	0.139	-0.117	-0.058	0.006	-0.978	-0.171	-0.126	-0.039	-0.035	-0.069	0.100
Core mean density	-0.019	0.173	-0.041	0.243	-0.065	0.001	0.945	0.186	0.114	-0.005	0.059	0.021	-0.075
Mean fuel temperature	0.049	-0.141	0.104	-0.151	-0.017	-0.014	-0.995	-0.111	-0.132	-0.032	-0.057	-0.050	0.128
Mean water temperature	0.014	-0.111	0.061	-0.155	0.099	0.008	-0.952	-0.164	-0.120	-0.001	-0.040	-0.060	0.067
Max peak	-0.060	0.154	-0.142	0.141	0.098	-0.001	0.974	0.150	0.121	0.065	0.052	0.060	-0.126
Max assemb. peak	-0.021	0.148	-0.059	0.196	-0.068	0.004	0.965	0.177	0.125	0.014	0.046	0.044	-0.074
Core mass flow	-0.003	-0.043	0.071	0.096	-0.733	0.038	0.179	0.037	0.097	-0.001	-0.001	-0.071	0.061
Press. difference over core	-0.016	-0.018	0.113	-0.053	-0.926	0.138	0.123	0.018	0.084	0.019	-0.019	0.015	0.083
Max fuel temperature	0.033	-0.161	0.110	-0.186	-0.005	0.017	-0.939	-0.341	-0.104	-0.044	-0.022	-0.055	0.037
Upper plenum press.	-0.154	0.291	0.153	0.730	0.214	0.047	-0.068	0.203	0.027	-0.023	0.163	-0.172	-0.064
PRZ press.	-0.154	0.288	0.154	0.729	0.215	0.046	-0.066	0.205	0.028	-0.024	0.167	-0.170	-0.064
CL1 temp.	0.030	-0.135	0.128	-0.125	-0.095	0.006	-0.972	-0.182	-0.129	-0.044	-0.039	-0.063	0.107
CL2 temp.	0.034	-0.132	0.127	-0.137	-0.102	0.004	-0.974	-0.182	-0.137	-0.039	-0.040	-0.060	0.112
CL3 temp.	0.035	-0.135	0.118	-0.130	-0.086	0.005	-0.974	-0.184	-0.136	-0.050	-0.043	-0.063	0.103
CL4 temp.	0.033	-0.137	0.126	-0.119	-0.089	0.009	-0.971	-0.180	-0.133	-0.047	-0.041	-0.059	0.104
HL1 temp.	0.214	-0.156	0.105	0.122	0.189	0.010	-0.571	-0.147	-0.085	-0.150	0.016	-0.078	0.005
HL2 temp.	0.012	-0.105	0.003	-0.233	0.058	0.010	-0.845	-0.120	-0.098	0.074	-0.069	-0.034	0.056
HL3 temp.	0.011	-0.109	0.007	-0.228	0.069	0.009	-0.861	-0.124	-0.098	0.069	-0.067	-0.038	0.061
HL4 temp.	0.010	-0.111	0.006	-0.223	0.072	0.009	-0.866	-0.125	-0.100	0.063	-0.066	-0.040	0.062
CL1 mass flow	0.117	-0.044	-0.096	-0.294	-0.206	-0.045	-0.148	0.060	-0.086	0.234	-0.094	-0.021	0.045
CL2 mass flow	-0.090	-0.010	0.067	0.277	-0.118	0.027	0.160	-0.041	0.112	-0.172	0.060	-0.048	-0.024
CL3 mass flow	-0.091	-0.011	0.068	0.276	-0.118	0.027	0.160	-0.042	0.111	-0.172	0.059	-0.048	-0.025
CL4 mass flow	-0.090	-0.011	0.068	0.276	-0.118	0.026	0.160	-0.042	0.111	-0.172	0.058	-0.048	-0.025

Table 10. The minimum, maximum and mean values and standard deviations (SD) with and without cross-section file variations (XS) of output parameters at the end of the HEXTRAN-SMABRE Scenario 2 simulations.

Output parameter	**Mean**	**Minimum**	**Maximum**	**SD (XS)**	**SD (without XS)**
Power (MW)	2128	2066	2176	29.16	21.81
Core mean density (kg/m^3)	713.7	710.8	716.8	1.44	0.69
Mean fuel temperature (°C)	496.3	470.0	528.5	16.74	15.01
Mean water temperature in core (°C)	305.3	304.0	306.4	0.62	0.32
Max peaking factor	2.526	2.454	2.595	0.034	0.009
Max assembly-wise peaking factor	1.287	1.241	1.331	0.020	0.002
Core mass flow (kg/s)	13295	13071	13655	178.70	168.28
Press. difference over core (MPa)	0.934	0.916	0.957	0.013	0.012
Max fuel temperature (°C)	1076.3	980.3	1179.0	50.74	32.58
Upper plenum pressure (MPa)	15.57	15.48	15.65	0.05	0.04
PRZ press (MPa)	15.52	15.43	15.61	0.05	0.04
CL1 temperature (°C)	286.0	285.5	286.4	0.22	0.16
CL2 temperature (°C)	286.1	285.6	286.6	0.24	0.17
CL3 temperature (°C)	286.3	285.7	286.7	0.24	0.17
CL4 temperature (°C)	285.8	285.3	286.2	0.22	0.16
HL1 temperature (°C)	275.3	275.0	275.5	0.12	0.12
HL2 temperature (°C)	310.8	309.6	312.1	0.64	0.49
HL3 temperature (°C)	311.2	310.0	312.5	0.65	0.48
HL4 temperature (°C)	309.9	308.8	311.0	0.59	0.45
CL1 mass flow (kg/s)	-1758	-1948	-1542	150.5	152.1
CL2 mass flow (kg/s)	5148	5082	5278	58.7	58.2
CL3 mass flow (kg/s)	5144	5078	5275	58.5	58.0
CL4 mass flow (kg/s)	5166	5100	5300	60.1	59.6

Table 11.1. The rank correlation coefficients from HEXTRAN-SMABRE Scenario 2 at the end of the simulations.

	FW limit	heater power	heater lower	heater upper	pump curve	CR worth	gas gap	fuel cond.	clad cond.
Power	0.146	-0.183	0.228	-0.186	-0.069	0.251	-0.954	-0.138	0.151
Core mean density	-0.097	0.282	-0.089	0.202	-0.100	-0.210	0.920	0.174	-0.013
Mean fuel temperature	0.116	-0.231	0.195	-0.233	-0.025	0.246	-0.994	-0.090	0.087
Mean water temperature	0.129	-0.271	0.123	-0.117	0.103	0.214	-0.924	-0.175	0.010
Max peak	-0.107	0.179	-0.236	0.258	0.101	-0.243	0.943	0.092	-0.149
Max assemb. peak	-0.087	0.274	-0.100	0.187	-0.076	-0.221	0.933	0.169	0.008
Core mass flow	0.004	0.146	0.125	-0.027	-0.305	0.012	0.166	0.133	0.251
Press. difference over core	0.058	0.113	0.124	0.036	-0.344	-0.025	0.141	0.137	0.277
Max fuel temperature	0.123	-0.230	0.150	-0.221	0.016	0.241	-0.945	-0.297	0.078
Upper plenum press.	0.268	0.142	0.193	0.689	0.063	-0.003	-0.035	-0.029	-0.004
PRZ press.	0.269	0.141	0.194	0.691	0.063	-0.005	-0.033	-0.028	-0.001
CL1 temp.	0.143	-0.161	0.242	-0.217	-0.078	0.244	-0.911	-0.107	0.196
CL2 temp.	0.161	-0.153	0.260	-0.204	-0.077	0.239	-0.880	-0.098	0.226
CL3 temp.	0.154	-0.163	0.236	-0.213	-0.070	0.247	-0.914	-0.114	0.199
CL4 temp.	0.138	-0.165	0.238	-0.217	-0.076	0.246	-0.921	-0.111	0.188
HL1 temp.	-0.028	-0.026	0.039	-0.120	0.019	0.174	-0.367	-0.130	-0.274
HL2 temp.	0.293	-0.203	0.166	-0.076	0.124	0.200	-0.756	-0.076	0.273
HL3 temp.	0.278	-0.215	0.157	-0.087	0.123	0.213	-0.803	-0.101	0.243
HL4 temp.	0.273	-0.219	0.160	-0.087	0.126	0.213	-0.814	-0.104	0.230
CL1 mass flow	0.242	-0.058	0.071	0.087	0.069	-0.026	-0.076	0.107	0.336
CL2 mass flow	-0.328	0.151	0.031	-0.157	-0.246	0.010	0.093	-0.013	-0.163
CL3 mass flow	-0.326	0.153	0.032	-0.156	-0.244	0.013	0.095	-0.014	-0.158
CL4 mass flow	-0.323	0.154	0.033	-0.156	-0.237	0.016	0.092	-0.013	-0.156

Table 11.2. The rank correlation coefficients from HEXTRAN-SMABRE Scenario 2 at the end of the simulations.

	fuel out. rad.	clad in. rad.	clad out. rad.	fuel in. rad.	spray	makeup	letdown	pump lock
Power	0.054	-0.036	-0.008	-0.179	0.157	0.177	0.092	0.187
Core mean density	-0.083	-0.082	-0.003	0.198	-0.143	-0.025	-0.056	0.065
Mean fuel temperature	0.065	0.005	0.011	-0.152	0.167	0.118	0.089	0.052
Mean water temperature	0.091	0.078	-0.017	-0.178	0.145	0.104	0.025	-0.063
Max peak	-0.043	0.050	0.006	0.153	-0.164	-0.112	-0.119	-0.197
Max assemb. peak	-0.079	-0.064	0.003	0.167	-0.158	-0.075	-0.052	0.124
Core mass flow	-0.097	-0.196	-0.060	0.035	-0.053	-0.017	0.095	0.593
Press. diff. over core	-0.092	-0.186	-0.080	0.039	-0.068	0.036	0.083	0.593
Max fuel temperature	0.078	0.000	-0.003	-0.220	0.141	0.107	0.077	0.055
Upper plenum pressure	0.066	-0.013	-0.088	0.090	-0.055	0.623	-0.268	-0.057
PRZ press	0.064	-0.010	-0.087	0.088	-0.057	0.621	-0.267	-0.053
CL1 temp.	0.058	-0.050	-0.009	-0.190	0.145	0.089	0.107	0.324
CL2 temp.	0.061	-0.055	-0.019	-0.206	0.133	0.093	0.114	0.400
CL3 temp.	0.064	-0.049	-0.016	-0.199	0.150	0.093	0.102	0.325
CL4 temp.	0.055	-0.049	-0.007	-0.187	0.149	0.094	0.103	0.296
HL1 temp.	-0.007	0.079	0.102	0.062	0.129	0.065	-0.026	-0.767
HL2 temp.	0.123	0.018	-0.047	-0.291	0.065	0.098	0.033	0.470
HL3 temp.	0.123	0.025	-0.047	-0.280	0.090	0.103	0.028	0.398
HL4 temp.	0.122	0.032	-0.043	-0.277	0.090	0.102	0.029	0.382
CL1 mass flow	0.045	-0.056	-0.035	-0.190	-0.107	-0.051	0.039	0.854
CL2 mass flow	-0.084	-0.092	0.032	0.241	0.152	0.009	0.024	-0.388
CL3 mass flow	-0.083	-0.095	0.032	0.239	0.150	0.012	0.024	-0.383
CL4 mass flow	-0.083	-0.098	0.032	0.240	0.148	0.012	0.024	-0.376

Table 12. The minimum, maximum and mean values and standard deviations of output parameters in TRACE at the end of simulations.

Output parameter	**Mean value**	**Minimum**	**Maximum**	**Standard deviation**
Upper plenum pressure (MPa)	15.20	14.95	15.37	0.07
PRZ press (MPa)	15.11	14.86	15.28	0.07
CL1 mass flow (kg/s)	-1167	-1175	-1160	4
CL2 mass flow (kg/s)	4855	4834	4882	13
CL3 mass flow (kg/s)	4840	4822	4864	12
CL4 mass flow (kg/s)	4888	4867	4914	13
CL1 temperature (°C)	555.4	554.9	555.9	0.2
CL2 temperature (°C)	556.9	556.4	557.4	0.3
CL3 temperature (°C)	557.2	556.7	557.7	0.3
CL4 temperature (°C)	555.0	554.6	555.4	0.2
HL1 mass flow (kg/s)	-1166	-1175	-1160	4
HL2 mass flow (kg/s)	4856	4834	4882	13
HL3 mass flow (kg/s)	4840	4823	4865	12
HL4 mass flow (kg/s)	4885	4864	4911	13
HL1 temperature (°C)	547.9	547.6	548.1	0.1
HL2 temperature (°C)	580.3	579.7	580.8	0.3
HL3 temperature (°C)	581.5	580.9	582.0	0.3
HL4 temperature (°C)	574.3	573.7	574.7	0.2
Core mass flow (kg/s)	13416	13362	13485	34

Table 13. The rank correlation coefficients between input parameters and output variables at the end of the TRACE simulations.

	pressure boundary condition	fuel cond.	clad cond.	heat loss	gas gap cond.	liquid to wall HTC	vapor to wall HTC	wall drag	power	heater power
upper plenum pressure	0.682	-0.053	0.008	0.047	0.137	0.157	-0.021	-0.469	-0.013	-0.032
PRZ pressure	0.687	-0.054	0.006	0.048	0.139	0.160	-0.022	-0.462	-0.014	-0.031
CL1 mass flow	0.054	0.030	-0.020	-0.023	-0.017	-0.055	-0.011	0.995	-0.060	0.016
CL2 mass flow	-0.051	-0.037	0.020	0.028	0.025	0.120	0.019	-0.986	0.044	-0.027
CL3 mass flow	-0.044	-0.038	0.020	0.030	0.020	0.139	0.024	-0.982	0.039	-0.029
CL4 mass flow	-0.054	-0.037	0.016	0.023	0.019	0.085	0.010	-0.992	0.054	-0.018
CL1 temp.	0.010	0.000	-0.045	-0.032	0.018	-0.983	-0.039	0.114	0.100	0.044
CL2 temp.	0.006	-0.001	-0.044	-0.011	0.014	-0.985	-0.036	0.100	0.100	0.042
CL3 temp.	0.006	-0.002	-0.048	-0.010	0.015	-0.986	-0.038	0.098	0.099	0.043
CL4 temp.	0.006	0.000	-0.046	-0.014	0.015	-0.985	-0.035	0.103	0.102	0.043
HL1 mass flow	0.054	0.031	-0.020	-0.022	-0.017	-0.058	-0.010	0.995	-0.060	0.016
HL2 mass flow	-0.052	-0.038	0.019	0.028	0.025	0.119	0.019	-0.986	0.044	-0.027
HL3 mass flow	-0.044	-0.038	0.021	0.029	0.020	0.138	0.024	-0.982	0.040	-0.030
HL4 mass flow	-0.052	-0.039	0.017	0.022	0.021	0.091	0.010	-0.991	0.051	-0.017
HL1 temp.	0.012	0.007	-0.051	-0.054	0.021	-0.975	-0.043	0.149	0.104	0.042
HL2 temp.	0.034	0.008	-0.055	-0.032	0.013	-0.926	-0.047	0.269	0.207	0.025
HL3 temp.	0.038	0.007	-0.055	-0.030	0.012	-0.928	-0.044	0.260	0.214	0.024
HL4 temp.	0.037	0.011	-0.049	-0.039	0.012	-0.918	-0.041	0.291	0.210	0.026
core mass flow	-0.049	-0.039	0.020	0.029	0.022	0.121	0.018	-0.986	0.044	-0.028

Table 14. The partial rank correlation coefficients between input parameters and output variables at the end of the TRACE simulations.

	pressure boundary condition	fuel cond.	clad cond.	heat loss	gas gap cond.	liquid to wall HTC	vapor to wall HTC	wall drag	power	heater power
upper plenum pressure	0.838	0.002	-0.038	0.126	0.266	0.334	-0.057	-0.744	-0.098	0.022
PRZ pressure	0.839	-0.001	-0.041	0.129	0.269	0.342	-0.058	-0.740	-0.098	0.026
CL1 mass flow	-0.230	-0.061	0.025	-0.138	-0.126	-0.769	-0.210	0.998	0.037	-0.065
CL2 mass flow	0.177	-0.040	-0.038	0.167	0.193	0.846	0.216	-0.996	-0.195	-0.057
CL3 mass flow	0.228	-0.047	-0.033	0.172	0.116	0.851	0.232	-0.995	-0.226	-0.068
CL4 mass flow	0.179	-0.058	-0.090	0.123	0.137	0.811	0.143	-0.997	-0.099	0.040
CL1 temp.	0.036	-0.033	-0.236	-0.468	0.109	-0.997	-0.120	0.864	0.773	0.033
CL2 temp.	0.012	-0.038	-0.224	-0.259	0.059	-0.997	-0.076	0.836	0.765	0.008
CL3 temp.	0.011	-0.064	-0.271	-0.253	0.069	-0.997	-0.109	0.838	0.767	0.023
CL4 temp.	0.009	-0.030	-0.243	-0.285	0.061	-0.997	-0.061	0.837	0.764	0.023
HL1 mass flow	-0.224	-0.037	0.018	-0.112	-0.123	-0.767	-0.184	0.998	0.036	-0.063
HL2 mass flow	0.172	-0.055	-0.042	0.167	0.186	0.842	0.207	-0.996	-0.191	-0.059
HL3 mass flow	0.225	-0.050	-0.027	0.170	0.117	0.851	0.236	-0.995	-0.216	-0.077
HL4 mass flow	0.190	-0.079	-0.074	0.105	0.156	0.818	0.135	-0.997	-0.133	0.055
HL1 temp.	0.031	0.047	-0.283	-0.596	0.138	-0.996	-0.159	0.891	0.765	0.003
HL2 temp.	0.140	0.043	-0.250	-0.352	0.057	-0.993	-0.172	0.935	0.887	-0.122
HL3 temp.	0.177	0.043	-0.247	-0.330	0.049	-0.993	-0.146	0.930	0.889	-0.128
HL4 temp.	0.149	0.066	-0.192	-0.386	0.051	-0.992	-0.121	0.941	0.887	-0.115
core mass flow	0.198	-0.062	-0.040	0.171	0.157	0.841	0.194	-0.996	-0.195	-0.064